NASA Contractor Report 159234

SCALE MODEL STUDIES FOR ESTABLISHING THE FLOW PATTERNS OF A LOW-SPEED TUNNEL

P. S. Barna

OLD DOMINION UNIVERSITY RESEARCH FOUNDATION
Norfolk, Virginia 23508

NASA Grant NSG-1563
March 1980

National Aeronautics and Space Administration
Langley Research Center
Hampton, Virginia 23665

SUMMARY

Experiments were conducted on a model tunnel scaled down from the full-size prototype, the V/STOL (Vertical Take-Off and Short Landing) tunnel located at NASA/Langley Research Center (LaRC) in a ratio of 1:24. The purpose of the tests was to study the flow characteristics around the tunnel and to document the location and causes of local flow separation and local recirculation. Cumulatively these adverse flow characteristics reduce the efficiency of the tunnel performance.

Preliminary experiments performed earlier on the V/STOL tunnel indicated that adverse flow conditions existed at various locations which suggested the need for a study of the interaction between the various components from which the tunnel is built. For this purpose an experimental setup similar to the sequence of tunnel circuit components was constructed which enabled the various components to be tested either individually or in combination. These components were tested both individually and in combination by the simple technique of blowing air through them, then measuring the velocity distribution at relevant sections.

The model experiments have been performed in the Aerodynamics Laboratory of the Old Dominion University Engineering School. While the tests are not fully completed, results obtained so far already show effects of interaction between the components which were absent when they were tested individually and which explain to some extent why the tunnel functions at reduced efficency.

INTRODUCTION

The calibration of full-scale wind tunnels is an accepted standard procedure which usually calls for the evaluation of flow conditions. A relatively simple evaluation concerns only the test section of the tunnel. At times, however, a need also arises for probing the flow conditions at other sections as well—occasionally even around the entire tunnel circuit, which of course proves to be

a more laborious and demanding procedure, requiring more time, more effort, and more equipment.

The employment of scaled-down tunnels has certain advantages. If model studies precede the construction of the full-scale "prototype," a fair conception of the flow distribution may be obtained ahead of time, thus allowing for corrections to be made. Although the prediction of flow distribution in the prototype may not be accurate owing to Reynolds number effects, the model studies would at least indicate trouble areas that could occur in various tunnel components where the flow pattern refuses to follow the anticipated distribution.

Experience teaches that in tunnels where one experiences "troubles" it is in the diffuser after the fan that flow separation most readily occurs. It is a well-known fact that, once the flow separates from the diffuser wall, the resulting fluctuations downstream become noticeable, affecting both the flow in the test section and the tunnel performance.

Recent studies on diffusers indicate that performance expressed in pressure recovery depends on the flow "quality" at inlet to the diffuser in addition to its geometry (ref. 1). Under quality comes, first, blockage at inlet that is closely linked to velocity distribution. Effects of viscosity come second (Reynolds number at inlet), and turbulence level comes third. Any other type of disturbance, such as a nacelle protruding into the diffuser or the diffuser changing cross-sectional configuration, adds to the complexity of the flow.

Since closed-circuit wind tunnels repeatedly turn around approximately the same air quantity, it is then the "history" of the flow that needs further consideration. This means that each component (corners, diffusers, etc.) of the tunnel through which the air passes affects the successive components downstream. Therefore, each component's performance, in addition to its design, is influenced by the flow conditions upstream.

Design and performance data available on components (corners, diffusers, etc.) are the results of tests which were most probably performed under a variety of flow conditions, but were nevertheless termed "ideal." For example, published results on the flow around a bend assume uniform velocity distribution right across the flow upstream. However, the flow even upstream of the first corner in a wind tunnel cannot be uniform right across because of the buildup of boundary layer in the preceding diffuser, which reduces the width of the uniform flow. Since the corner has to turn uniform as well as nonuniform flow (near the walls), it would be unreasonable to expect a completely uniform flow to emerge on the downstream side of it! Furthermore, if the duct downstream from the first corner is a diffuser, an additional boundary-layer buildup is experienced, and the uniformity of flow becomes further impaired. Consequently, the flow after the corner may altogether become non-uniform. It may even become asymmetric as well, owing to the fact that, in the process of turning, flows generally develop a pressure gradient across the stream, the higher pressure being on the outer side to balance centrifugal forces. Downstream from the corner, during the process of pressure equalization, parts of the stream run ahead, which explains why the flow becomes neither uniform nor axisymmetric. Should the fan be located downstream from the second corner, it may reasonably be anticipated that the velocity distribution in the flow annulus will neither be uniform nor symmetric.

For axial flow fans with fixed blade settings, however, there is no provision to compensate for unsymmetric through flow conditions, which results in a flow that is <u>again</u> unsymmetric downstream from the fan.

The large diffuser (following the fan) suffers from the disadvantage of receiving a turbulent and nonuniform flow from the fan, thus preventing the diffuser from performing satisfactorily. In transit through the diffuser the flow profile further

deteriorates. Since the third and fourth corners are considered incapable of restoring uniformity to flow, the contraction upstream from the test section can improve the flow to a limited extent and only if the contraction ratio is large. It cannot reduce the prevailing turbulence to the level anticipated by its geometry because of the nonuniform flow distribution at entry. As a result, the turbulence level in the test section is also higher than the desired level, and so the first diffuser downstream from the test section may be affected.

Ultimately, the operation of the wind tunnel depends on the performance of its components. This in turn depends on the history of the flow, the starting point for which may be the velocity distribution in the test section and possibly the prevailing turbulence level therein.

At this time data are lacking on the effects of turbulence on diffuser performance. Therefore, it is not yet possible to predict the effects of turbulence level on the diffuser's operation. Nevertheless, studies of interaction between components can be made by a technique described in this report.

SYMBOLS

d	wire diameter of screens (m)
p	center distance between screen wires (pitch) (m)
R	radius (m)
r	radial distance from centerline (m)
s	wire screen solidity defined as $2d/p$
y	distance measured from the tunnel wall (m)
u	velocity of stream at distance y measured from the inner wall (m/s)
U_{max}	maximum velocity of the stream (m/s)

w tunnel width (m)

T.S. traverse station

H horizontal traverse

V vertical traverse

BRIEF DESCRIPTION OF THE V/STOL TUNNEL COMPONENTS

In order to make recognizable the characteristic features of the V/STOL tunnel, the curcuit will be briefly reviewed. The various components are noted on figure 1, which shows the plan view of the tunnel. Table 1 gives the relevant details of these components.

The test section or testing area is followed by the first diffuser, which is provided with an air breather (air intake) that can be operated open, closed, or half open. At the end of the first diffuser is the first corner, provided with equally spaced turning vanes, which is followed by the second diffuser. The flow control vanes, placed into the second diffuser, provide better speed control at very low test section velocities. A wire screen is fitted right across the second corner, which is followed by the third diffuser, designed for transition from a rectangular cross section to a circular cross section. The axial flow fan is located in a cylindrical shell and is fitted with a nacelle that protrudes into the large fourth diffuser, which is designed for transition from a circular to a rectangular cross section. The air exhaust is located at the end of the fourth diffuser. The third and fourth corners are connected with a rectangular duct of constant cross section. Finally, the contraction closes the return circuit. A set of two screens is fitted over the entire cross section at inlet to the contraction. Note that neither the rectangular section of the testing area nor any of the other components with rectangular sections were provided with corner fillets.

Table 1. Approximate cross-sectional area of components.

Component	Inlet Area m^2	Inlet Area ft^2	Outlet Area m^2	Outlet Area ft^2	Area Ratio Outlet/Inlet
Contraction	263.5	2835.75	29.3	315.4	1:8.99
Test section	29.3	315.4	32.8	353.5	1.12:1
First diffuser	32.8	353.5	79.0	850.5	2.41:1
Second diffuser	79.0	850.5	98.3	1057.86	1.244
Third diffuser	98.3	1057.86	115.9	1247.5	1.18
Fourth diffuser	141.3	1521.55	254.9	2743.6	1.8
Fan section	115.9	1247.5	141.3	1521.55	1.22
Return duct between 4th diffuser and contraction	--	--	--	--	1.033

APPARATUS FOR THE SCALE MODEL TESTS

The apparatus employed for the blowing experiments was an open-ended, through-flow wind tunnel, powered by a 11.19-kW (15-HP) variable speed motor, shown in figure 2. The exit area of the tunnel was stepped down through a suitable transition duct to fit the model ducts. Specifically, the transition duct was provided with a 76.2-cm (30-in.) diameter at inlet, which changed to a rectangular exit measuring 37.8 × 40 cm (14.875 × 15.75 in.) over a length of 0.914 m (3 ft). All linear dimensions of the model ducts were reduced from the full scale in a ratio of 1:24.

The setup for testing the various components varied according to the arrangement for each tunnel configuration. Some components were tested individually, while others were tested in combination. For example, the corner downstream from the first diffuser was tested first as an individual component, and various types of turning vanes were inserted in order to test their effectiveness for turning the flow. With the diffuser attached to the corner, the setup became a combination. When tests were conducted on diffusers without the presence of the corners, the setup was referred to as the "straight blowing-through mode."

The following setup combinations were tested:

A. Straight blowing-through the third diffuser, followed by the annular duct and the large fourth diffuser without the nacelle (fig. 3);

B. Same as A, but with the nacelle installed (fig. 4);

C. Second corner alone, with various turning vanes employed (fig. 5);

D. Second corner, followed by a short parallel duct (fig. 6);

E. Second corner, followed by third diffuser, annular duct and the fourth diffuser, without the nacelle (fig. 7);

F. Same as E, but with the nacelle installed (fig. 8);

G. Same as F, except the fourth diffuser was followed by the third corner (fig. 9);

H. Same as G, but with the fourth corner added (fig. 10); and

I. Same as H, but followed by the contraction leading to the testing area of the tunnel (fig. 11).

METHOD OF TESTING

Most tests were conducted with two fan speeds: No. 2 and No. 4 respectively, 2 being the low speed and 4 being the highest. However, some tests were also conducted with other fan speeds. (Each combination resulted in a different speed because of the variation in the duct size.) The speeds produced are noted in the results. In all tests a standard pitot-static traversing procedure was employed. In some tests a wire screen was stretched across the flow and its effects on the downstream velocity distribution were studied. At traverse location 11, a 14-mesh screen was used; at traverse location 15, a 16-mesh screen, and at traverse location 16, a 20-mesh screen was used. (Note that the 14-mesh screen was used only once, while the 16-mesh screen at location 15 was used most frequently.)

EXPERIMENTAL RESULTS

All results presented in this report are normalized, and u/U_{max} is plotted against y/w, where U_{max} was the maximum speed attained in any traverse across the particular duct where the width was w. In figures 3 to 11, all horizontal traverses are marked with "(H)" at the outside contour of the tunnel, while the vertical traverses are marked with "(V)" in the center near the axis of symmetry.

Results of Setup A

Figure 3 shows the geometry of setup A. This setup was arranged to discover the flow characteristics in three empty ducts following each other by blowing uniformly distributed air through the third diffuser, followed by the annular duct and the fourth diffuser, without the presence of the nacelle and fan.

The results show that this setup produced a satisfactory velocity distribution all the way along the duct as presented in figures 12(a) to 12(g). Uniform velocity distribution extended almost all the way across the section—except for the boundary layer. The distribution appeared symmetrical for practical considerations, and the shoulder regions near the wall showed no signs of separation. Naturally, the boundary layer was very thick at exit from the fourth diffuser (T.S. 16), but 25 to 28 percent thickness was to be anticipated and may be considered no worse than expected under "normal circumstances" when the blockage at diffuser inlet is low (refs. 2, 3).

The implication of this experiment is important: given a uniform velocity distribution upstream, without introduction of high intensity turbulence, the return "leg" of the tunnel produces satisfactory flow conditions.

Results of Setup B

Figure 4 shows the geometry of setup B. In these tests the setup remained essentially the same as in A, except that the nacelle was installed in its proper place.

These experiments established the velocity distribution at a section of the tunnel where the fan would be located, and the effect of the nacelle on the downstream flow condition was studied.

Figures 13(a) and 13(b) show the velocity distribution in the horizontal and vertical planes between the nacelle and tunnel wall at the fan location when the straight through-flow conditions applied.

It appears that at T.S. 13 the flow velocity dropped sharply from the radial location y/R = 0.15 to the tunnel wall. This velocity drop could cause tip stall for a fan designed on the basis of constant axial velocity. The hemispherical hub caused a nonuniform velocity distribution between radial locations y/R = 0.2 to 0.6, which could be improved by employing a more suitable hub.

Immediately downstream from the nacelle (at T.S. 15), a dip appeared in the center region and the velocity decreased sharply to $u/U_{max} \approx 0.39$, as shown in figure 13(c). Further downstream, at T.S. 16, the defect extended only to $u/U_{max} \approx 0.68$, as shown in figure 13(d), while the velocity distribution near the wall remained about the same as in setup A, shown in fig. 12(f). The presence of the nacelle did not seem to affect the velocity distribution near the walls downstream.

Results of Setup C

Figure 5 shows the geometry of setup C. In these tests, flow around a 90-degree bend was studied. The bend was fitted with corner vanes of various designs: thick vanes consisting of two circular arcs, as used commercially, and thin circular arc vanes either spaced equally or in geometric progression (see fig. 14).

Figure 15 presents results first obtained with the readily available thick turning vanes generally favored in commercial practice because of their stiffness. In addition to obtaining velocity distribution downstream from the vanes, angles of yaw and pitch were also measured.

The results show a remarkably uneven distribution, and large variations in velocity were observed across the stream, resembling "humps and hollows." In addition, the average velocity was found to decrease towards the outer wall. Furthermore, variations in the pitch and yaw angles up to ±4 degrees were noted.

Corrective measures were initiated to eliminate these adverse effects: a honeycomb was installed immediately downstream from the vanes to correct yaw and pitch and also to decrease the

variations in velocity; the 45-degree diagonal setting of the vane row was changed by 5 degrees, and a large-radius turning vane was placed near the outer corner. However, these modifications did not produce the desired uniform flow in the horizontal plane and the vertical traverses; and so the thick turning vanes were replaced by thin circular arc vanes.

The thin circular arc vanes were made of 16-gage aluminum with a 5.1-cm (2-in.) radius and 8.2-cm (3.2-in.) chord. The experiments were performed both with equal spacing and with varied spacing when the gap between the vanes increased outwardly in a geometric progression, as prescribed by the Royal Aeronautical Society's Data Sheet (see refs. 4 and 5).

The experimental results for both thin vane configurations showed a substantially uniform velocity distribution (ref. 6), and the velocity defects due to vane thickness were markedly reduced, as shown in figures 16 and 17. It may be noticed that, when the corner vanes were followed by a diffuser, some change in the velocity distribution occurred immediately downstream at a distance of 3.8 cm (1.5 in.) from the trailing edge. The maximum velocity then occurred near the inner wall and gradually decreased toward the outer wall [fig. 17(b)]. A slight "dish" near the center also became noticeable. At a distance 36.8 cm (14.5 in.) further downstream, the center dish (or trough) widened and two velocity peaks appeared, while the boundary-layer flow near the inner wall thickened, as shown in fig. 17(c). The distribution could probably be further improved by employing vanes of smaller chord, but these are more difficult to obtain, and their alignment causes additional problems.

Results of Setup D

Figure 6 shows the geometry of setup D. In these tests static pressure distribution across the flow downstream from the equally spaced thin corner vanes was studied. While the general arrangement

remained the same as in setup C, the corner was followed by a short parallel duct. Since the flow pattern in the return leg of the tunnel differed considerably between the straight flow-through mode and the mode employing turning vanes ahead of the diffuser, some explanation for this difference had to be found.

A short parallel duct, 61-cm (24-in.) long, was fitted downstream from the turning vanes, and the static pressure distribution was measured across the horizontal plane at 4 traverse planes at increasing distances from the trailing edge of the vane located at the inner corner. The results are shown in figure 18, where the static pressure is plotted against distance across the flow.

Right at exit from the corner the variation was larger than anticipated, while in going downstream the pressures equalized quite rapidly. As a result, some redistribution of the flow downstream from a corner took place when the corner was followed by a duct. As the pressure equalized, the flow ran ahead at the inner regions, causing also a crossflow and ultimately nonuniform flow distribution [see fig. 17(b)].

Results of Setup E

Figure 7 shows the geometry of setup E. In these tests the effects of the second corner on the downstream flow taking place in the third diffuser, annular duct and fourth diffuser were studied, in this case without the presence of the nacelle. First the effects of a corner fitted with thick turning vanes were studied. These vanes are widely used in commercial practice and were readily available. Subsequently the thick vanes were replaced by equally spaced thin turning vanes, and their effects on the downstream flow were studied and compared with those of the thick vanes.

The results show that the velocity distribution at entry to the test setup at T.S. 10 was fairly uniform upstream from the thick vanes as presented in figure 19(a). The small defect noticeable between $y/w = 0.6$ and 1.0 amounted to about 2 to 4 percent,

and this most probably was due to inertia effects. The thick turning vanes have been found to produce markedly nonuniform flow downstream. Immediately downstream from the thick turning vanes, at T.S. 11, the flow pattern was affected by the wake of each vane, as shown in figure 19(b), and several dips in the profile show the traverse location where the defects were in alignment with the trailing edge of the vanes. Flow separation at the inner wall also became noticeable.

In going further downstream, transformation of the velocity profile took place because of boundary-layer buildup on the walls. At T.S. 13 and 14 a dip developed near the center of the accelerating core as shown in figures 19(c), (d), and (e). In addition, the pattern became more and more unsymmetric. The flow appeared to be sensitive to Reynolds effects, and the dip deepened at the low speed of the fan, while a marked change in the distribution occurred when the speed was increased. Only one peak appeared at high speed and was located off-center near the outer wall, as shown at T.S. 15 and 16, figures 19 (f) and (g).

The experiments previously described were repeated after the thick turning vanes were replaced with thin vanes made in a circular arc shape. First vanes with variable spacing were employed; subsequently vanes with equal spacing were also tested. The difference was found to be small between the equally and variably pitched vanes.

The results of tests with the thin vanes showed a marked improvement in the velocity distribution, as presented in figure 20. The velocity distribution at T.S. 13 was more even [fig. 20(a)], and the velocity defects were less pronounced than with the thick vanes shown in figure 19(c). However, further downstream the velocity distribution again became unsymmetric, and the peak in velocity shifted towards the outer wall at T.S. 15 and 16, as shown in figures 20(b) and (c).

Results of Setup F

Figure 8 shows the geometry of setup F. The combination of ducts remained the same as in E, except that the nacelle was now installed and variably pitched vanes were installed in the second corner.

With the nacelle installed, the flow immediately downstream from the nacelle trailing edge showed a marked velocity defect in the center, approximately $u/U_{max} = 0.25$, while the two velocity maxima off center were approximately equal [fig. 21(a)]. However, at T.S. 15 the velocity at the center began to increase, while the peak near the inner wall decreased and the flow on the inner wall showed signs of separation [fig. 21(b)]. Further downstream at T.S. 16, only the velocity peak at the outer wall remained, while the flow between the center and inner wall receded (most probably separated) as shown in figure 21(c).

Results of Setup G

Figure 9 shows the geometry of setup G. To the test setup described under F was added the third corner with thick turning vanes, and its effects on the upstream flow were studied.

Addition of the third corner brought about some changes in the velocity profiles at T.S. 15 and 16, but direct comparison cannot be made between the experiments described in setup F because of a change from the variably pitched vanes employed in F to equally spaced vanes employed in G.

At T.S. 16 two peaks in velocity distribution occurred, each off center. The one nearer the inner wall lagged behind the peak nearer the outer wall, which was the maximum, as shown in figure 22(a). When compared with figure 21(c), one finds that only one peak occurred near the outer wall, while the peak near the inner wall did not occur as a peak but as a flat portion of the distribution

where the velocity remained unchanged. This may be called the "zone of hesitation," [1] (a phenomenon quite similar to that experienced at T.S. 15 in the full-scale tunnel). The velocity distribution near the inner wall indicated a very thick boundary layer that may even have been separated, while at the outer wall the distribution appeared satisfactory.

After the flow turned the third corner at T.S. 17, the flow showed some changes. While the velocity peaks remained approximately the same (both in shape and location), the defect moved up from 0.75 to 0.84, as shown in figure 22(b). The flow near the inner wall further deteriorated. Note that both the third and fourth corners were provided with thick turning vanes.

Results of Setup H

Figure 10 shows the geometry of setup H. The fourth corner with thick turning vanes was added to setup G, and studies were made to determine its effects on the flow upstream. In one set of experiments the second corner was provided with the variably spaced vanes, and in another set of tests the equally spaced vanes were employed.

Results of tests with the variably spaced vanes are shown in figures 23 (a), (b) and (c). While the flow far upstream remained unchanged, as shown in figures 23(a) and 23(b) (T.S. 15 and 16), two peaks in the velocity again occurred at exit from the fourth corner; however, both moved closer to the center, as shown in figure 23(c). Further boundary-layer growth was also experienced. Results of tests with equally spaced vanes are shown in figure 23(d). With the changeover to equally spaced vanes in the

---

1 "Zone of hesitation" is a term used here to mark a certain width of flow across which constant velocity is observed.

second corner, one observed two velocity peaks at T.S. 16 [fig. 23(d)], as compared to one peak at the same location with the variably spaced vanes. This is of considerable interest because it shows that the flow distribution at inlet to the third diffuser had a marked effect on the flow distribution downstream.

Results of Setup I

Figure 11 shows the geometry of setup I. To the setup H, which used variably spaced, thin turning vanes in the second corner, was added the contraction downstream from the fourth corner. Measurements of velocity distribution were made at the entrance and at the exit of the contraction section. The results show that the velocity distribution was uniform at exit as presented in figure 24(a), which is a rather interesting result when one considers the rather poor velocity distribution of the flow at inlet to the contraction (T.S. 19) as shown in figure 24(b). Certainly the large contraction ratio (9:1) was responsible for the uniform velocity distribution at exit of the contraction.

Changes in the Velocity Profile at the Nacelle

When setup B was changed to setup I, there appeared a change in velocity distribution upstream from corners 3 and 4; hence a check on the velocity distribution at the nacelle was felt desirable.

For setup I, figures 25(a) and 25(b) present the velocity distribution in the horizontal and vertical planes respectively. When comparing figure 25 with figure 13, one may observe velocity distributions which differ. In both traverses of setup I from a position near the wall to a position near the hub the velocity increases fairly uniformly. However, in setup B, an abrupt change in the rate of velocity increase was noticeable; in the horizontal traverse, shown in figure 13(a), this occurred at $y/w = 0.18$, while in the vertical traverse (where the traverse proceeded from the nacelle to the wall) the abrupt change occurred at $y/w = 0.83$.

These differences are of considerable interest as they affect the fan design and its performance. Their most probable cause is the effect of the corner upstream.

Effects of Screen on the Flow

Application of a screen affected the flow distribution both up and downstream. Screens are known to even out adverse velocity distributions; they tend to reduce high velocity peaks and at the same time advance motions in regions where slow or sluggish flow appears, especially at the walls of diffusers with thick boundary-layer growth (refs. 7, 8).

In these experiments, the effects of screens on the turbulence were also examined. Since the intensity of turbulence increased with speed, the effects of screens on the flow were different at high speed as compared with low speed. For this reason, screens stretched across wind-tunnel sections where the flow velocity was high (such as at T.S. 11) had effects on the flow which differed from those observed when the screen was inserted into low-speed regions (such as at T.S. 15 or 16).

Results of tests with the setup A employing a 20-mesh screen (solidity = 0.32) stretched across T.S. 11 are shown in figure 26. With the variation of airspeed, the effect of the screen on the flow in this setup produced a slight velocity peak near the outer wall, but only in the case when the air velocity was high. This result was found consistently through traverse stations 13, 14, 15 and 16 as shown in figures 26(a), (b), (c), and (d).

When the screen was removed from T.S. 11 and was placed further downstream at T.S. 16, the velocity distribution shown in figure 26(e) became almost identical to the flow without the screen [shown earlier in fig. 12(f)], except that the flow near the inner wall improved slightly. A more marked change occurred, however, when the screen was moved upstream to T.S. 15. Downstream from the screen the flow changed, and the previously uniform portion of the flow

profile at T.S. 16 widened while the flow near the wall advanced, as shown in figure 26(f). At the same time, the flow became less steady and a wavy flow pattern became noticeable which could no longer be considered as uniform. (Some of these effects could have been caused by uneven tension in the screen.)

In setup B, introduction of a 16-mesh screen (solidity = 0.64) at T.S. 15 resulted in a marked improvement in the downstream flow at T.S. 16. When comparing figure 27 with figure 13(d), one finds the velocity distribution improved. Near the walls the flow was more satisfactory, while at center the defect produced by the nacelle was shallower.

When changing to setup E, with the introduction of the second corner (thick turning vanes), the effect of the screen on the flow varied, depending on the screen location. When the screen was located at T.S. 11, a slight improvement of the flow became noticeable at T.S. 13, as shown by comparison of figures 28(a) and (b) with figures 19(c) and (d). However, further downstream at T.S. 16, the flow pattern changed considerably when turning from low to high speed. In the horizontal traverse, shown in figure 28(c), the higher peak occurred near the inner wall, while in the vertical traverse the flow appeared separated at the top, as shown in figure 28(d). In addition, presence of the screen produced a defect which was found much larger with the screen than without. Also, marked changes occurred when the airspeed was increased, showing sensitivity to viscous effects which were due both to the presence of the corner and of the screen. When comparing figure 28(c) with figure 19(g), one finds that the velocity peak shifted from the location $y/w = 0.67$ to 0.2, a rather surprising result, which showed the combined effects of screen and corner vanes on the downstream flow distribution.

With the screen removed from T.S. 11 and placed at T.S. 15, a marked improvement in the flow occurred near the walls, as shown in the figure 29. In comparing figure 29 with figure 28(c), one also finds that the higher velocity peak changed location, having moved from $y/w = 0.2$ to 0.7.

When changing to setup F, with the screen placed at T.S. 15, the flow at T.S. 16 improved. When comparing figure 29 with figure 21(c), one finds the greatest improvement occurred between the inner wall and the center. The sharp peak near the outer wall became more rounded and the gradient near the outer wall seemed more satisfactory as well.

When changing to setup G, the effect of the third corner on the upstream flow at T.S. 16 showed only a slight improvement. When comparing figure 30 with figure 29, the distribution shown in setup G (fig. 30) shows about five percent improvement near the inner wall. However, when figure 30 is compared with figure 22(a), it is seen that the improvement of flow near the inner wall was very marked indeed!

When changing to setup H, one may observe some changes both up and downstream. At T.S. 17 [(fig. 31(a)], the outer peak decreased to $u/U_{max} = 0.97$ while the inner peak and the flow velocity ratio near the inner wall increased to 1.0. The flow near the outer wall slowed, and this effect shows up well when comparing figure 31(a) with figure 30. After turning around the fourth corner at T.S. 18 [fig. 31(b)], the flow near the outer wall showed further deterioration, while near the inner wall it remained about the same as observed at T.S. 17 [(see fig. 31(a)].

While the experiments are not yet conclusive as far as determining the most effective and suitable screen, the application of a screen halfway along a diffuser (here at T.S. 15) seemed definitely to produce beneficial effects downstream and presumably upstream as well. However, these effects were limited to the neighborhood of the screen. For example, the third corner introduced a new disturbance to the flow, and so the effective turning by the fourth corner was affected by the disturbance set up by the third corner. Therefore the necessity may arise of introducing a screen between the third and fourth corner, and so on, between the fourth corner and the contraction as well, which is, of course, a well-recognized fact in wind tunnel design.

CONCLUSIONS

An investigation into the flow characteristics of a scale-model wind tunnel has been conducted. The tunnel components have been scaled down in a ratio of 1:24 from the prototype V/STOL tunnel located at NASA/LaRC. The results of this investigation show the following conclusions:

1. As expected, there was an interaction between the tunnel components, each component having an effect on the other components, both up and downstream. The components which appeared to have the largest influence on the flow were the corners.

2. The flow straight through the empty return leg of the tunnel was found satisfactory (setup A)—an indication that when the flow at inlet to the diffuser was uniform the diffuser performed to satisfaction. Contrary to anticipation, the addition of the nacelle did not stall the fourth diffuser (setup B).

3. Results of tests on the various corners (setups C and D) showed that when the discharge from the corner took place into the atmosphere, the velocity distribution was uniform for the thin circular arc sheet metal vanes. If, however, the corner discharged into a parallel duct or into a diffuser, the velocity distribution no longer remained uniform. In this case the corners set up a pressure gradient across the tunnel that may be considered large enough to set up a cross flow, hence causing circulation. As a result, the flow into the large diffuser developed undesirable characteristics, resulting in separation downstream (setups E and F).

4. Screens introduced into the flow appeared to have beneficial or adverse effects depending on their location. A screen inserted halfway along the large diffuser substantially improved the flow downstream. However, if the screen was

was inserted upstream into a high-velocity region, it introduced turbulence which appeared to cause undesirable flow characteristics further downstream.

5. The screens appeared to have significant influence on the flow in the regions close by; further away, where a "fresh" disturbance is introduced, additional screens may become necessary.

6. Flow over the nacelle was also affected by the corner, and changes were observed when the corner was removed.

7. Contrary to expectation, the third and fourth corners did not improve the flow, and the distribution downstream from the fourth corner was found rather unsatisfactory. Interestingly, at exit from the contraction the velocity distribution was found fairly uniform.

8. There appeared to be no advantage to using variably spaced, turning vanes.

REFERENCES

1. Runstatler, W.; Dolan, F.X.; and Dean, R.C., Jr.: Diffuser Data Book Creare Inc. Report TN-186, May 1975.

2. Cockrell, D.J.: The Diffuser Inlet Flow Parameter. J. R. Aero. Soc. G.B., Vol. 69, May 1965, p. 350.

3. Reneau, L.R.; Johnston, J.P.; and Kline S.J.: Performance and Design of Straight, Two Dimensional Diffusers. J. Basic Eng., March 1967, p. 141.

4. Salter, C.: Experiments on Thin Turning Vanes. Aero. Res. Council of G.B., R & M 2469, 1952.

5. Pressure Losses in Curved Ducts: Single Bends. Engineering Sciences Data Unit 77008, 1977. (Royal Aero. Soc.)

6. Ahmed, S.; and Brundett, E.: Performance of Thin Turning Vanes in Square Conduits. Dept. of Mech. Eng., Univ. of Waterloo (Ont. Canada), 1967.

7. Pressure Drop in Ducts Across Round Wire Gauzes Normal to the Flow. R. Aero. Soc. Data Sheet 02.00.01, 1963.

8. Dryden, H.L.; and Schubauer, G.B.: The Use of Damping Screens for the Reduction of Wind Tunnel Turbulence. J. Aero. Soc., Vol. 14, No. 4, April 1947, pp. 221-228.

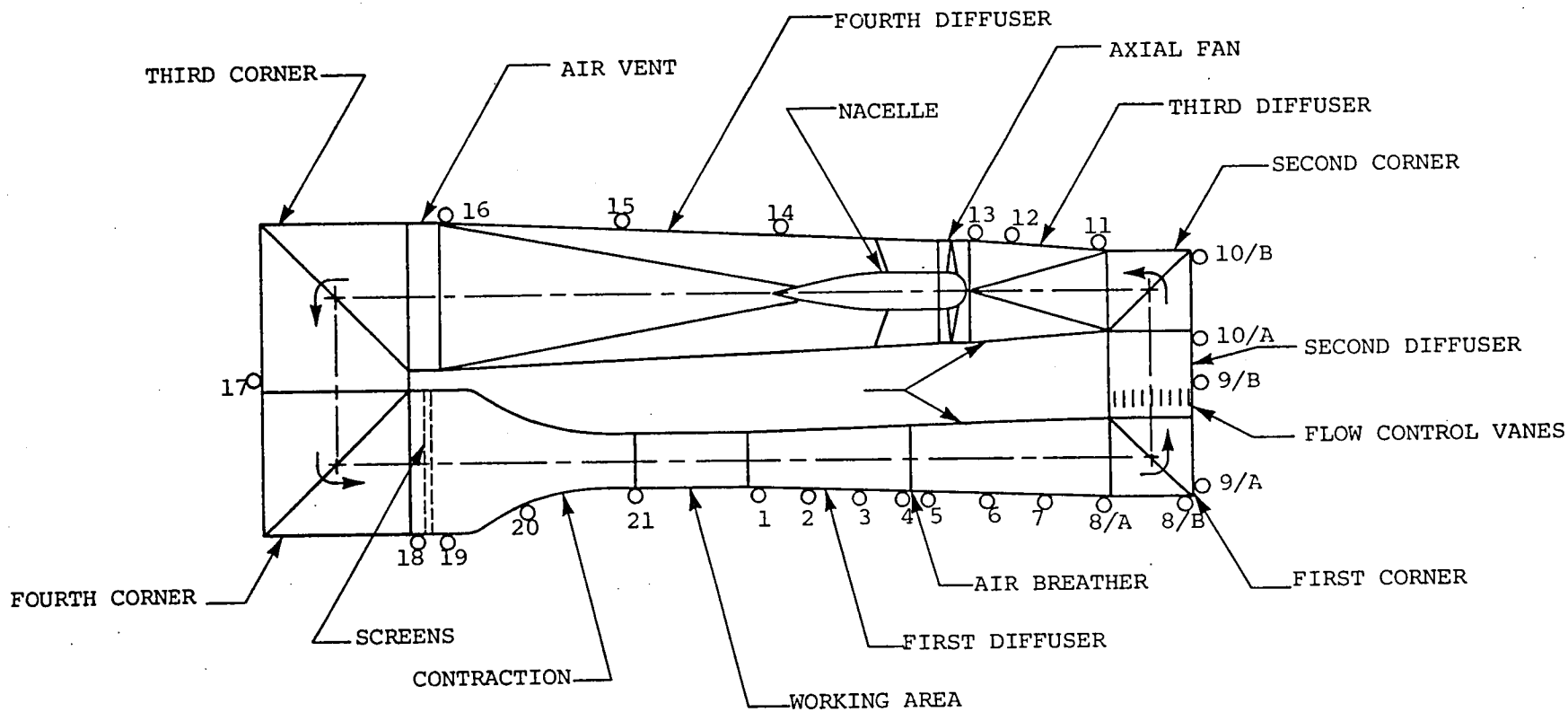

Figure 1. Plan view of the V/STOL tunnel.

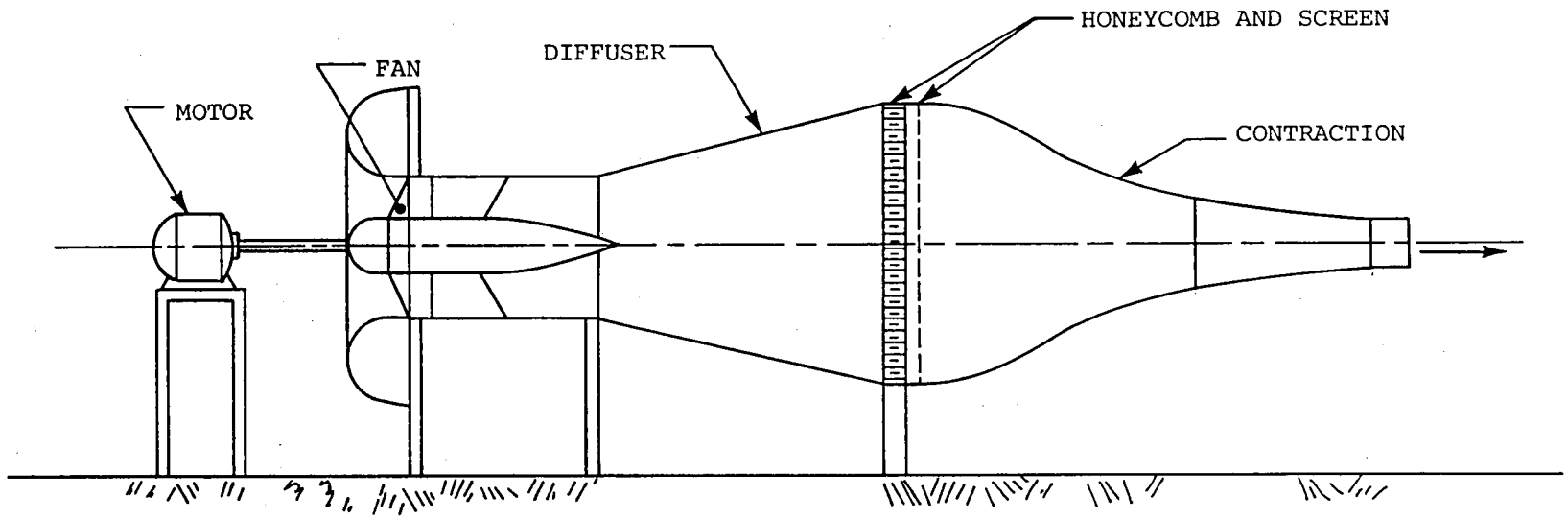

Figure 2. Schematic view of apparatus employed for blowing air through ducts.

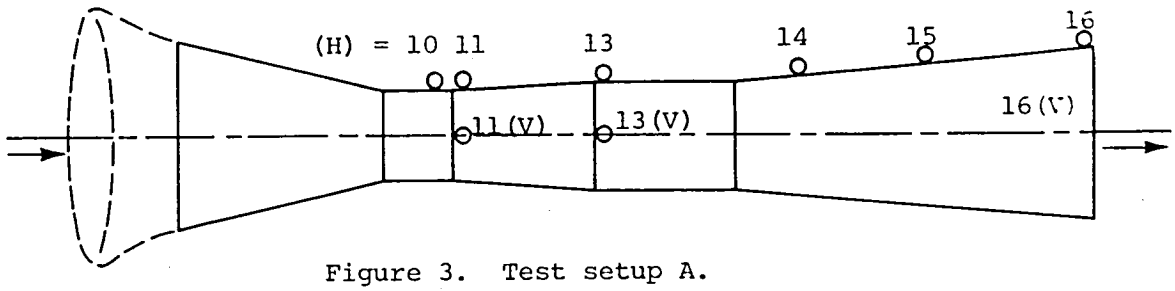

Figure 3. Test setup A.

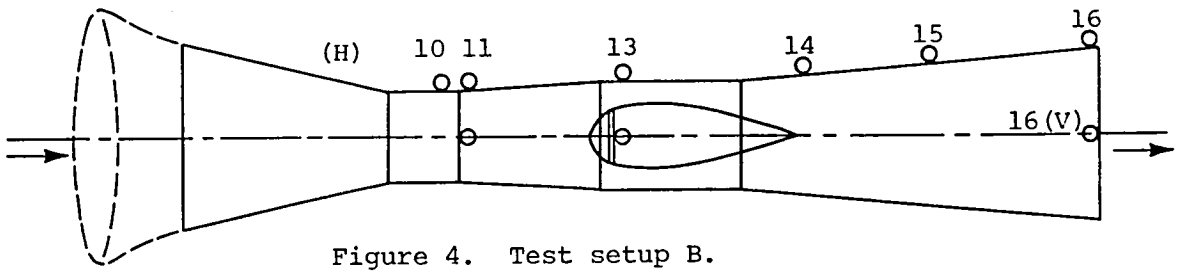

Figure 4. Test setup B.

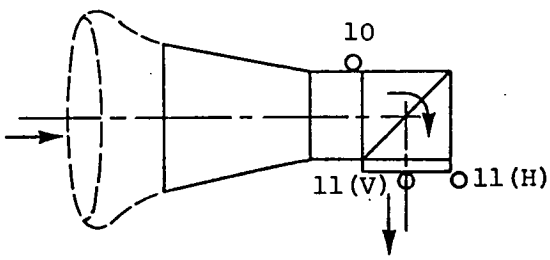

Figure 5. Test setup C.

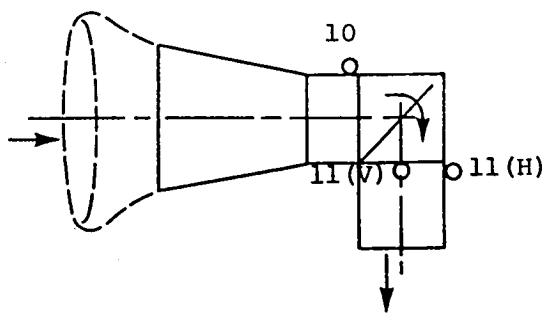

Figure 6. Test setup D.

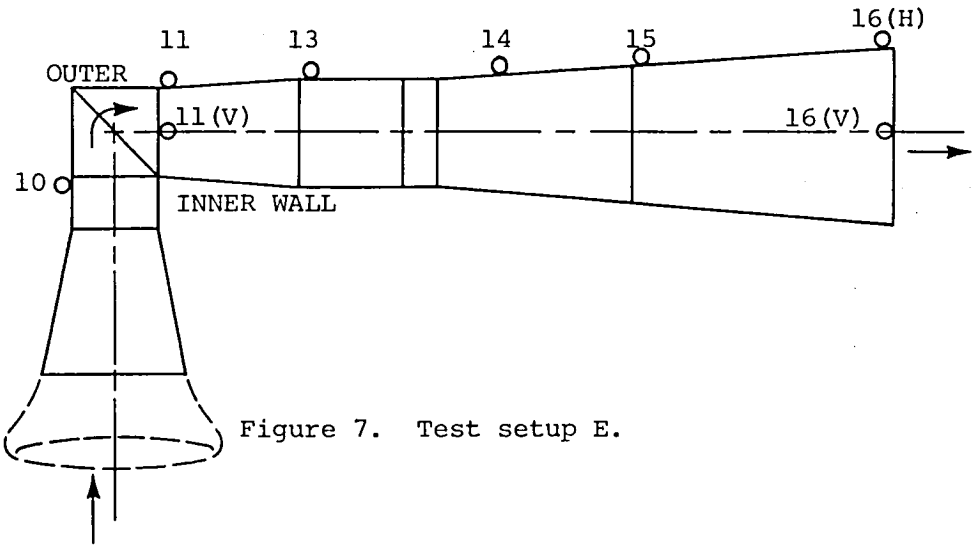

Figure 7. Test setup E.

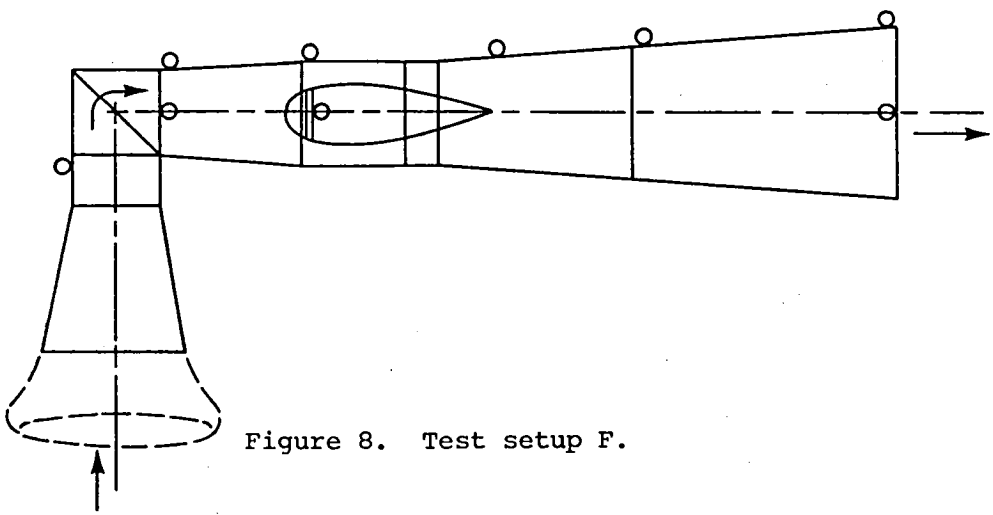

Figure 8. Test setup F.

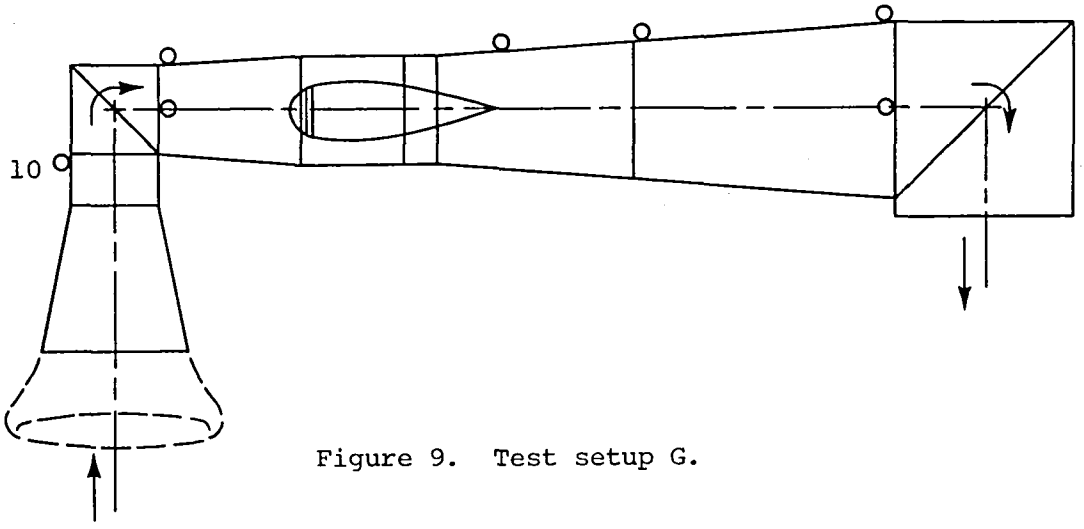

Figure 9. Test setup G.

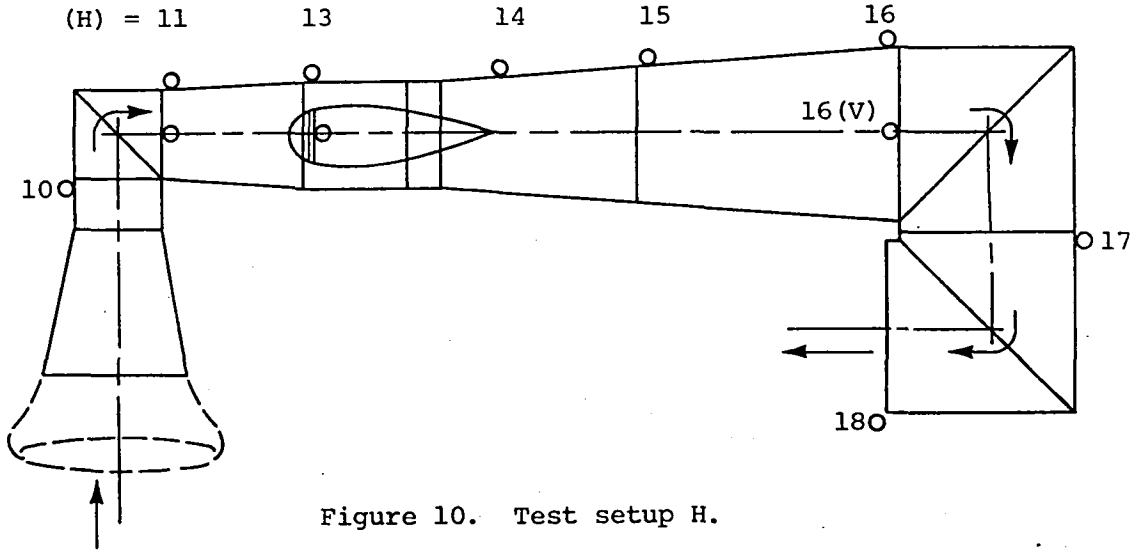

Figure 10. Test setup H.

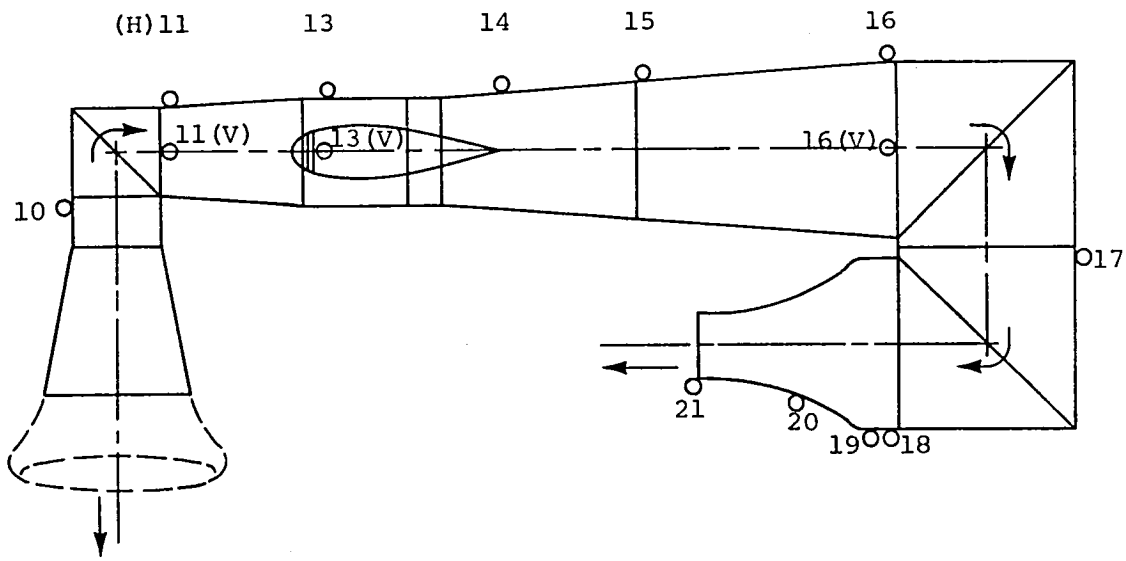

Figure 11. Test setup I.

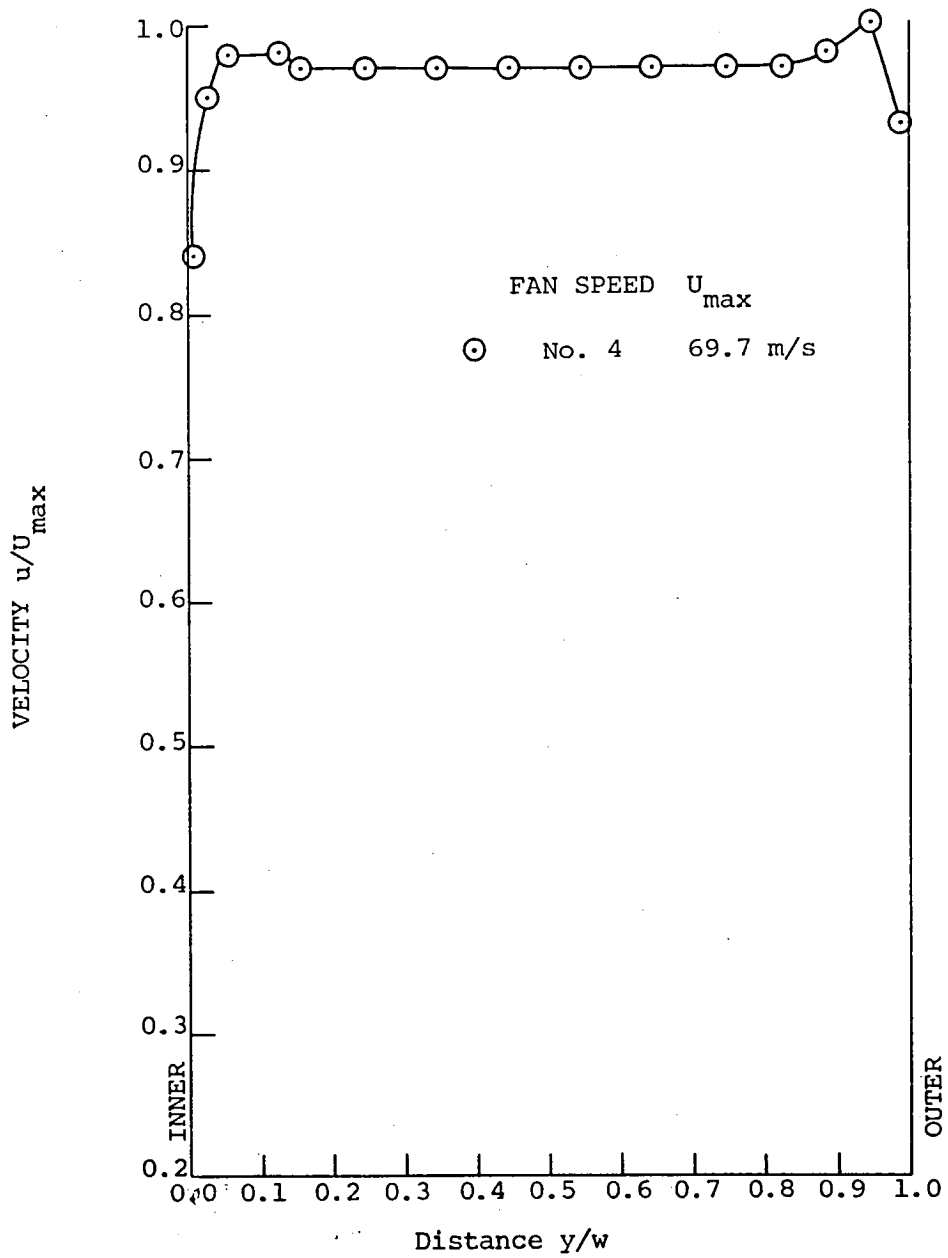

(a) Traverse station 11 (H).

Figure 12. Setup A: velocity distribution across the flow (straight through flow).

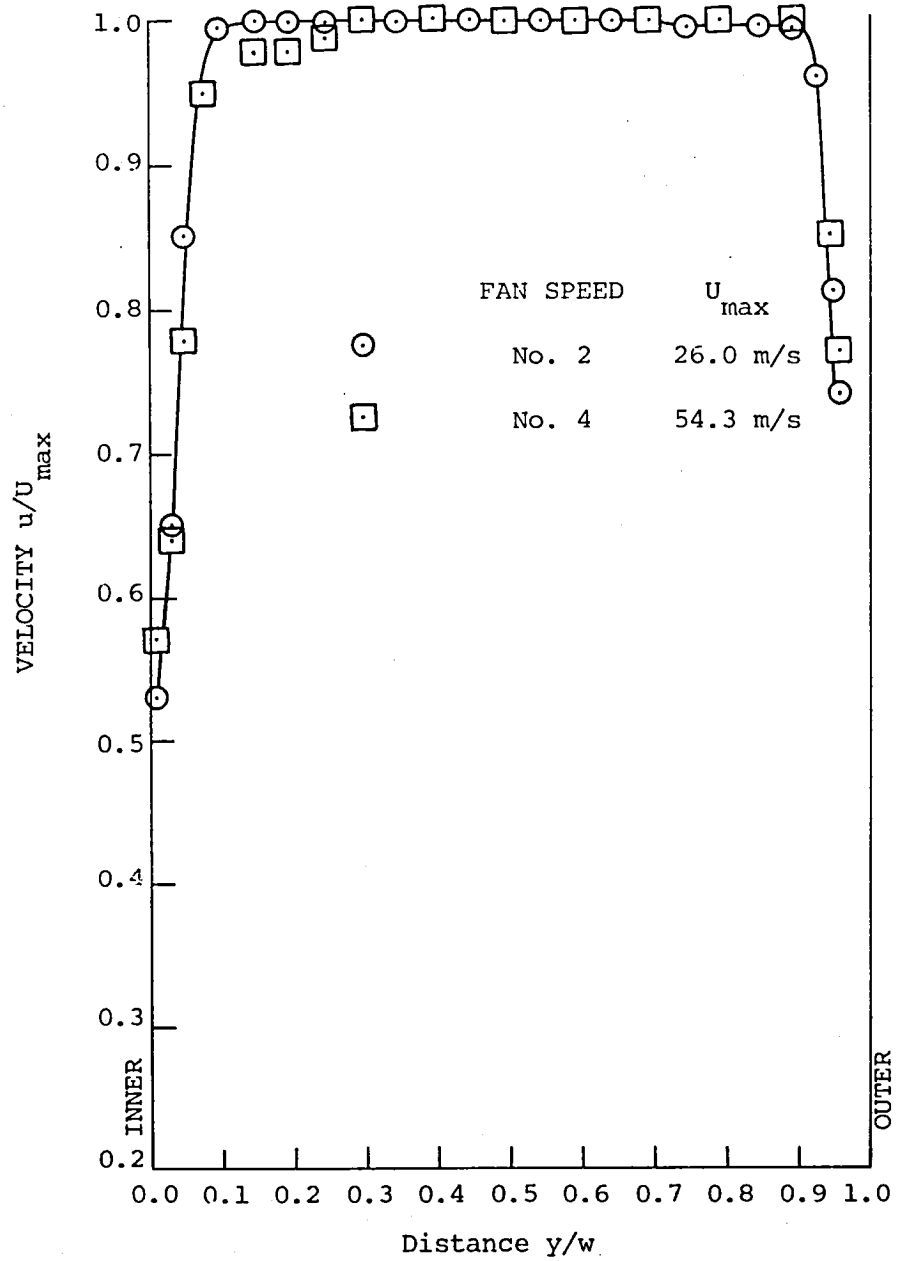

(b) Traverse station 13 (H).

Figure 12. (Continued).

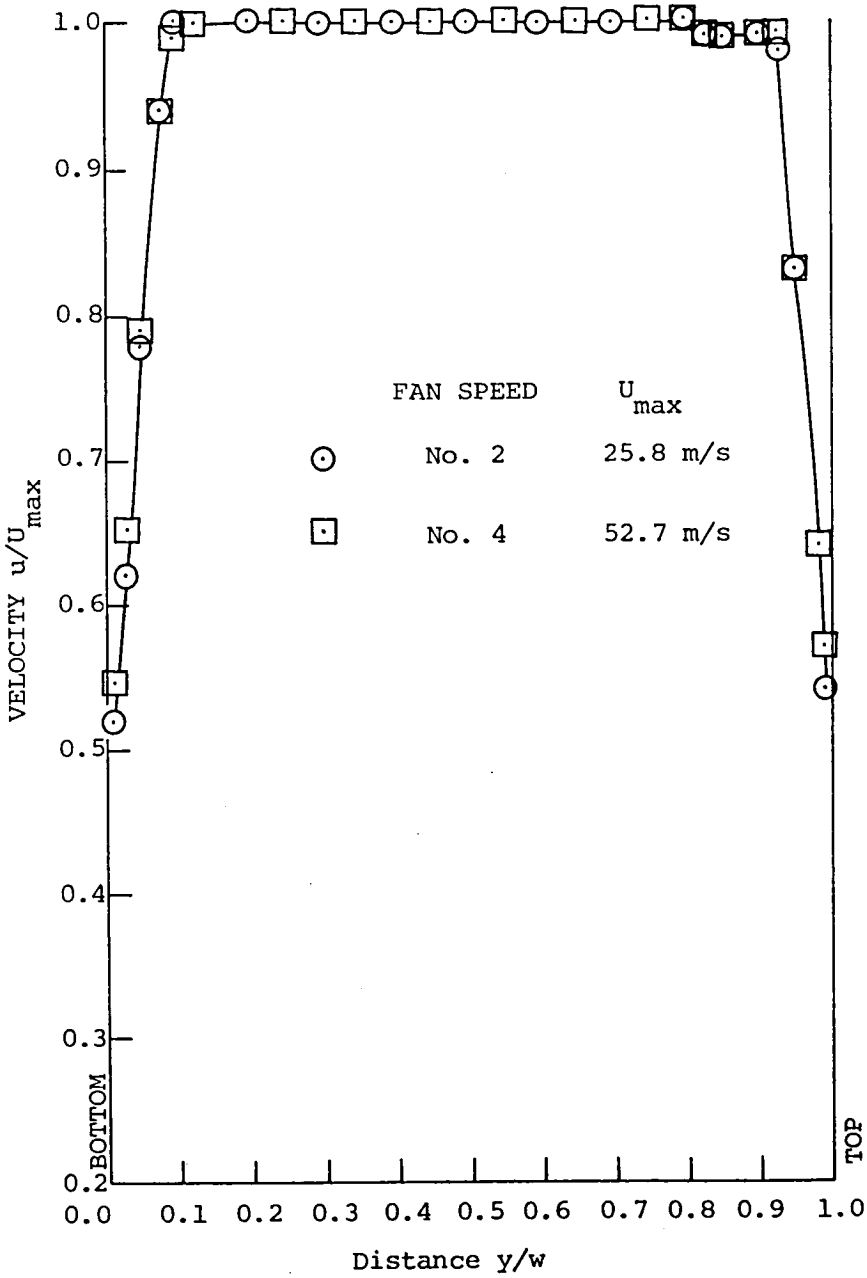

(c) Traverse Station 13 (V).

Figure 12. (Continued).

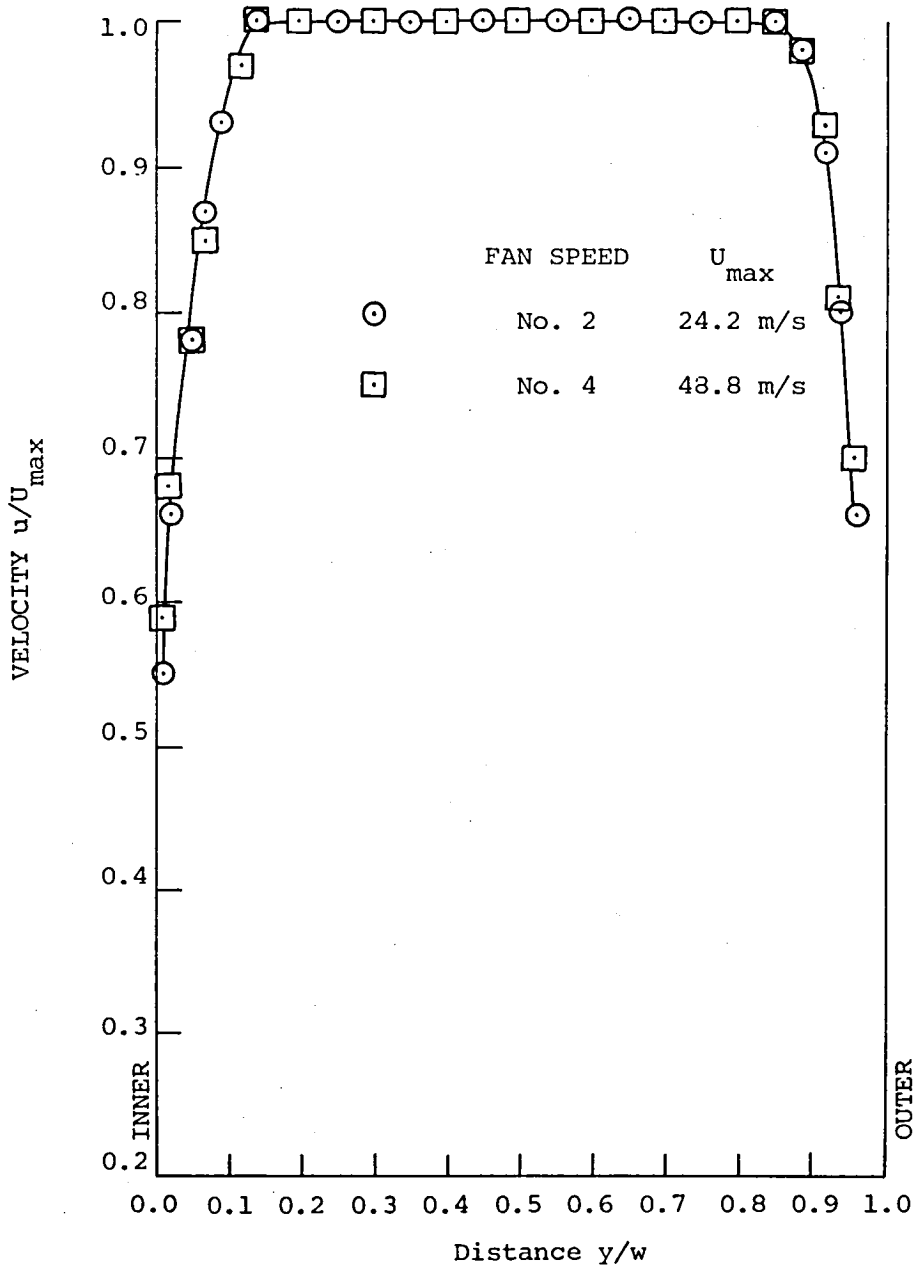

(d) Traverse station 14 (H).

Figure 12. (Continued).

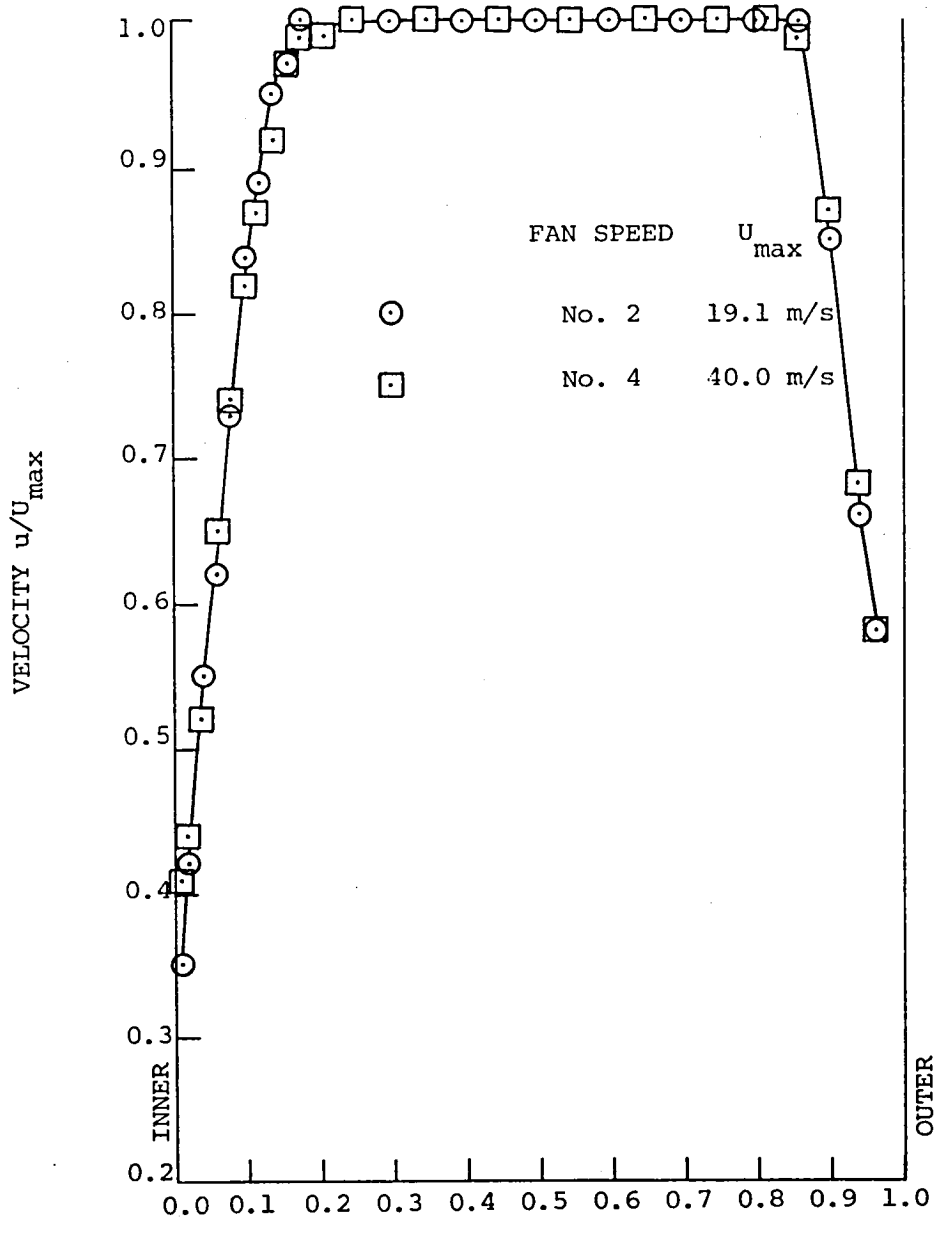

(e) Traverse station 15 (H).

Figure 12. (Continued).

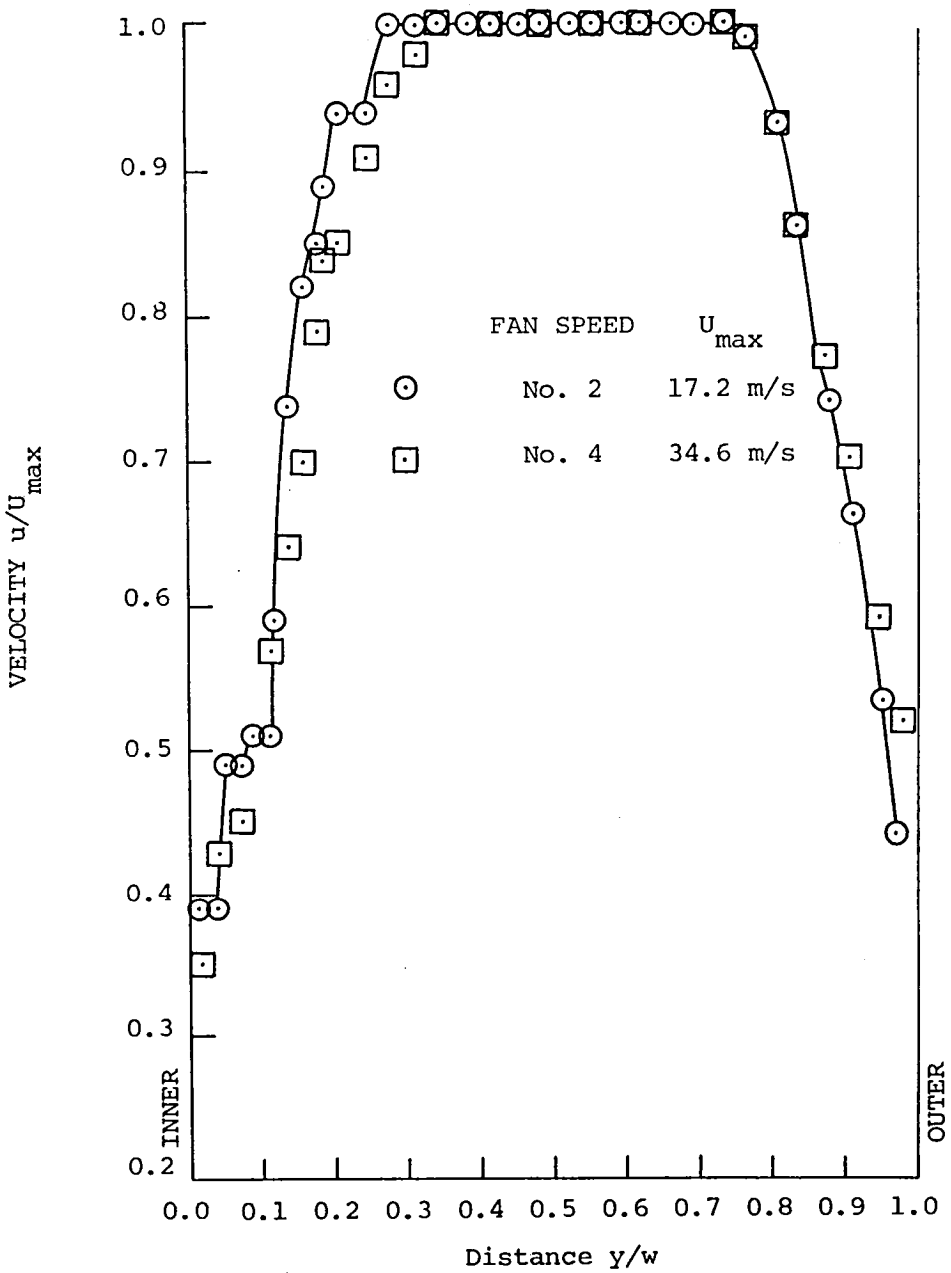

(f) Traverse station 16 (H).

Figure 12. (Continued).

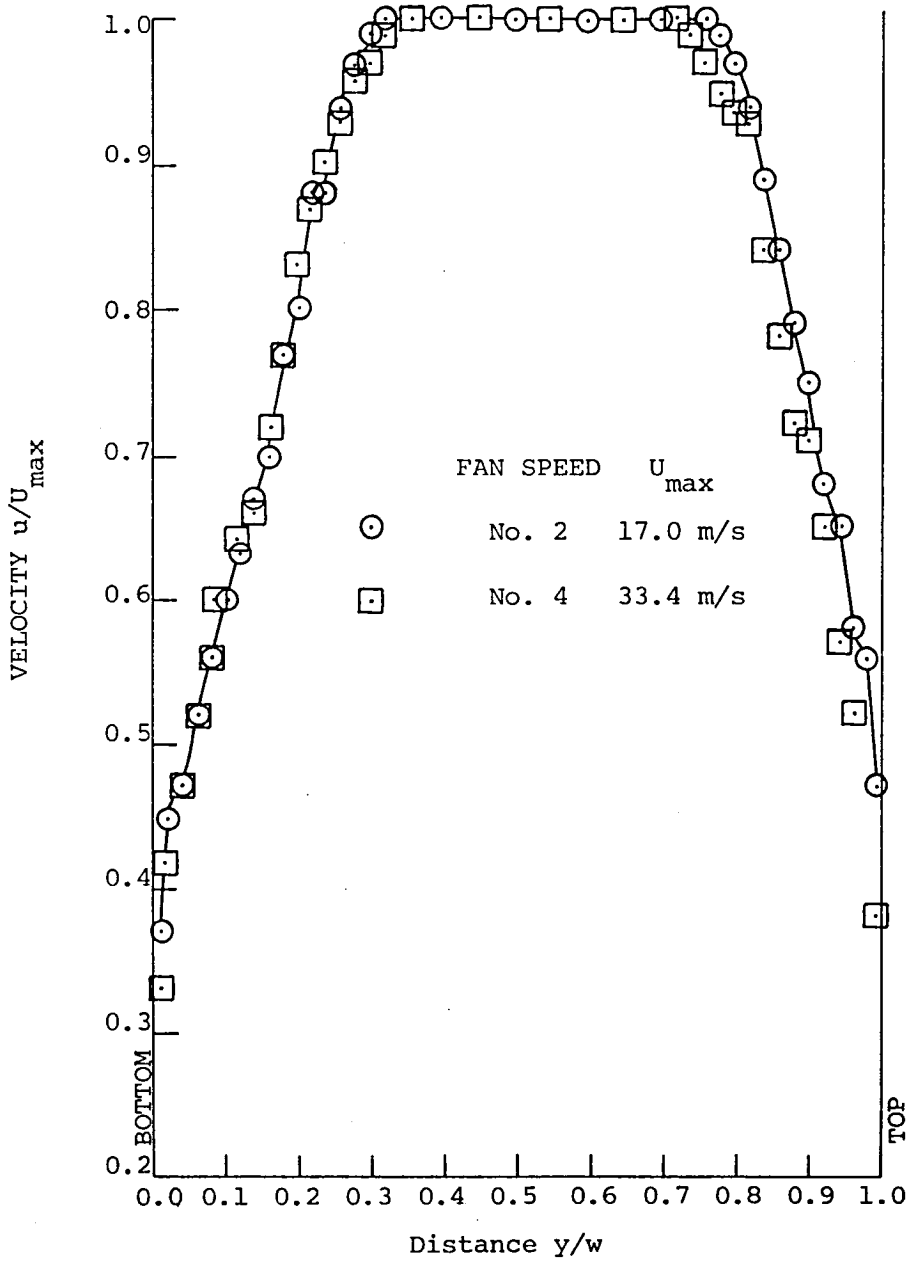

(g) Traverse station 16 (V).

Figure 12. (Concluded).

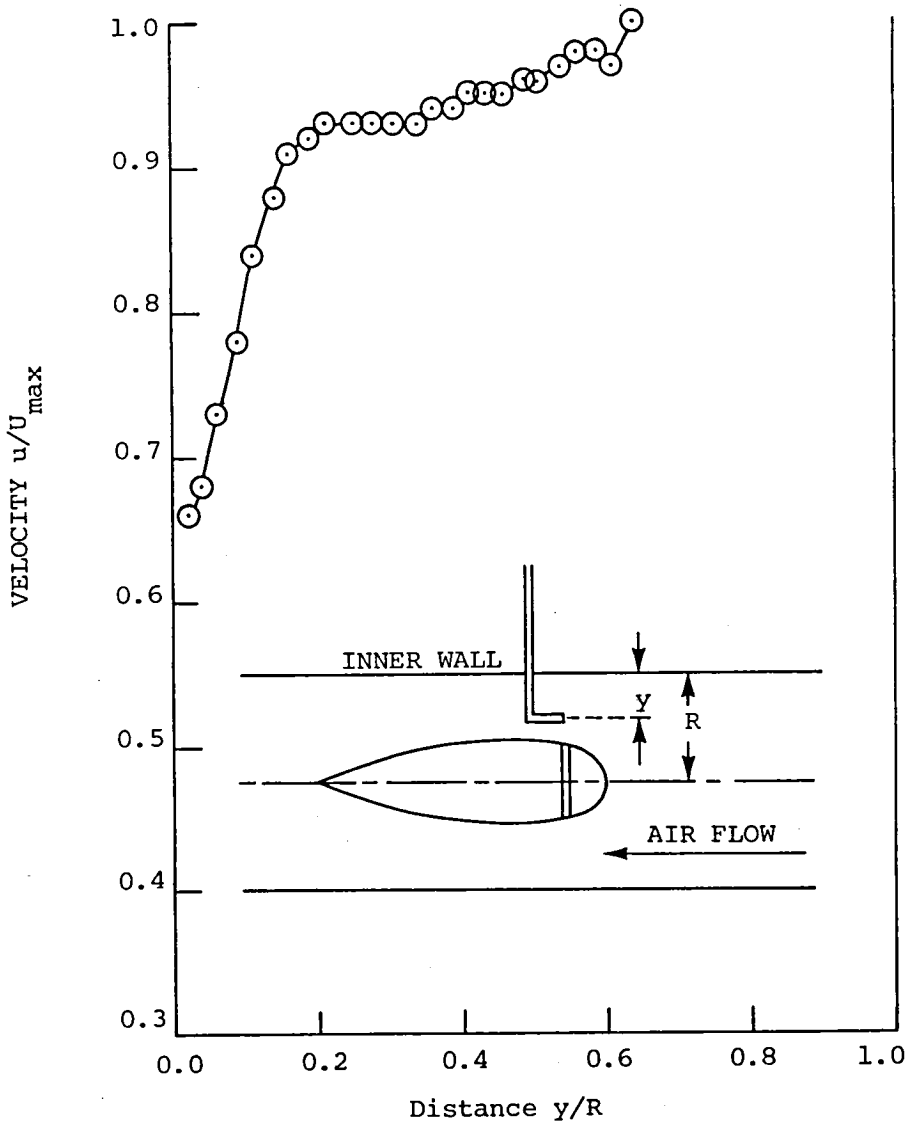

(a) Traverse station 13 (H).

Figure 13. Setup B: velocity distribution across the flow (influence of the nacelle).

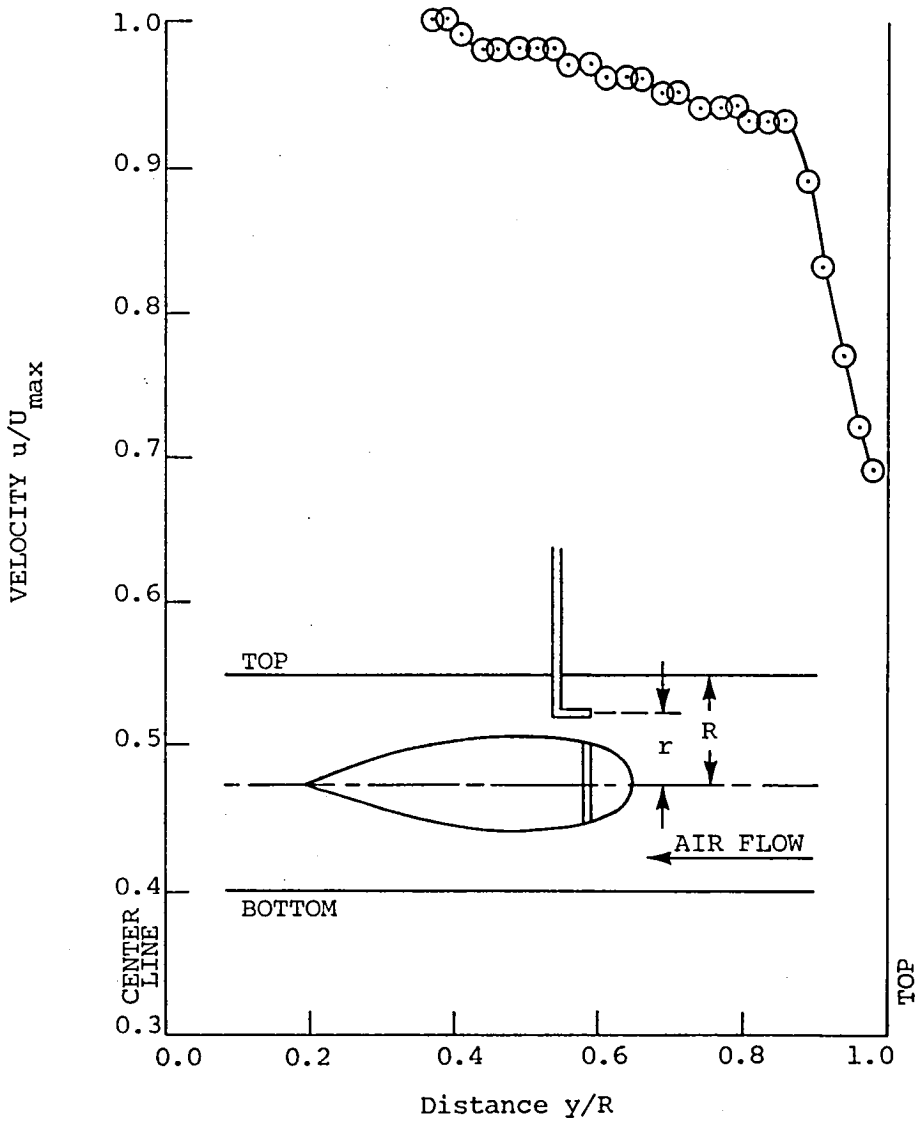

(b) Traverse station 13 (V).

Figure 13. (Continued).

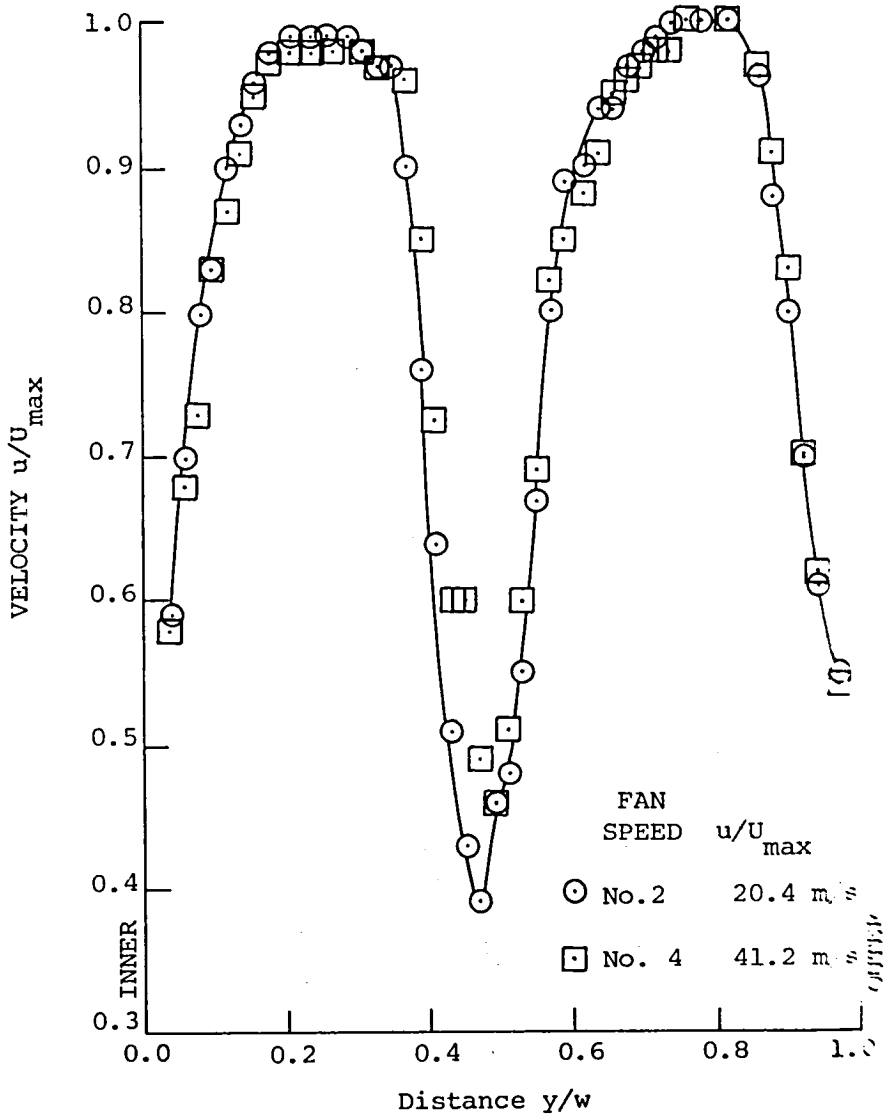

(c) Traverse station 15 (H).

Figure 13. (Continued).

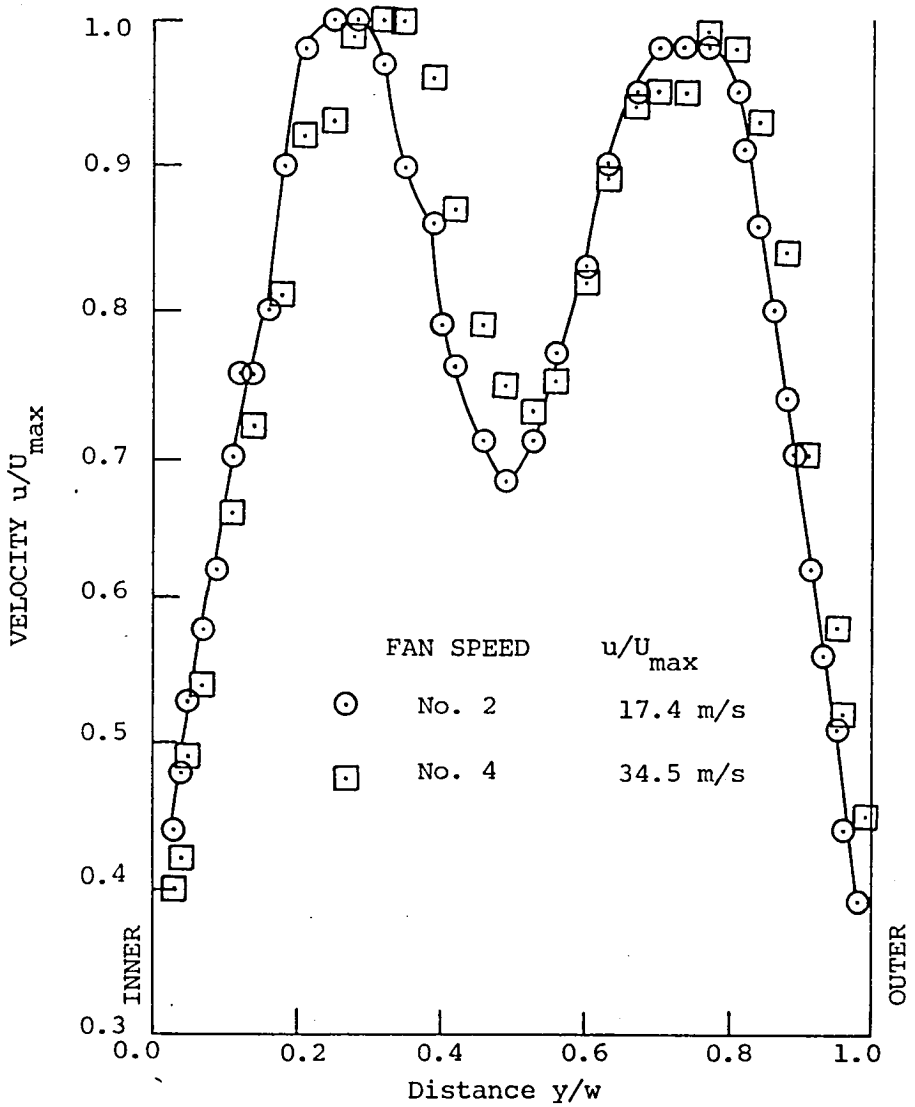

(d) Traverse station 16 (H).

Figure 13. (Concluded).

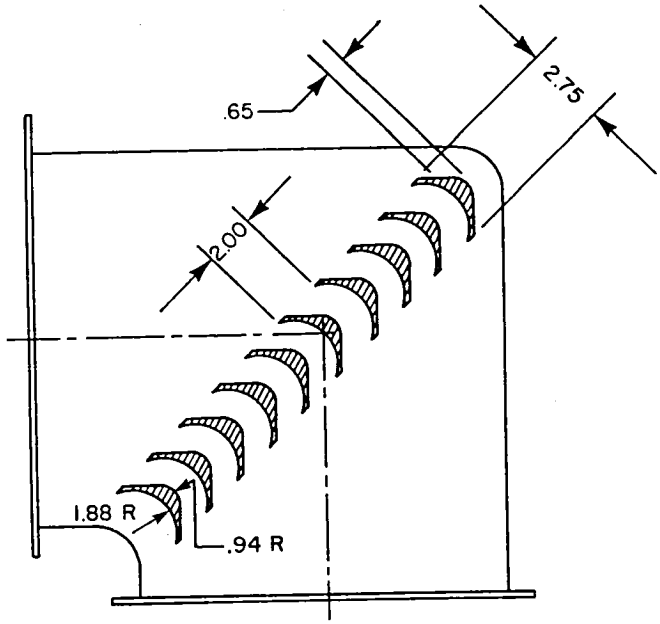

(a) Thick vanes.

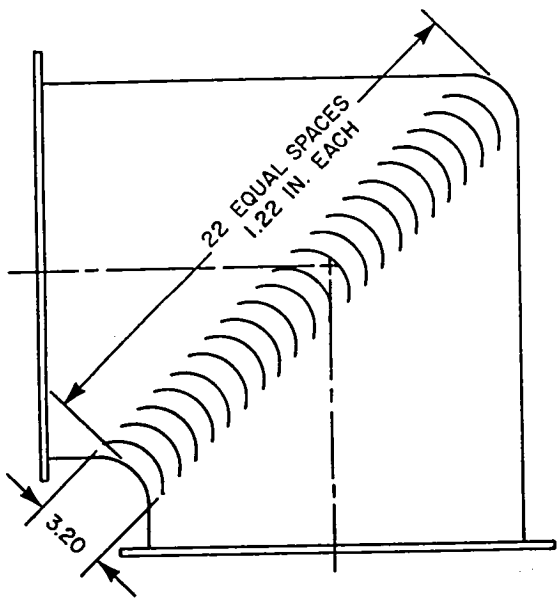

(b) Thin vanes equally spaced.

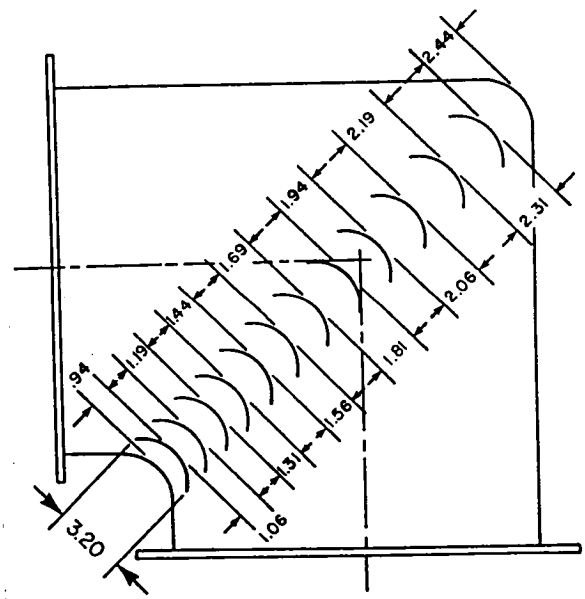

(c) Thin vanes variably spaced.

Figure 14. Design details of various corner vanes employed in the tests. (Dimensions are given in inches; i in. = 2.54 cm).

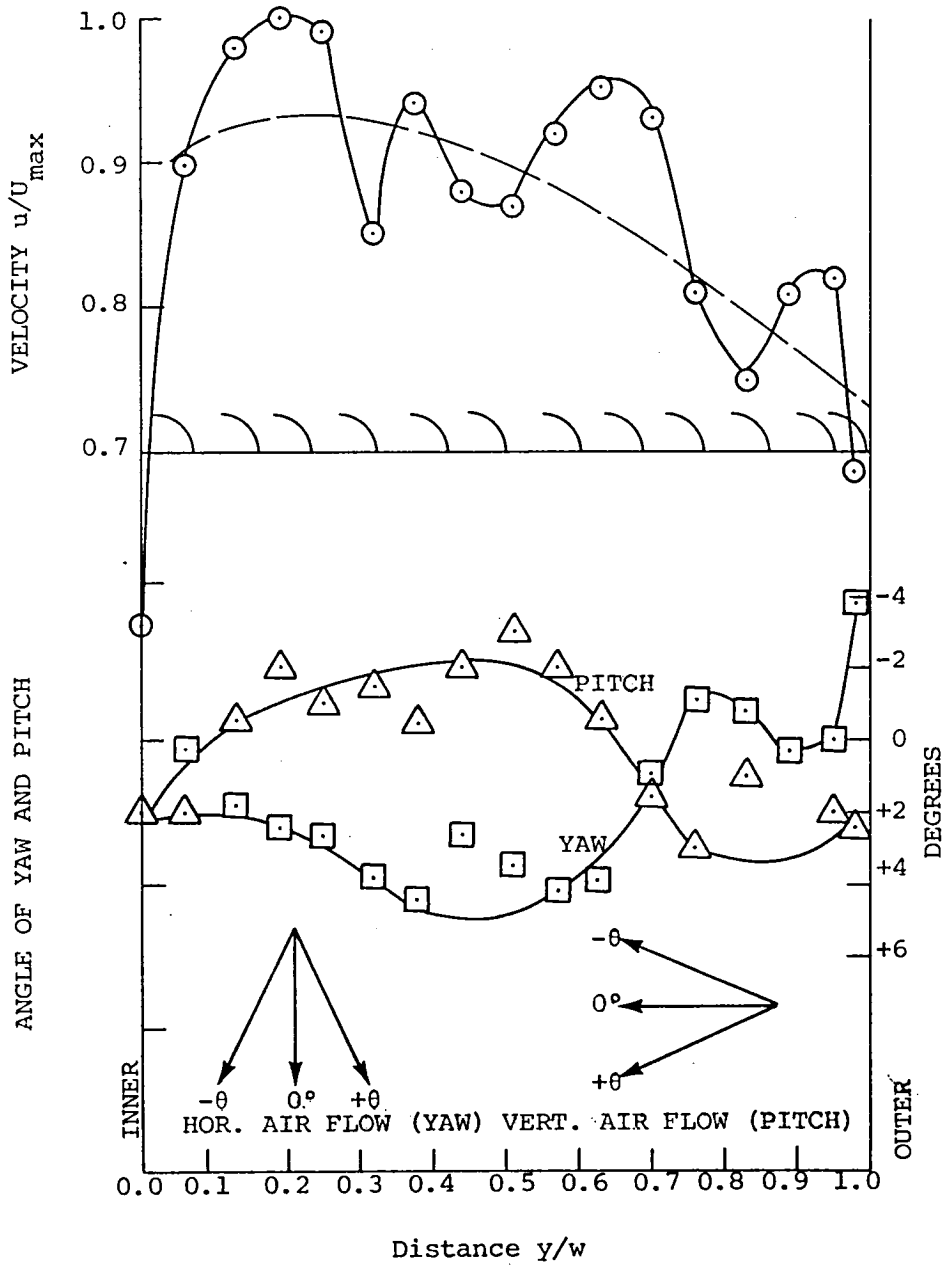

(a) Traverse (H) at centerline; Reynolds number $R_e = 0.9 \times 10^5$.

Figure 15. Setup C: velocity distribution at Traverse 11—thick vanes equally spaced.

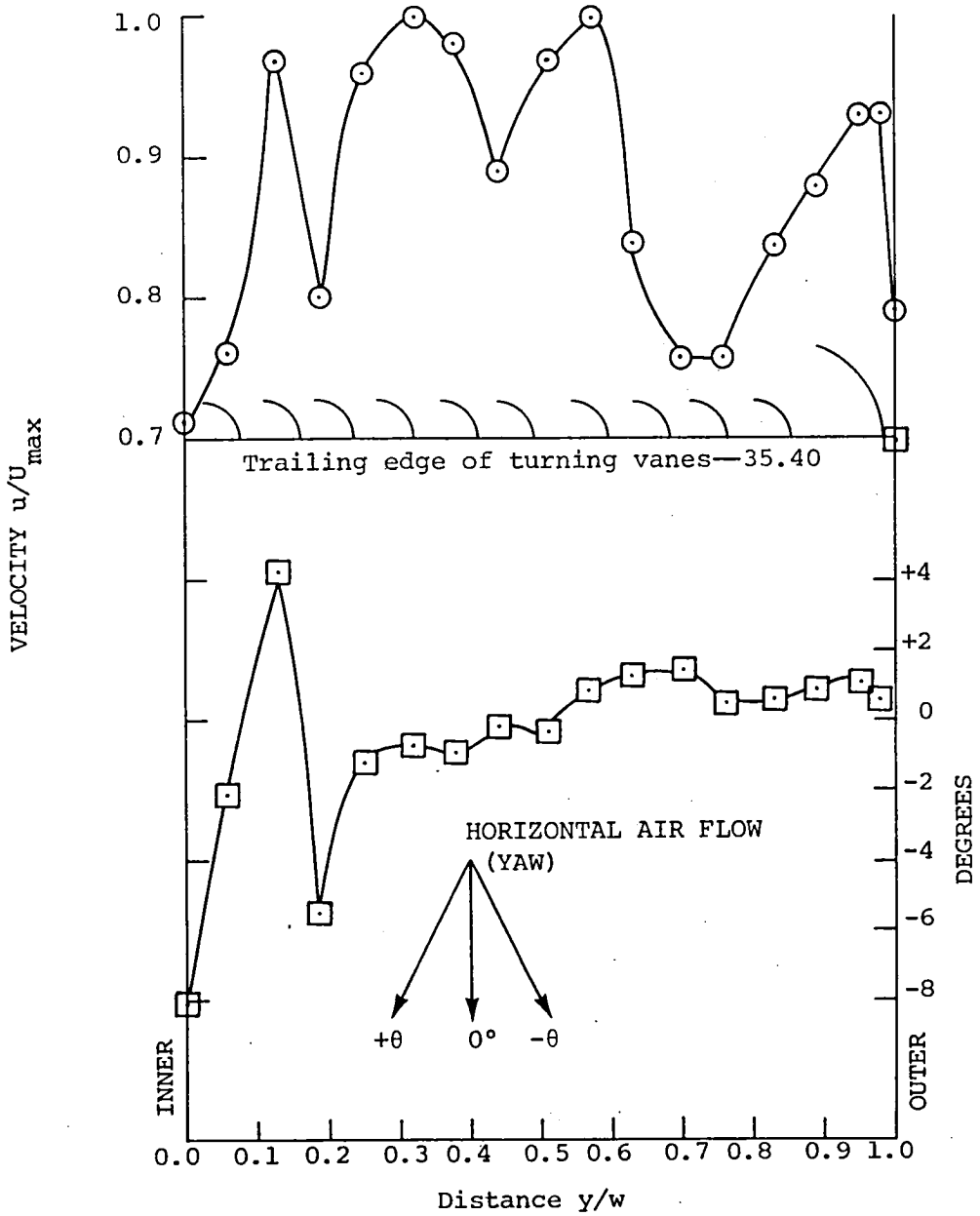

(b) Traverse (H) at centerline; large radius vane at outer corner; $R_e = 0.9 \times 10^5$.

Figure 15. (Continued).

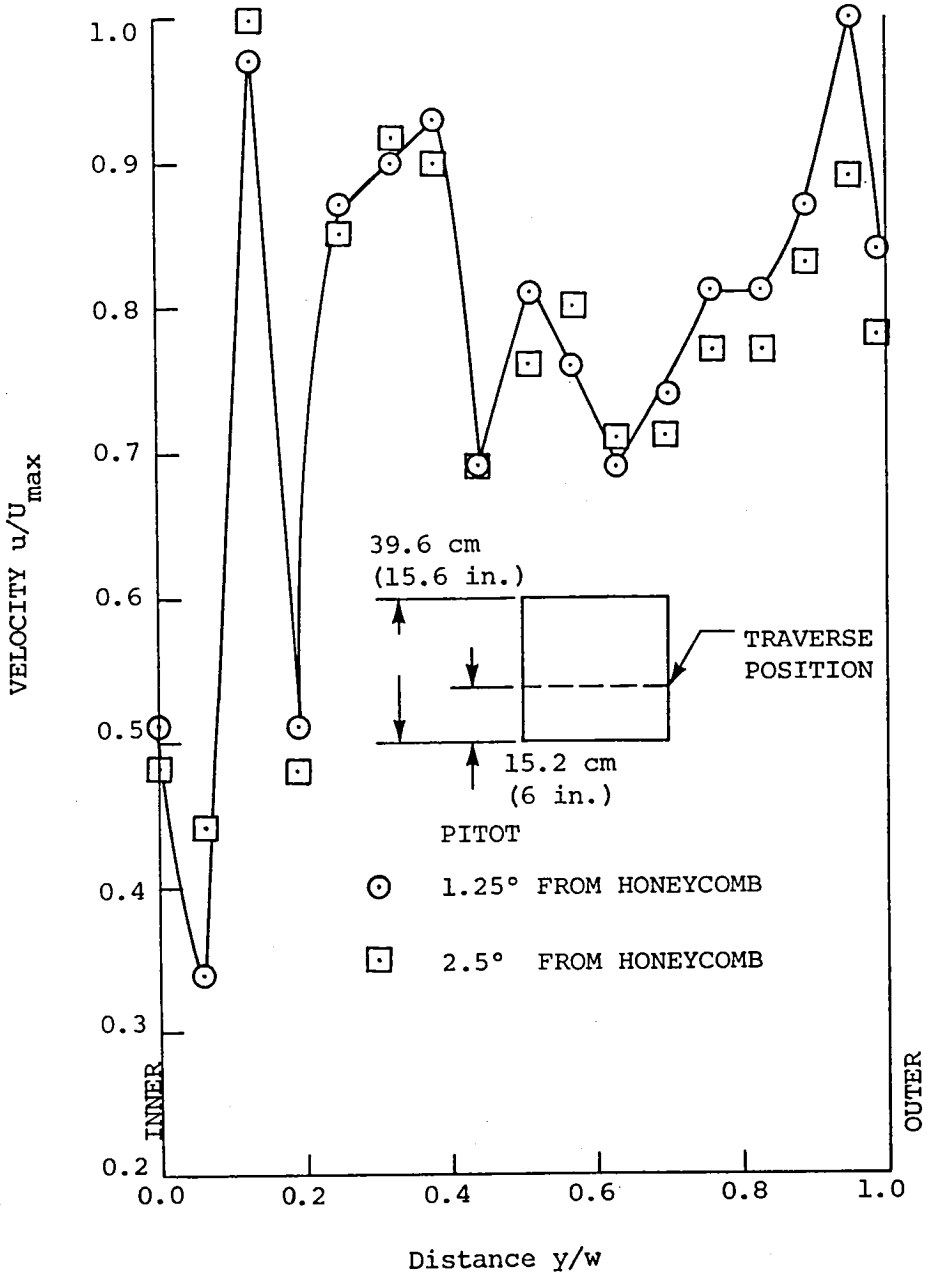

(c) Traverse (H), 15.2 cm (6 in.) from bottom; $R_e = 0.9 \times 10^5$.

Figure 15. (Continued).

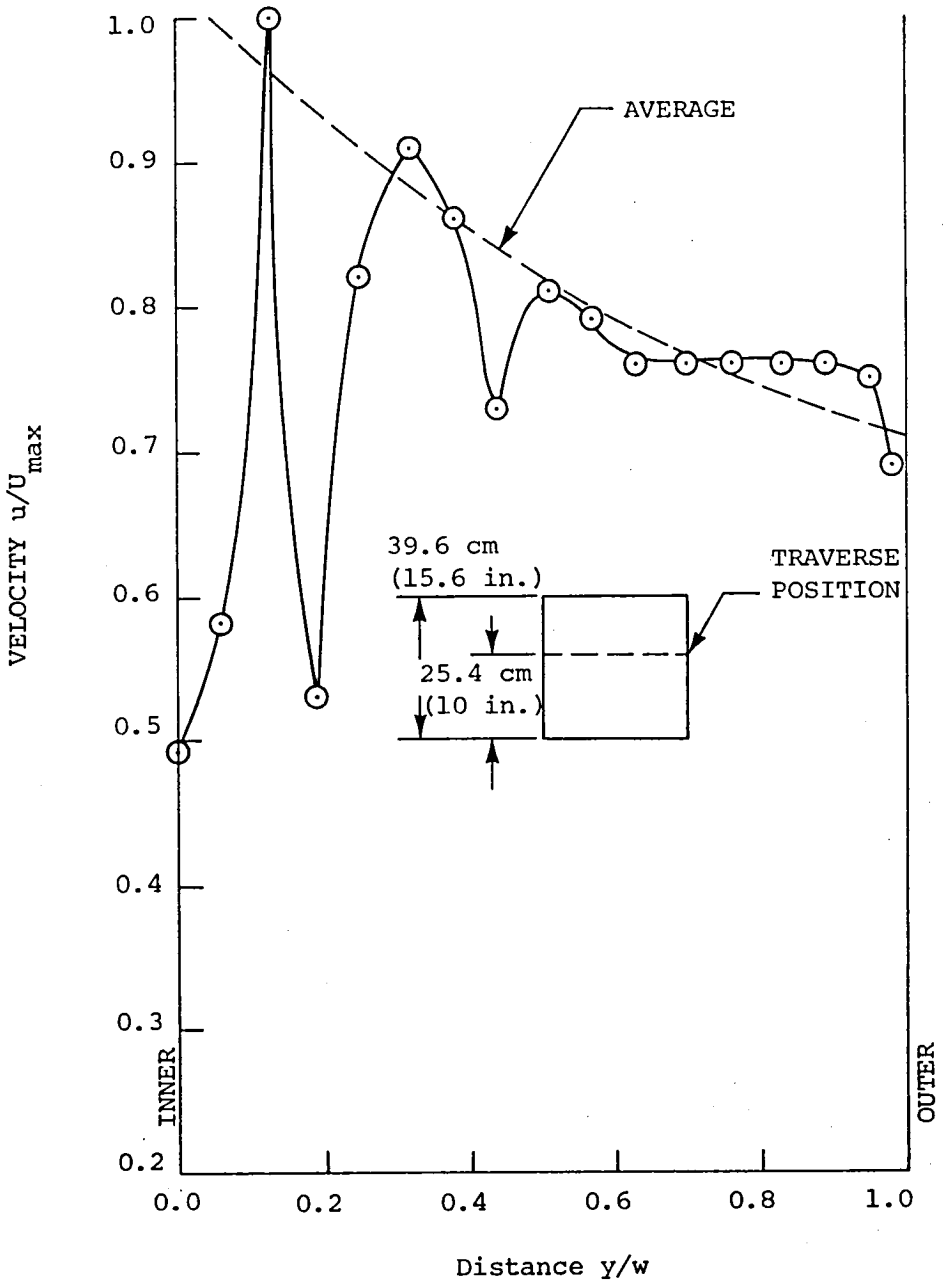

(d) Traverse (H), 25.4 cm (10 in.) from bottom; $R_e = 0.9 \times 10^5$.

Figure 15. (Continued).

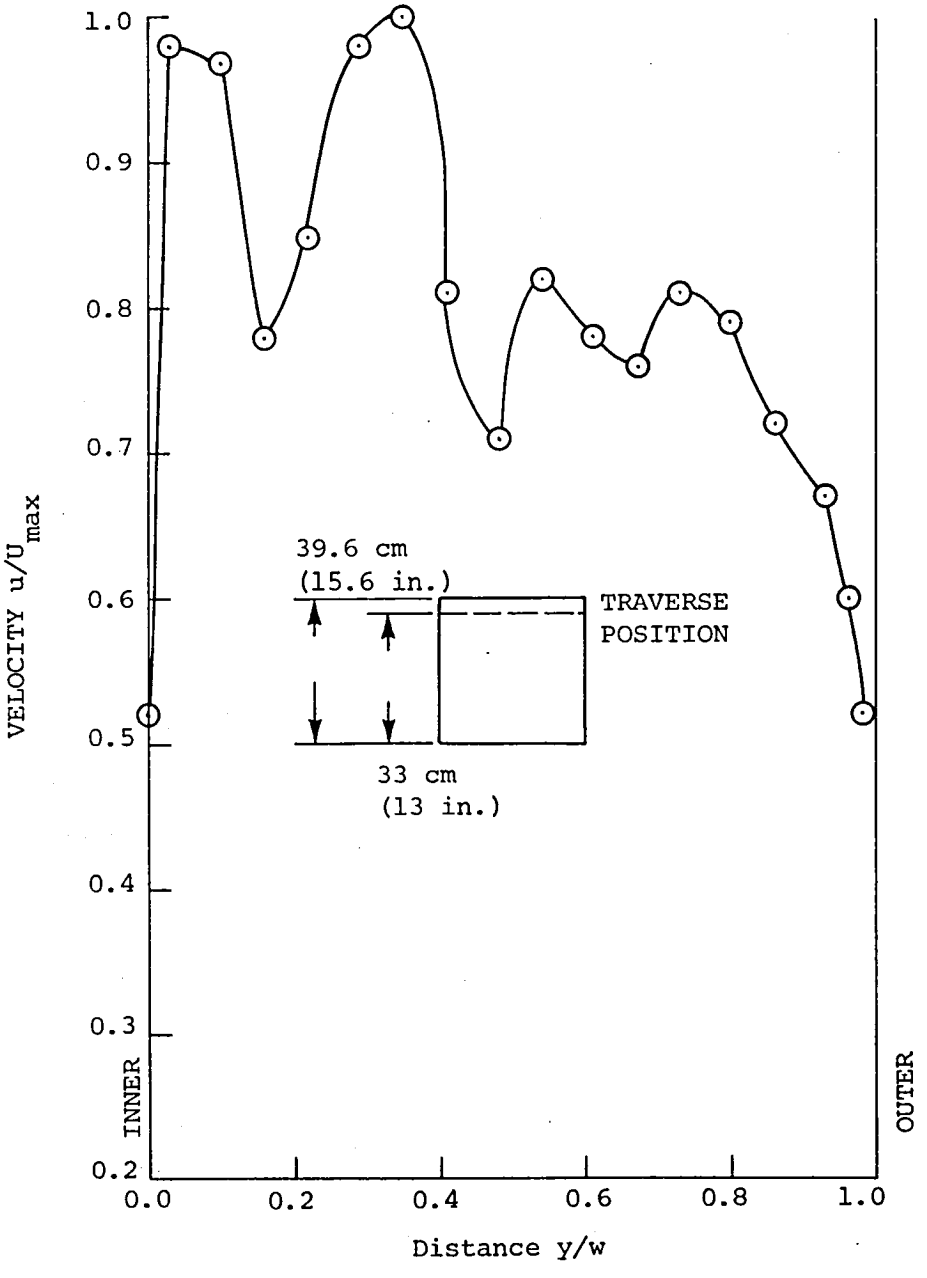

(e) Traverse (H), 33 cm (13 in.) from bottom; $R_e = 0.9 \times 10^5$.

Figure 15. (Continued).

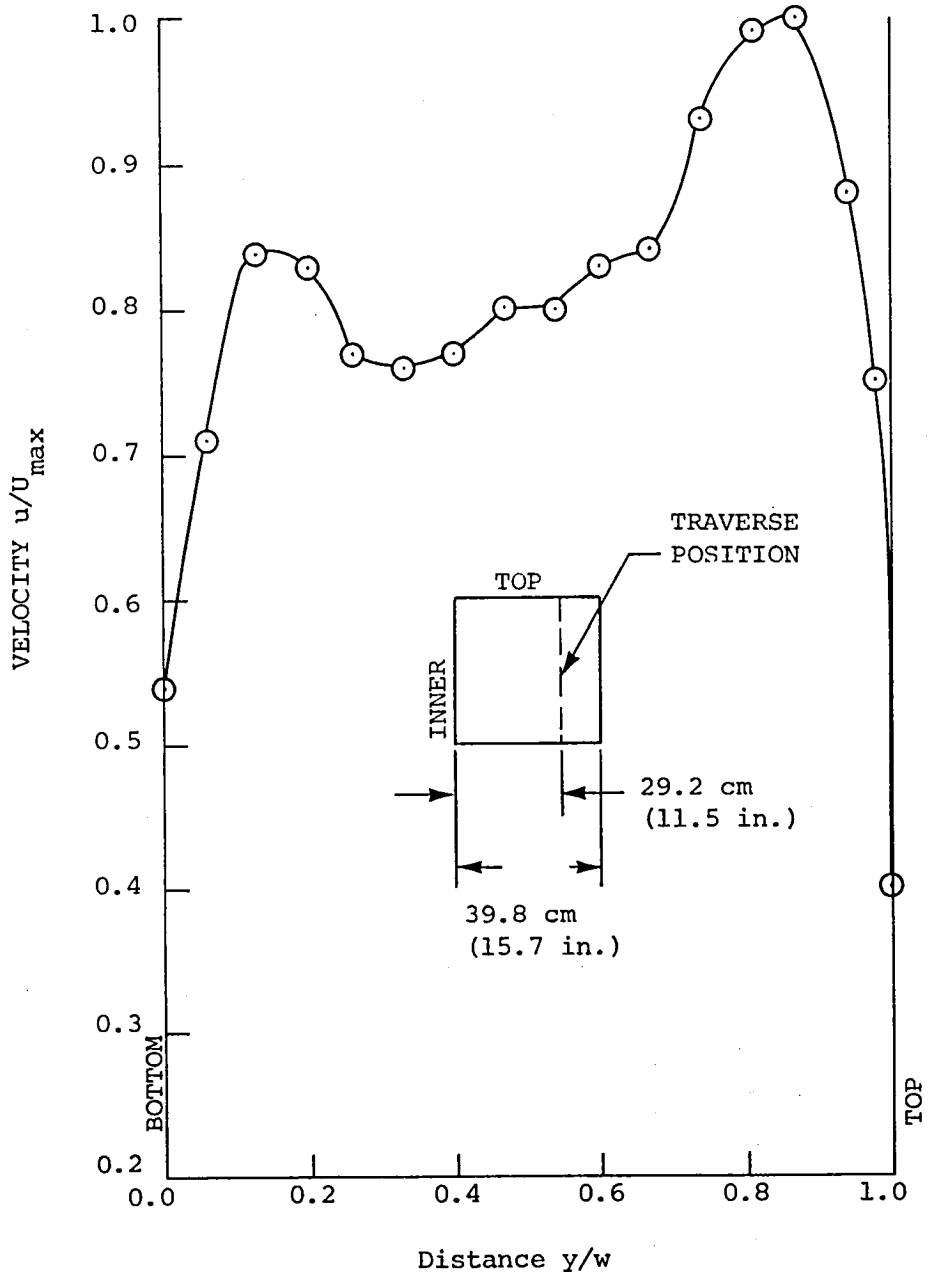

(f) Traverse (V), 29.2 cm (11.5 in.) from inner wall; $R_e = 0.9 \times 10^5$.

Figure 15. (Concluded).

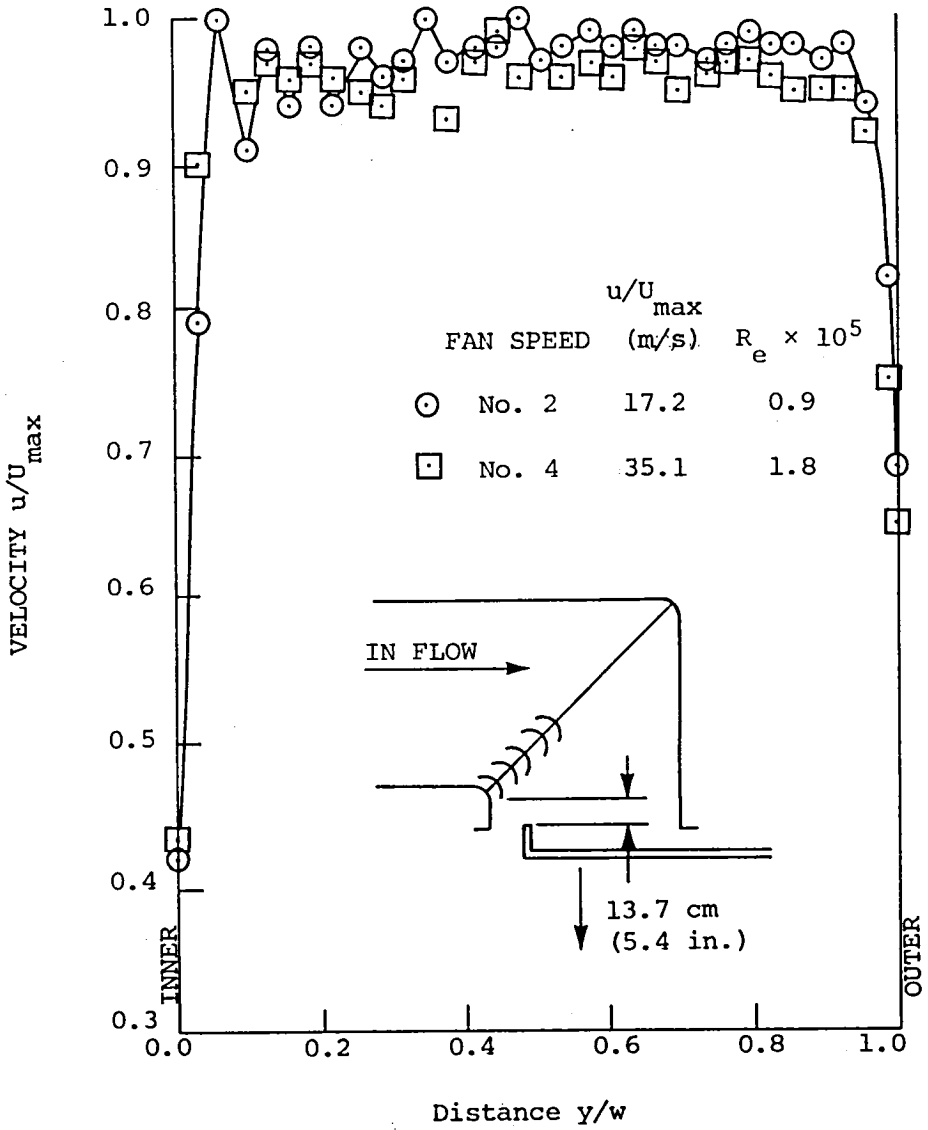

(a) Traverse (H) at centerline.

Figure 16. Setup C: velocity distribution at Traverse 11—thin vanes equally spaced.

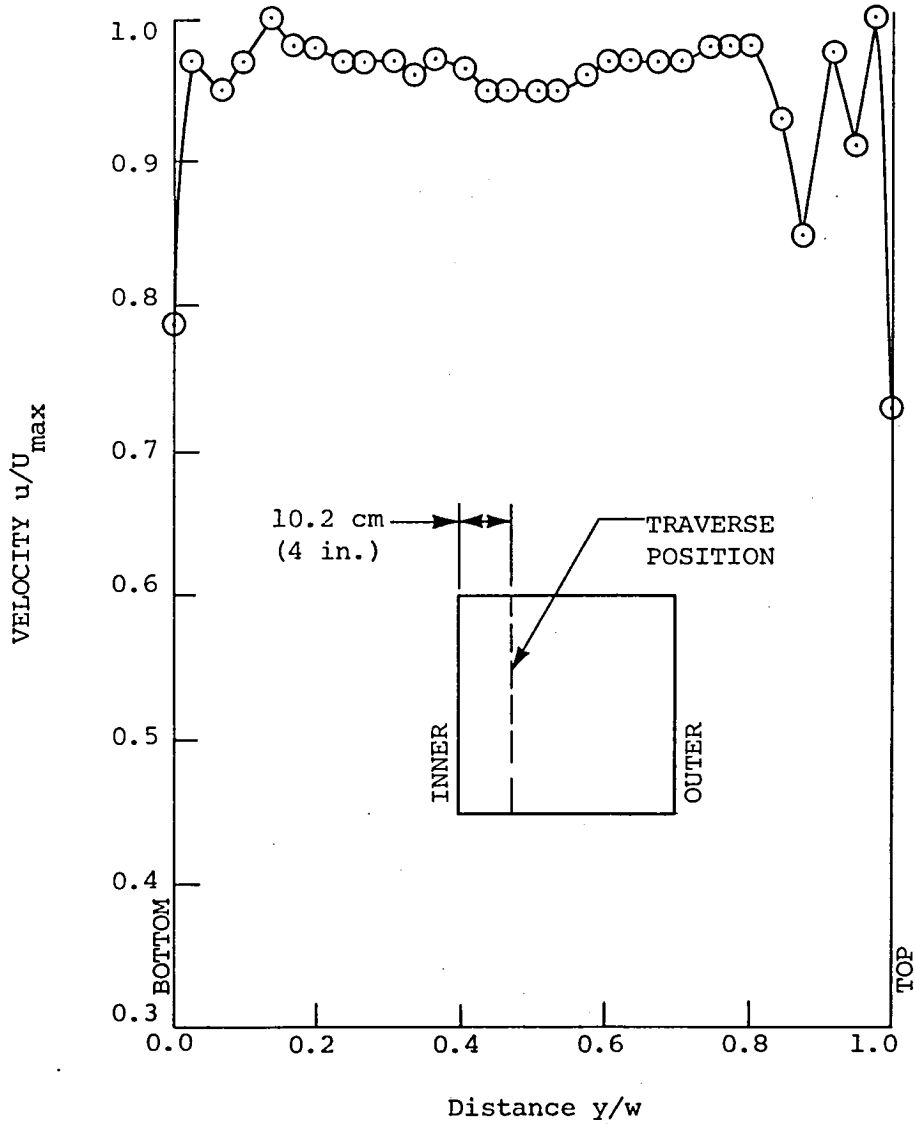

(b) Traverse (V), 10.2 cm (4 in.) from inner wall; $R_e = 0.9 \times 10^5$.

Figure 16. (Continued).

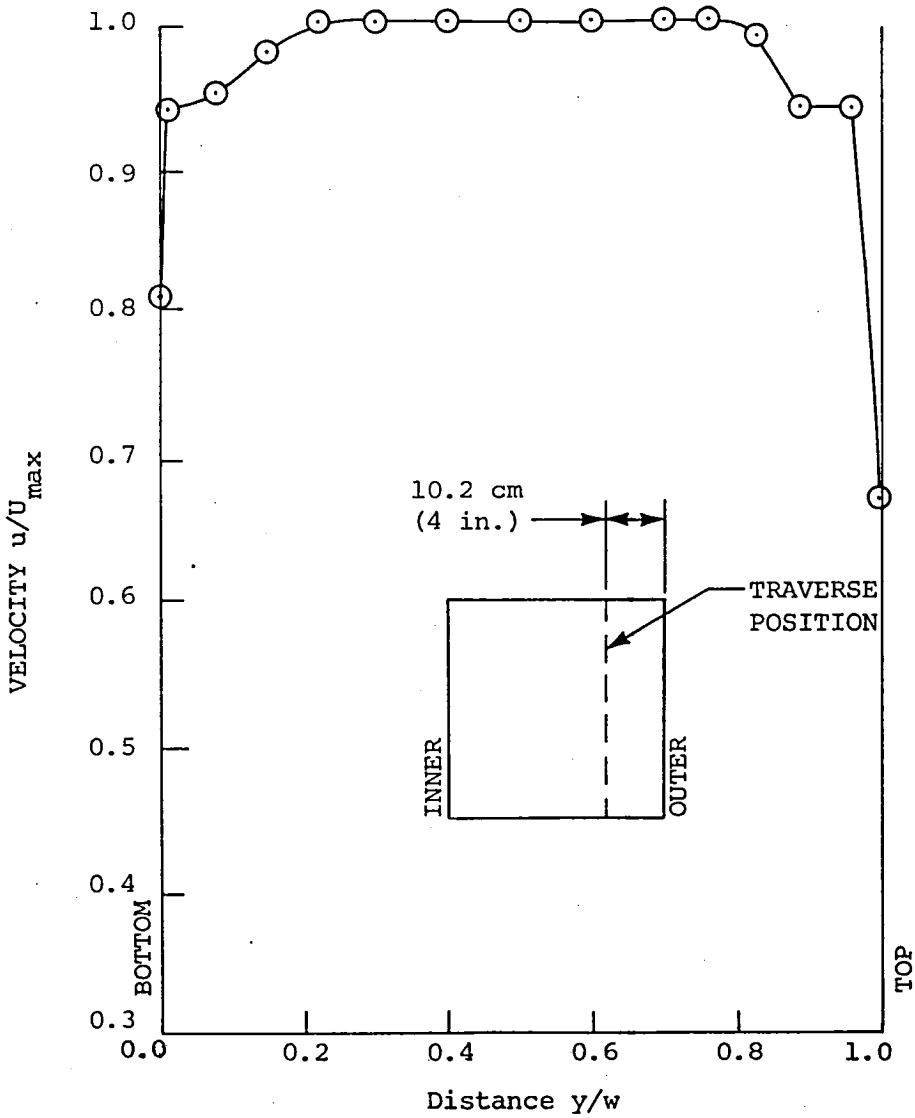

(c) Traverse (V), 10.2 cm (4 in.) from outer wall; $R_e = 0.9 \times 10^5$.

Figure 16. (Concluded).

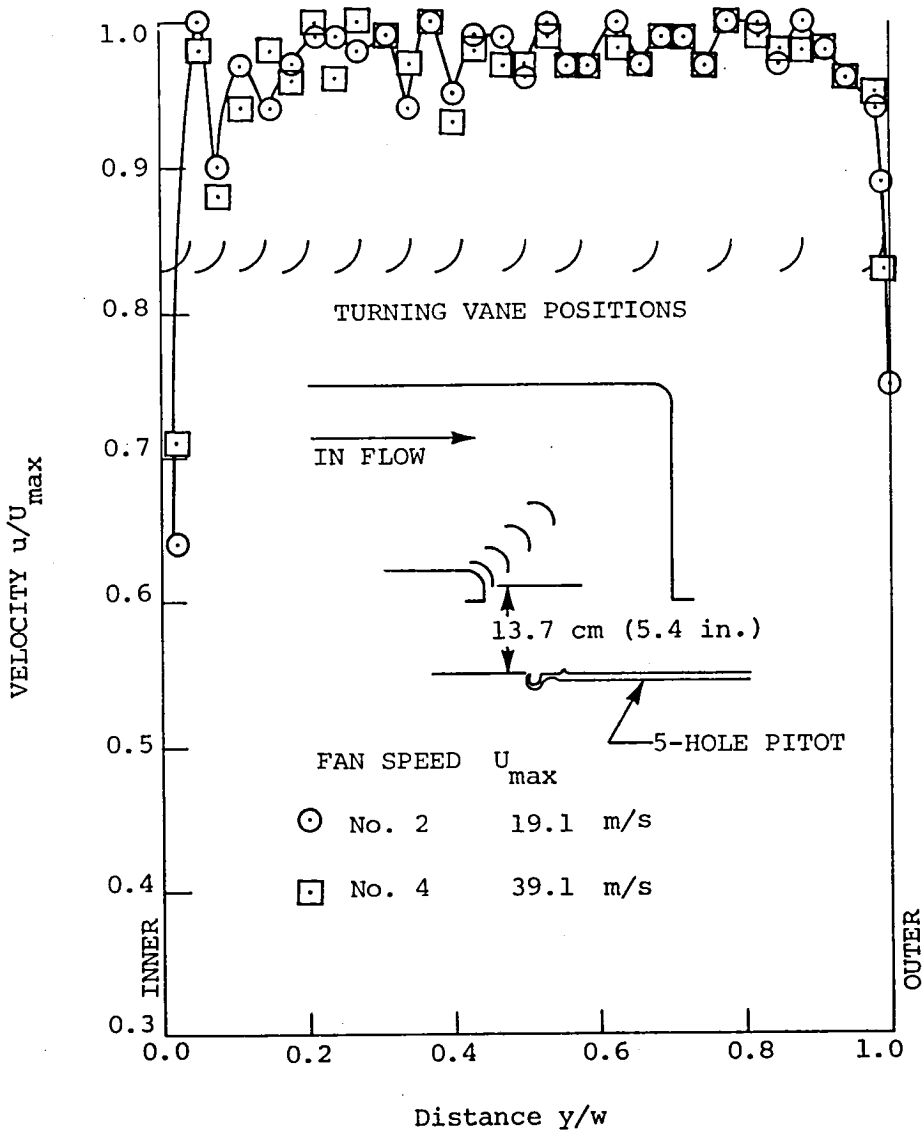

(a) Traverse (H) at centerline distance 13.7 cm (5.4 in.); discharge into free air.

Figure 17. Setup C: velocity distribution at Traverse 11—thin vanes variably spaced; $R_e = 0.9 \times 10^5$.

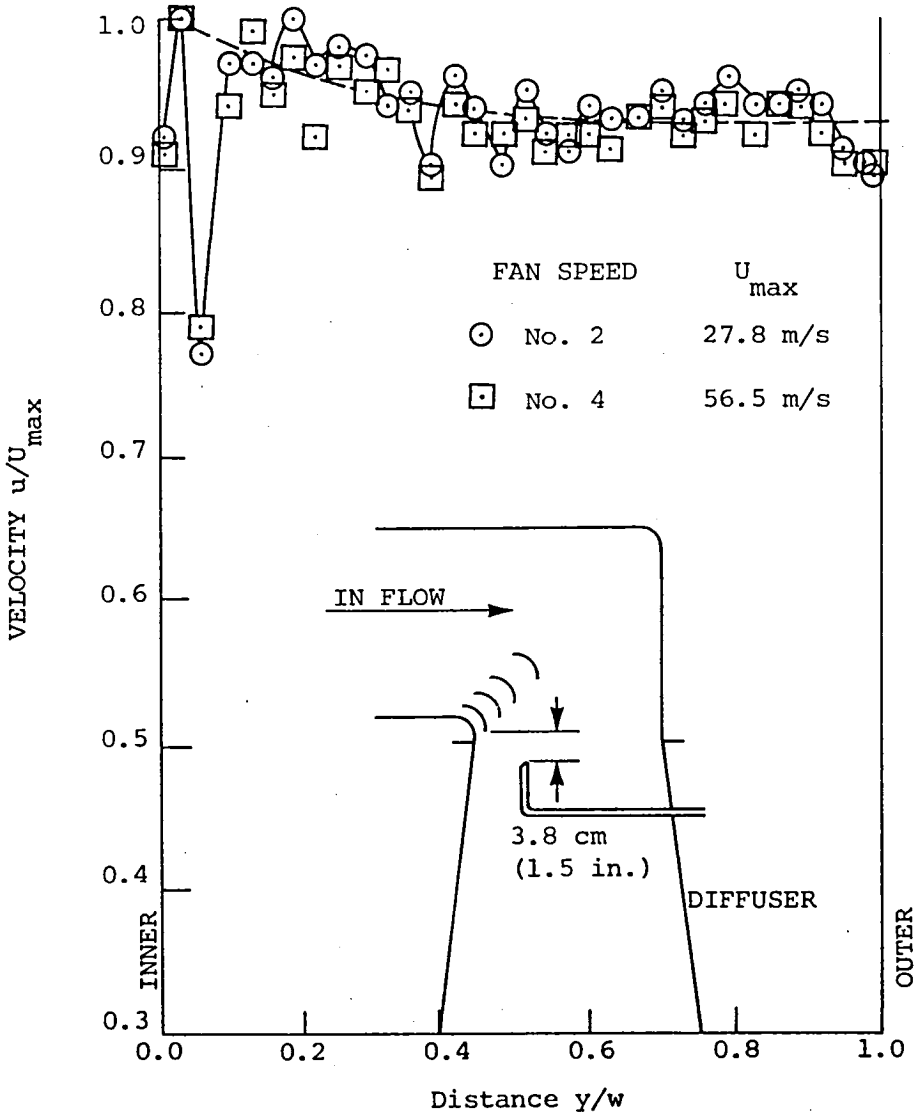

(b) Traverse (H) at centerline distance 3.8 cm (1.5 in.); discharge into a diffuser.

Figure 17. (Continued).

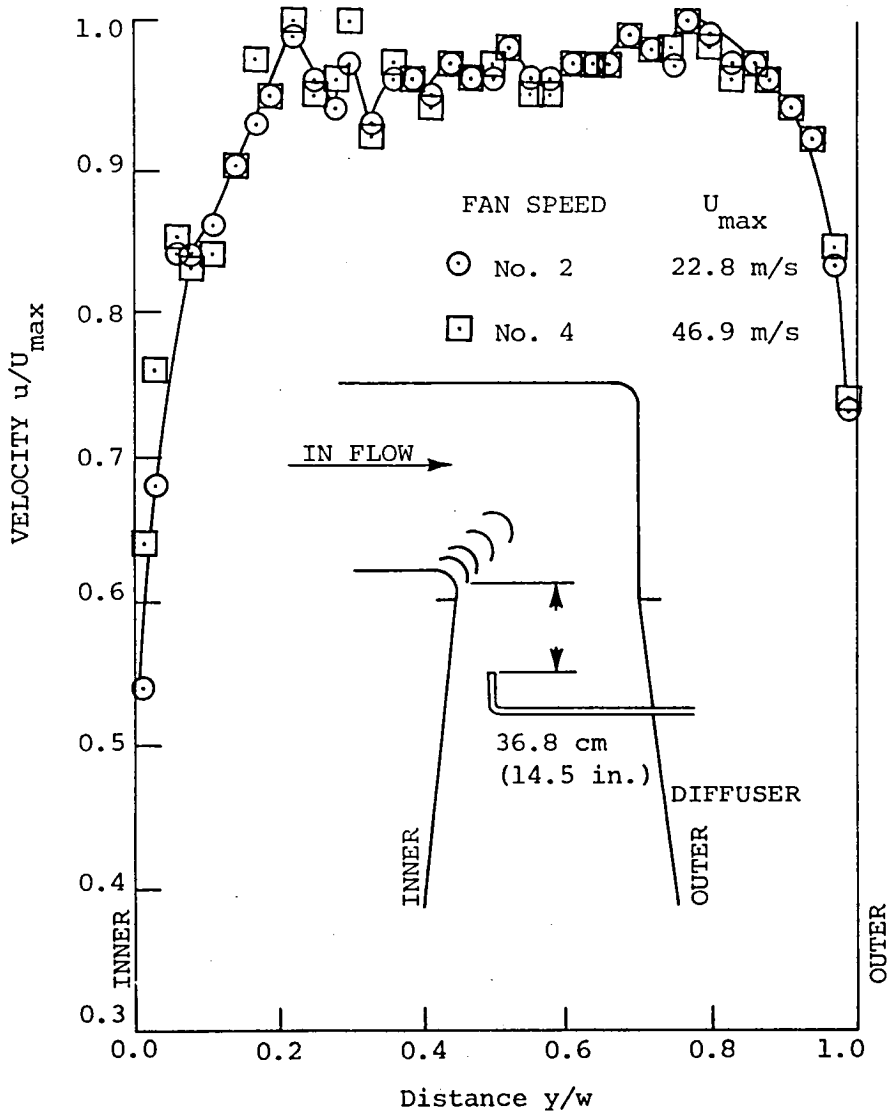

(c) Traverse (H) at centerline distance 36.8 cm (14.5 in.); discharge into a diffuser.

Figure 17. (Concluded).

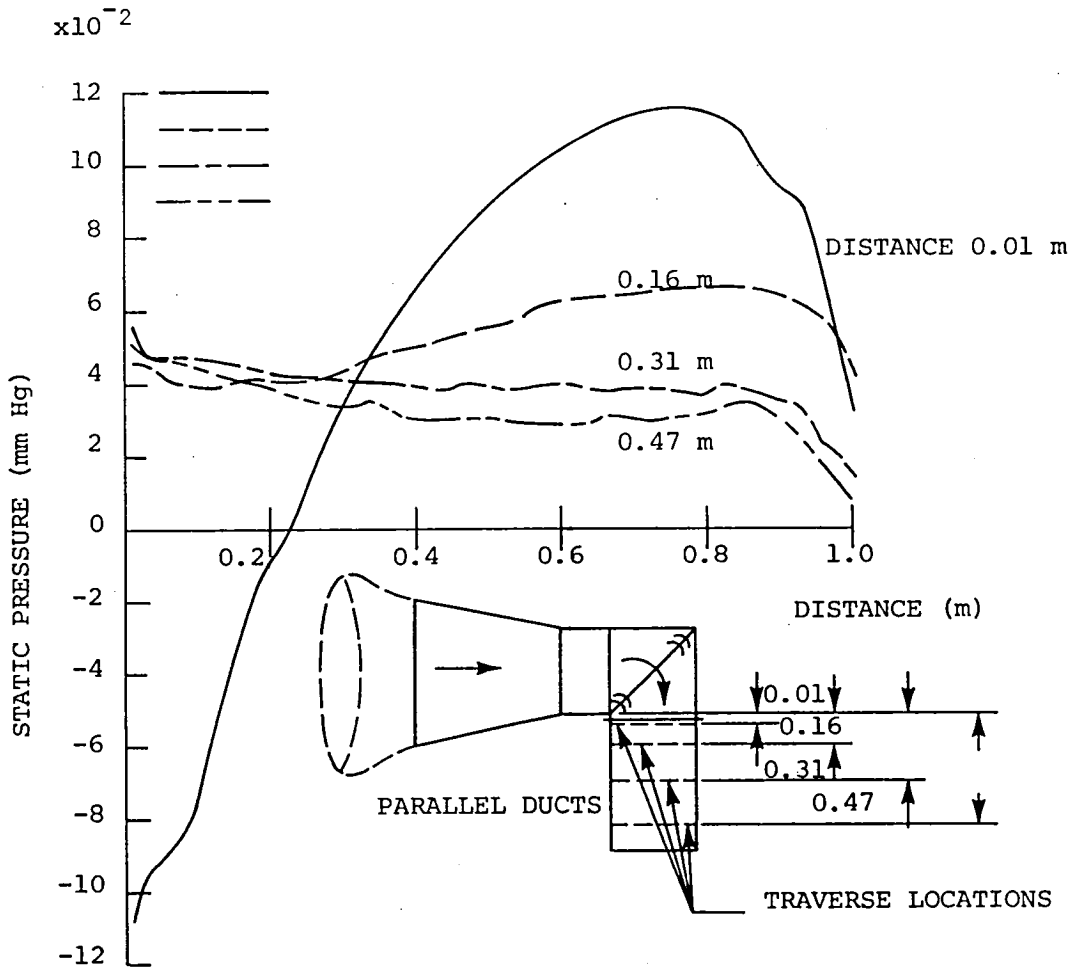

Figure 18. Setup D: pressure distribution across the flow downstream from a corner provided with equally spaced thin vanes.

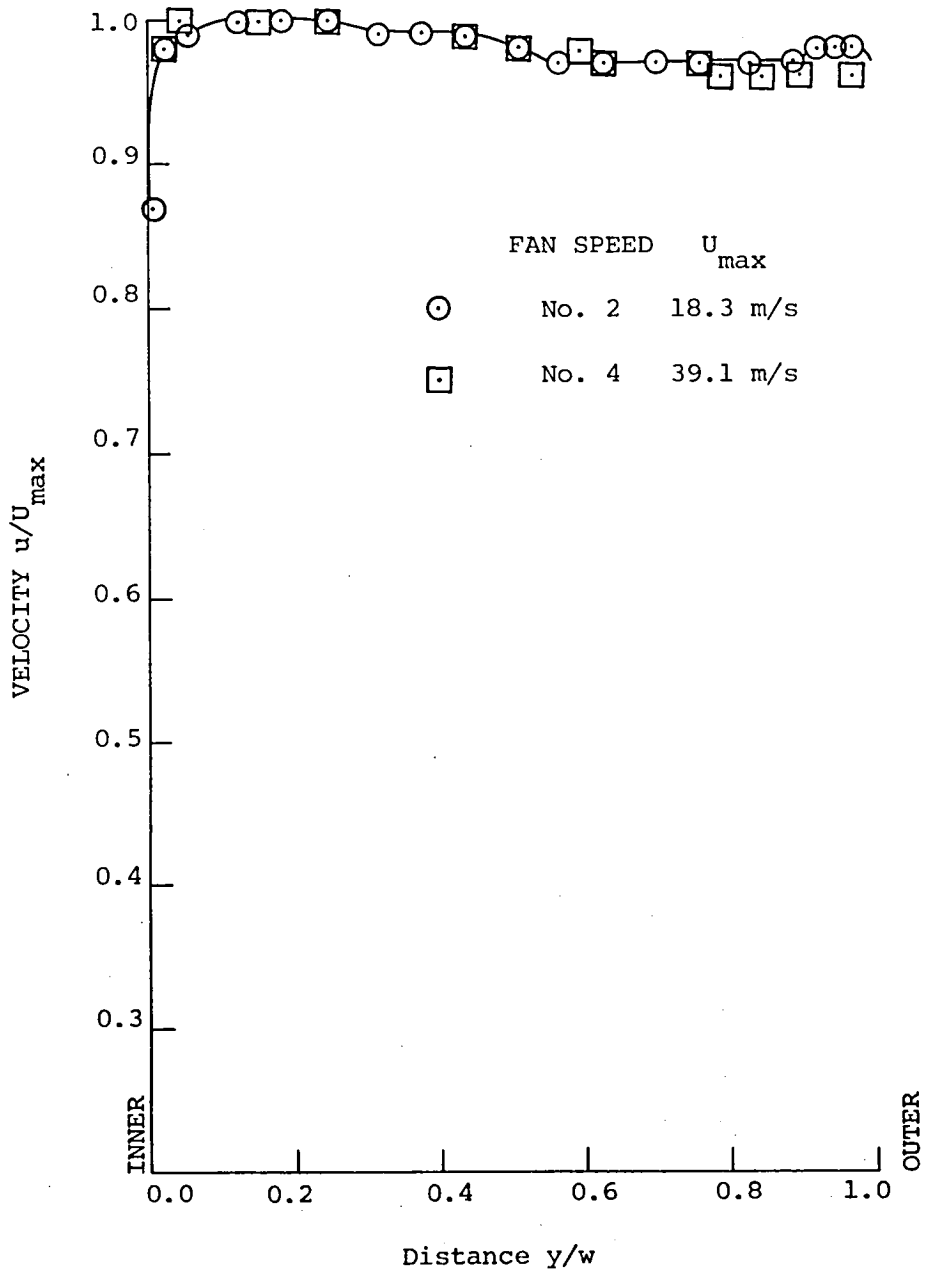

(a) Flow upstream from the corner at T.S. 10.

Figure 19. Setup E: effects on the flow in the third and fourth diffusers caused by thick corner vanes.

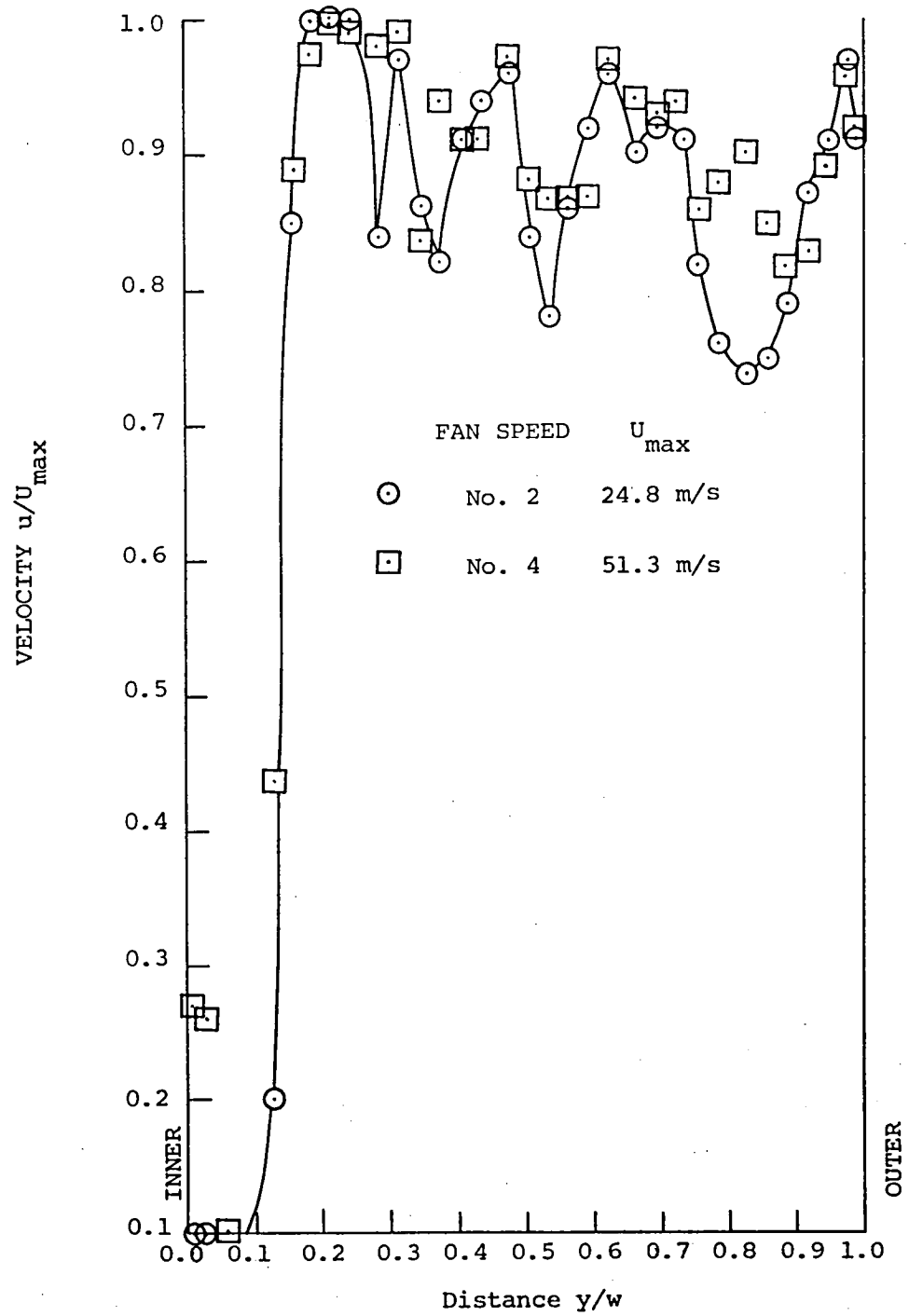

(b) Velocity distribution at T.S. 11 (H).

Figure 19. (Continued).

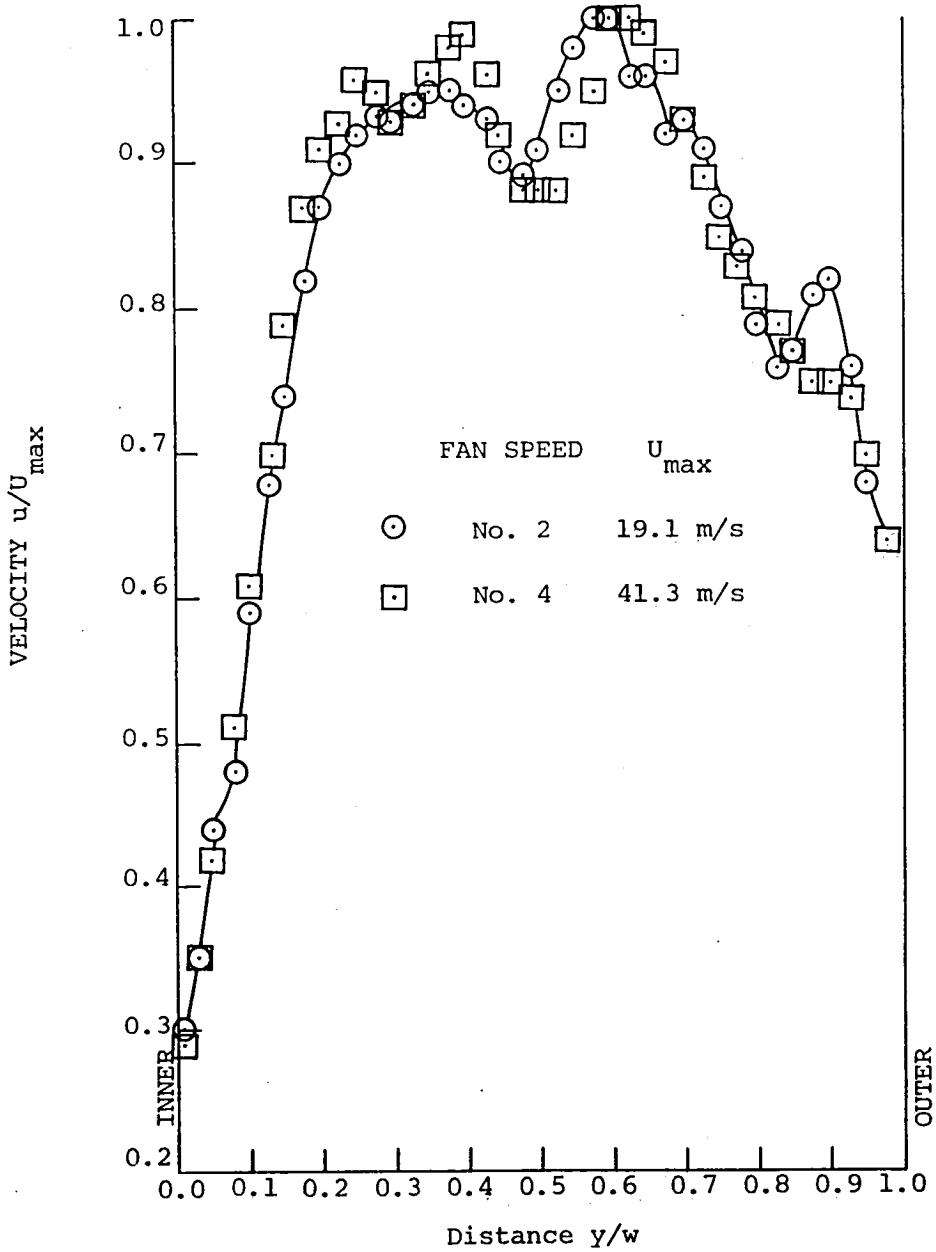

(c) Velocity distribution at T.S. 13(H).

Figure 19. (Continued).

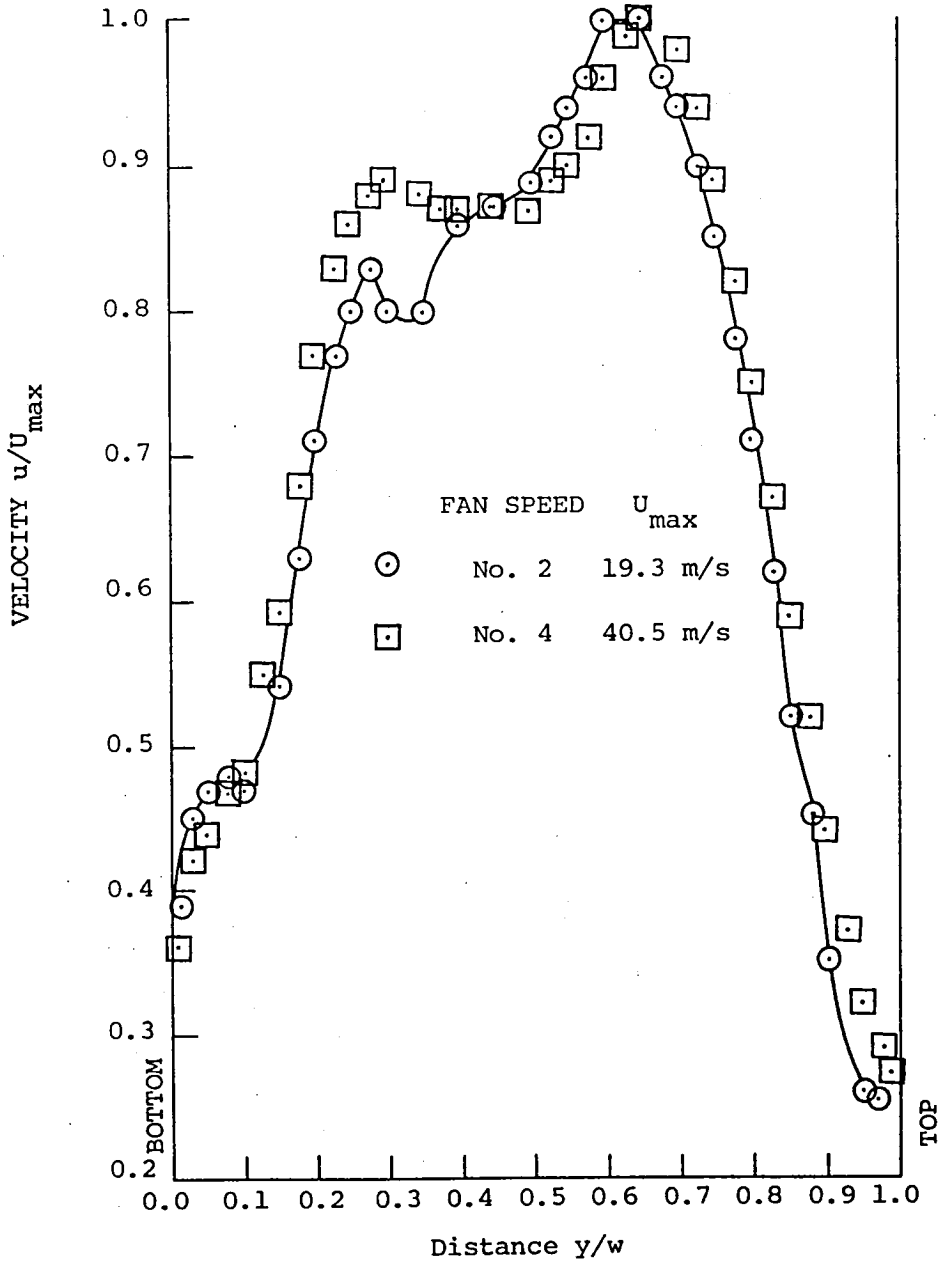

(d) Velocity distribution at T.S. 13(V).

Figure 19. (Continued).

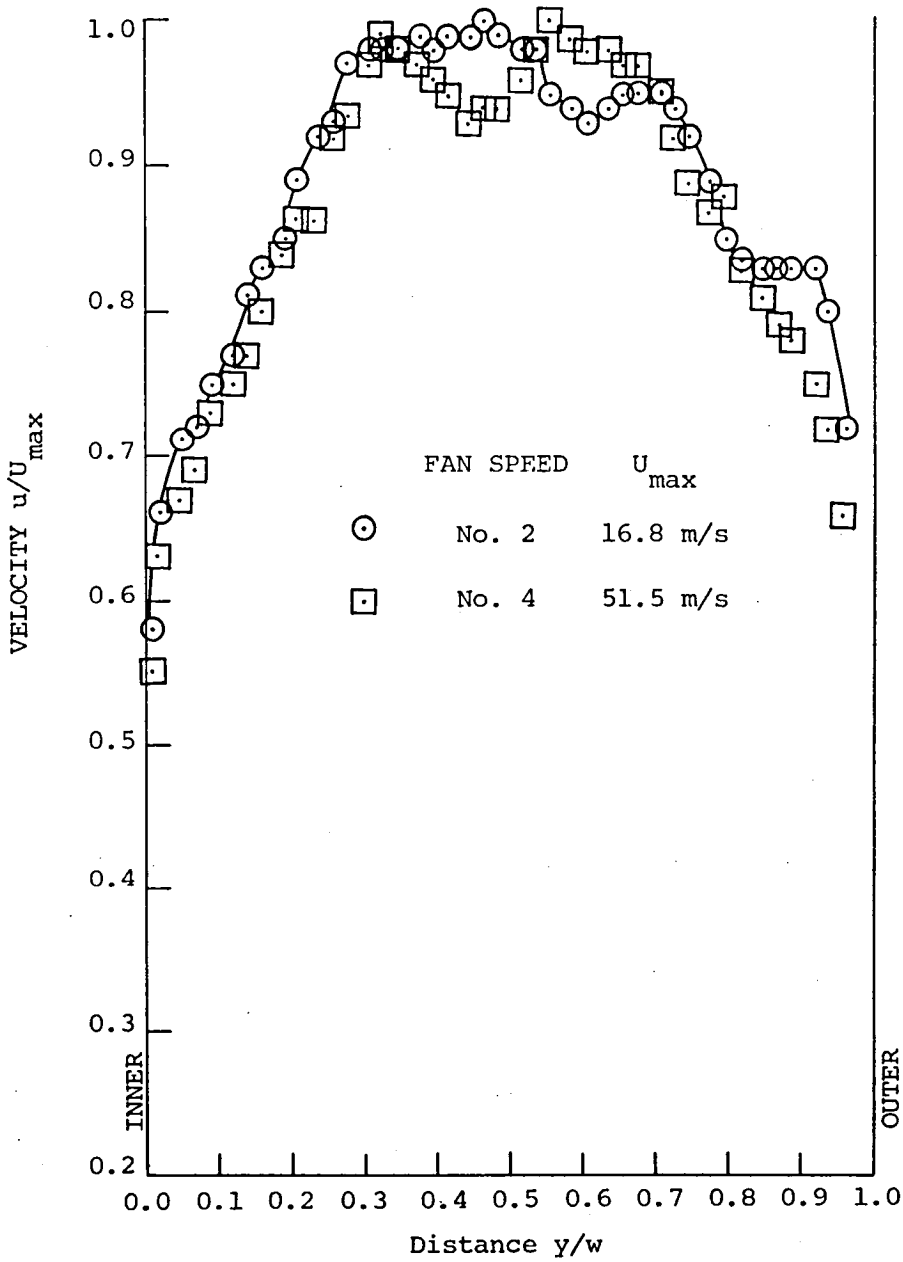

(e) Velocity distribution at T.S. 14(H).

Figure 19. (Continued)

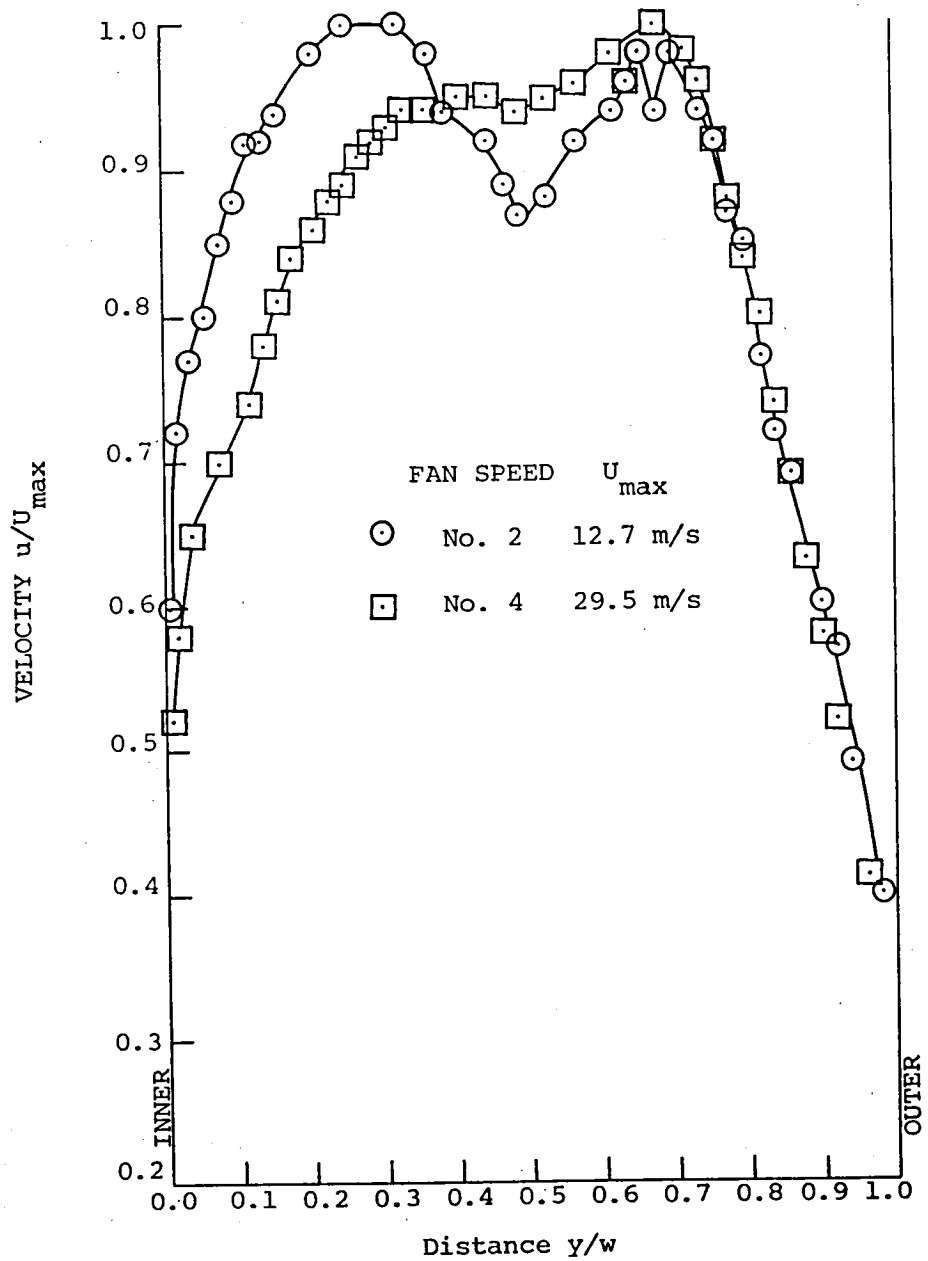

(f) Velocity distribution at T.S. 15(H).

Figure 19. (Continued).

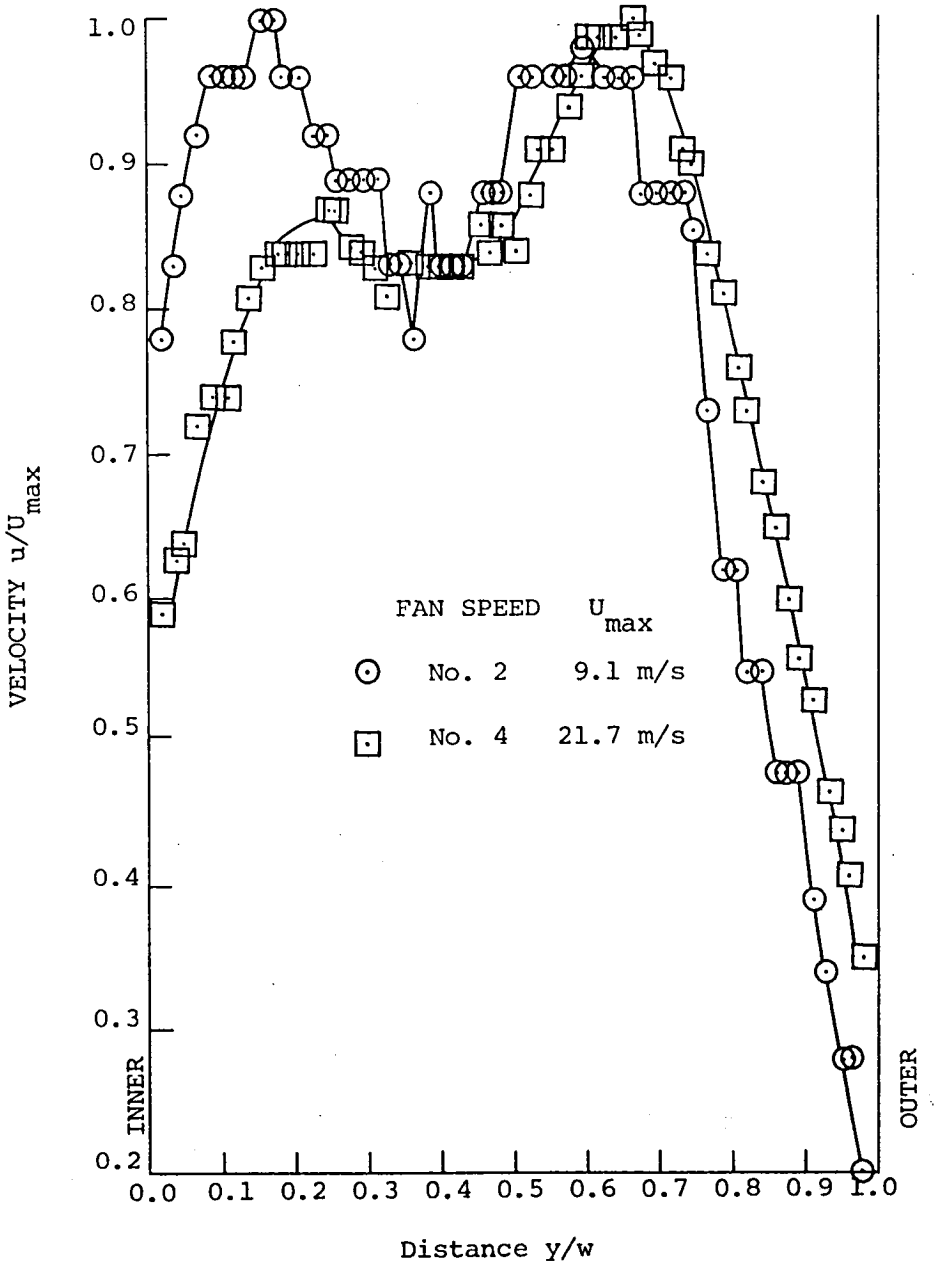

(g) Velocity distribution at T.S. 16(H).

Figure 19. (Concluded).

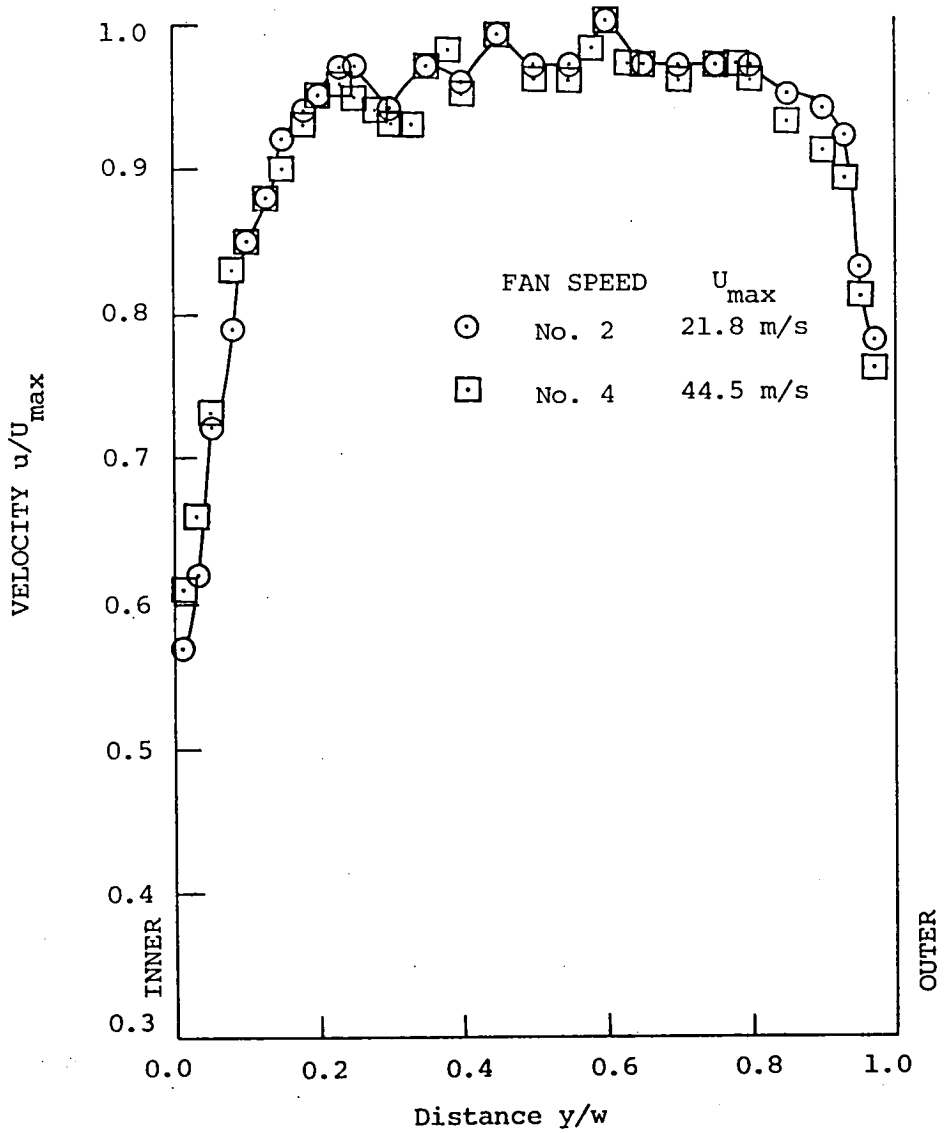

(a) Velocity distribution at T.S. 13(H).

Figure 20. Setup E: effects on the flow in the third and fourth diffusers caused by thin corner vanes equally spaced.

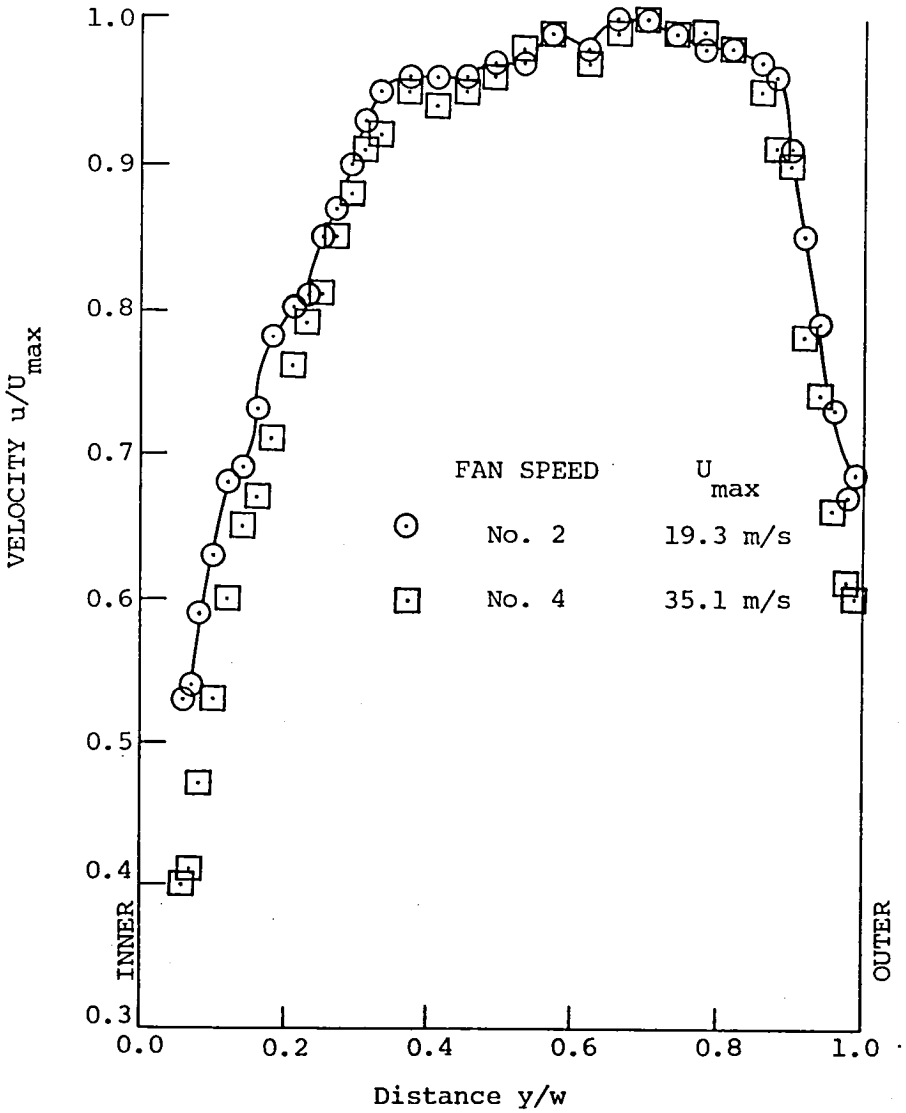

(b) Velocity distribution at T.S. 15(H).

Figure 20. (Continued).

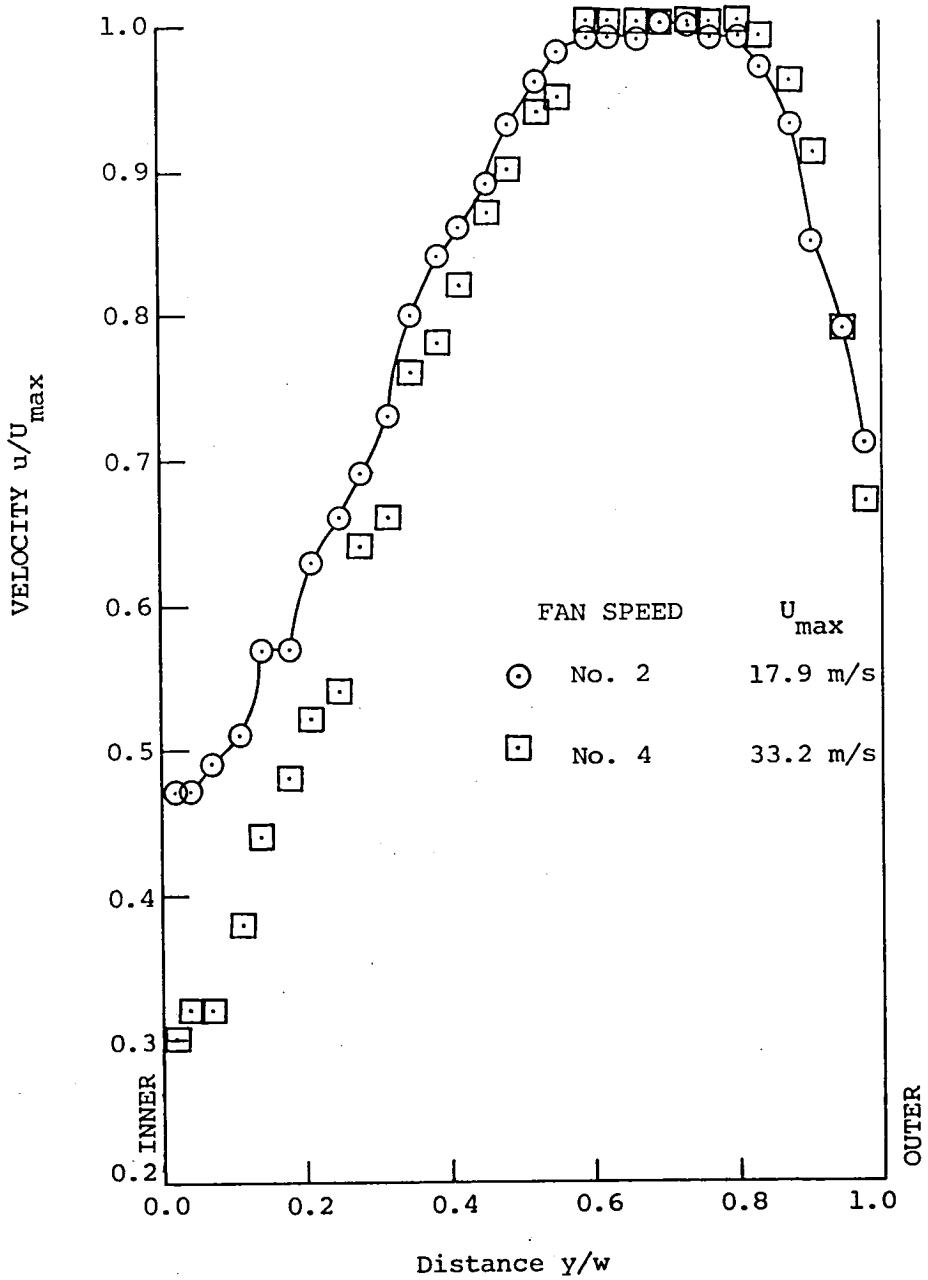

(c) Velocity distribution at T.S. 16(H).

Figure 20. (Concluded).

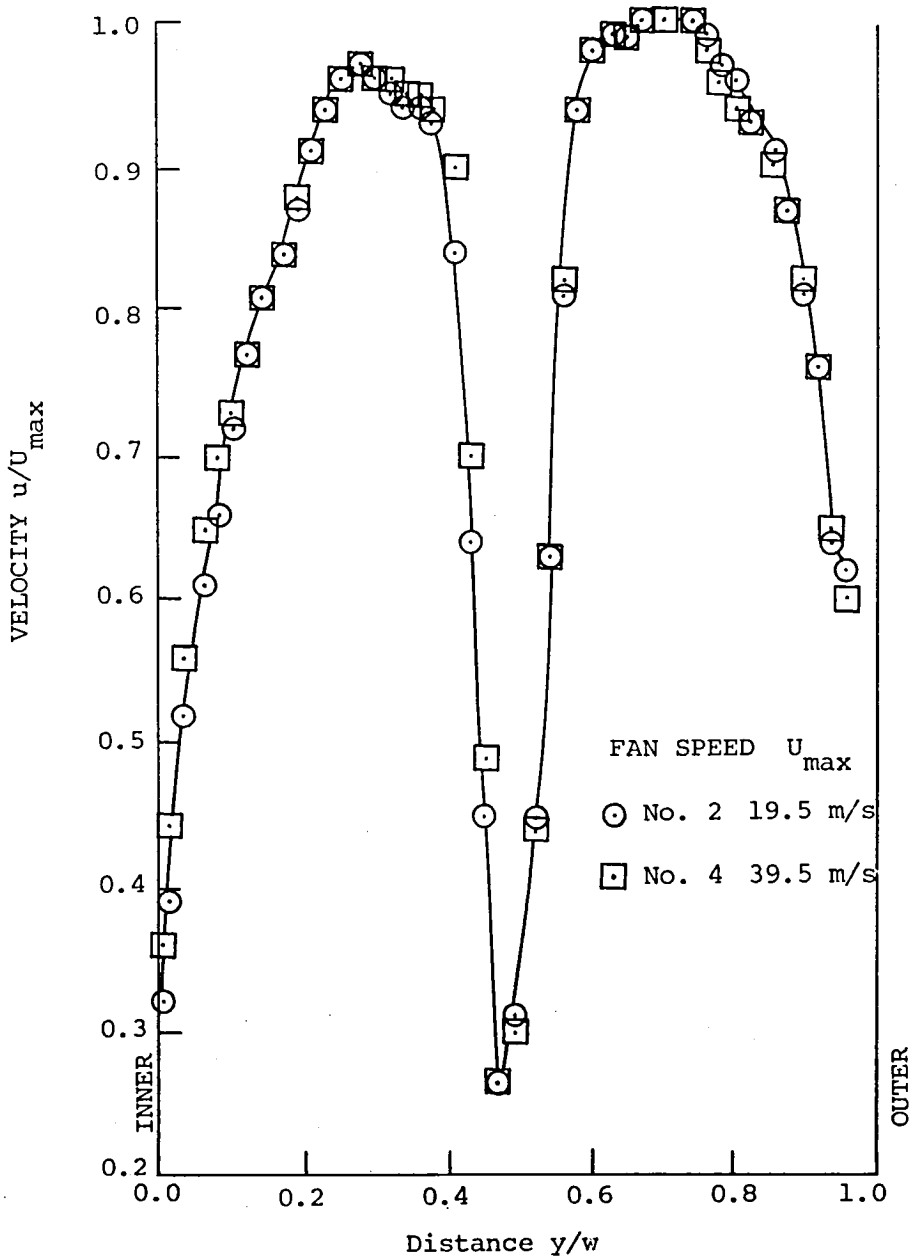

(a) Traverse station 14(H).

Figure 21. Setup F: effects on the downstream flow caused by the nacelle and by variably spaced vanes.

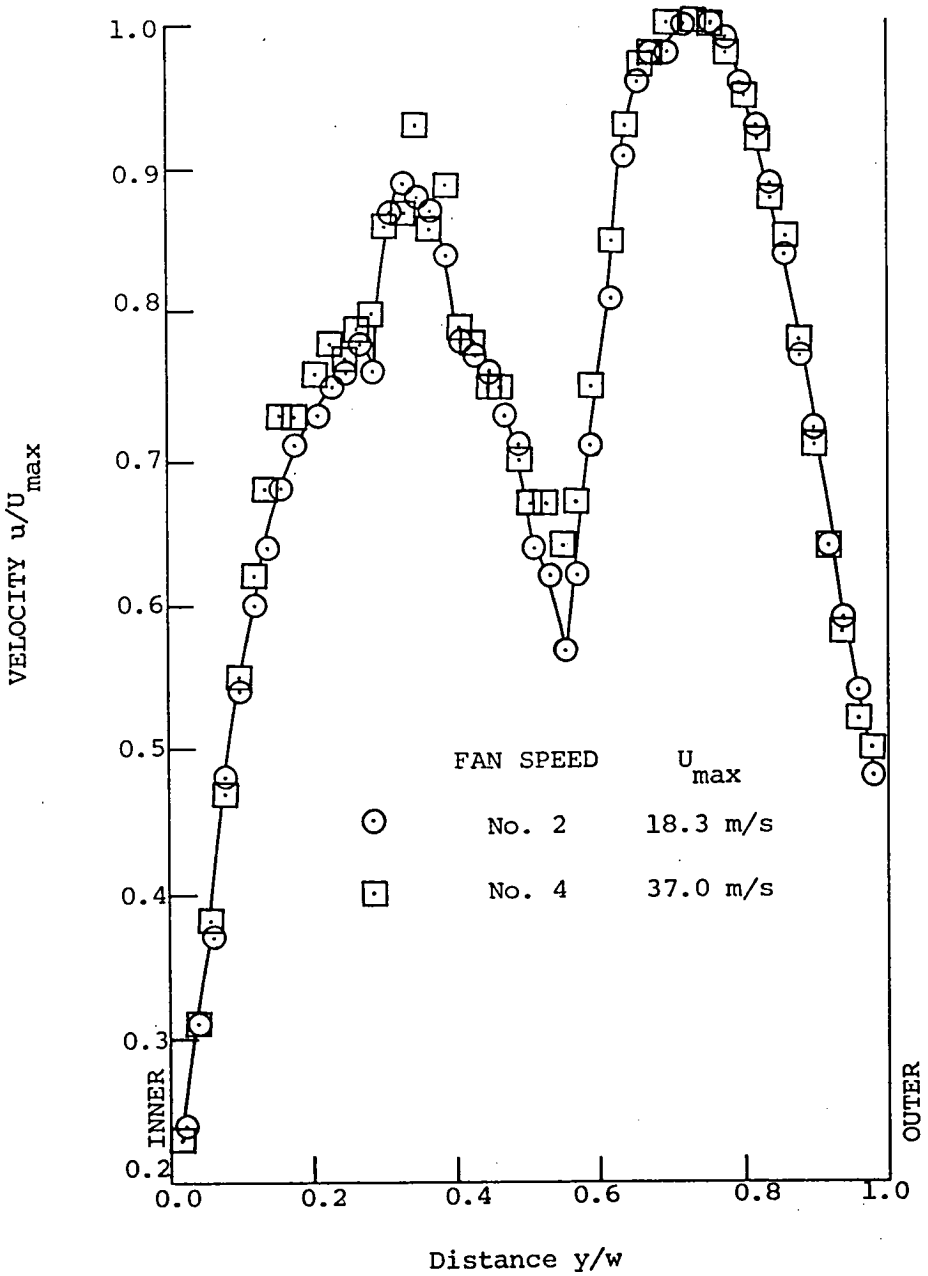

(b) Traverse station 15(H).

Figure 21. (Continued).

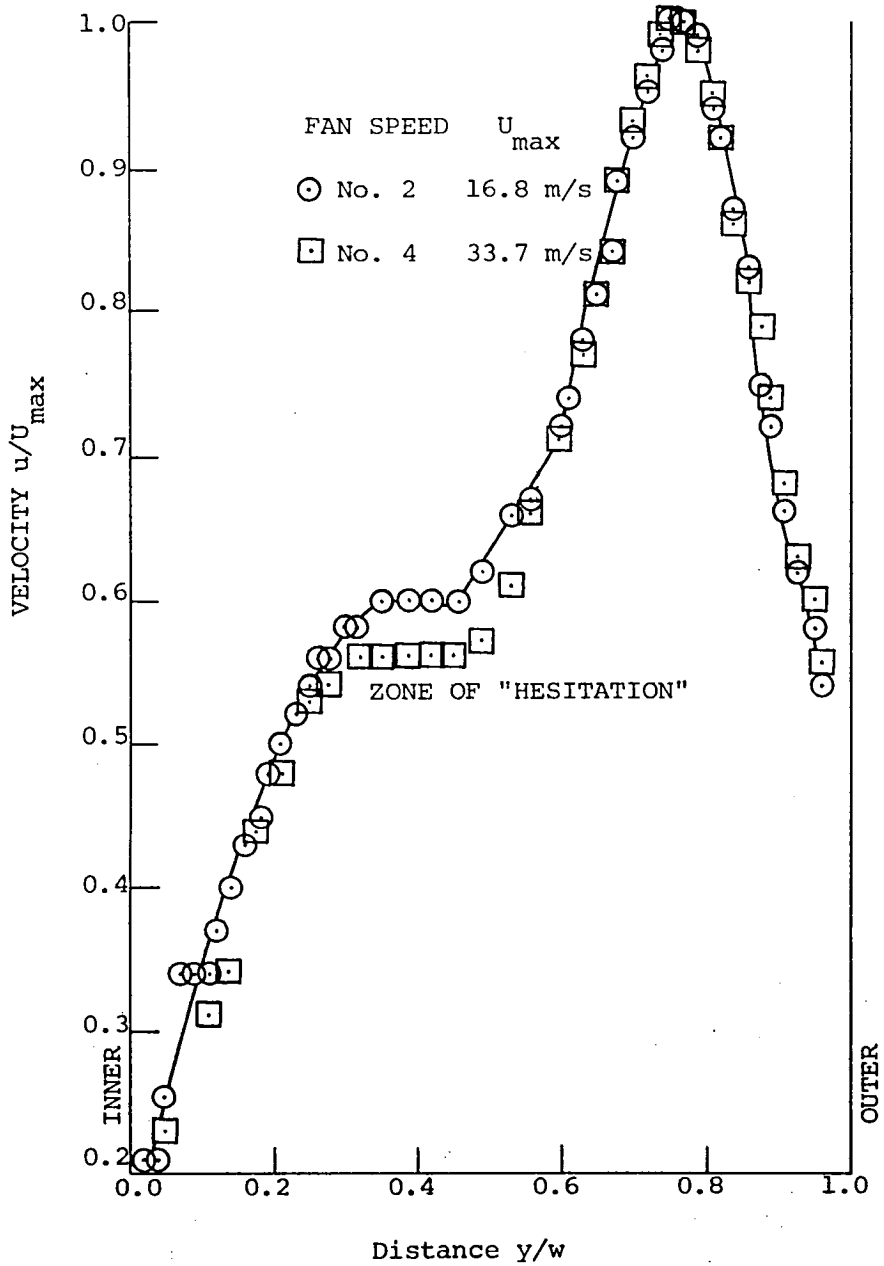

(c) Traverse station 16(H).

Figure 21. (Concluded).

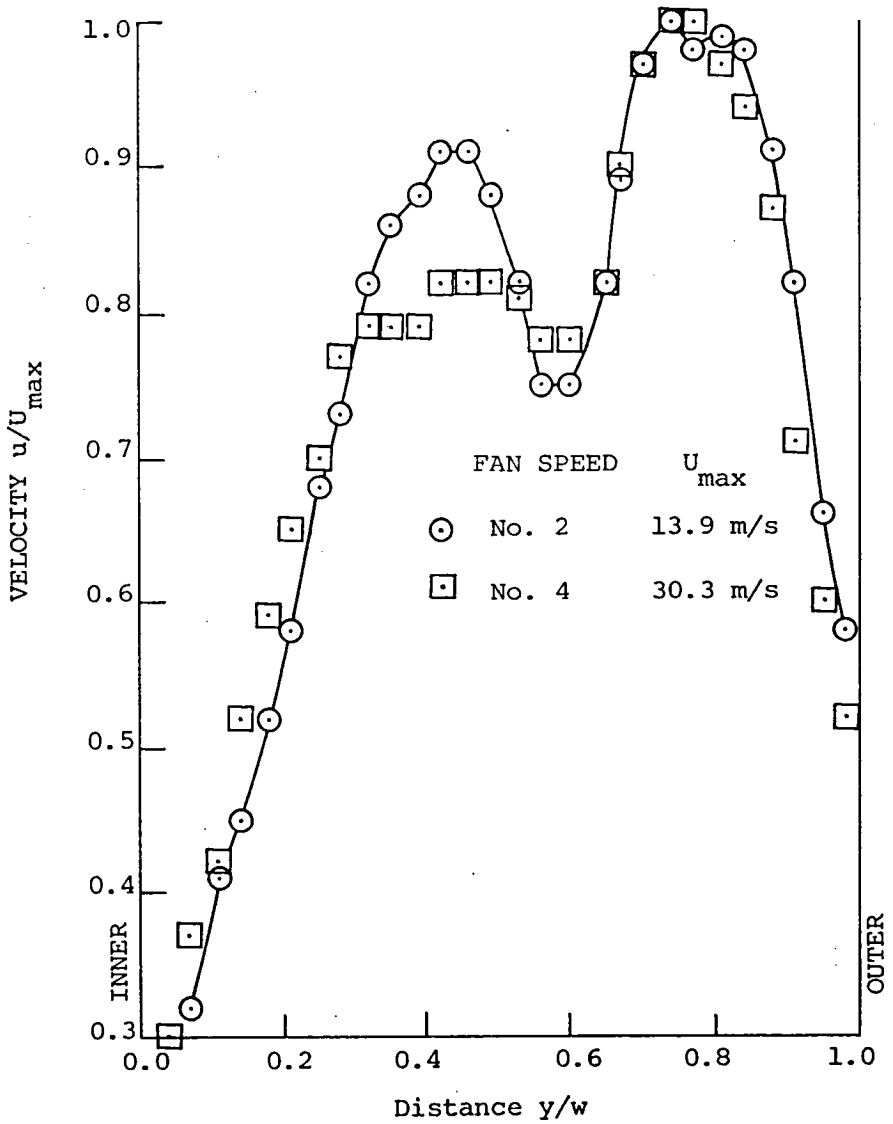

(a) Traverse station 16(H).

Figure 22. Setup G: effects on the downstream flow caused by nacelle and by equally spaced vanes.

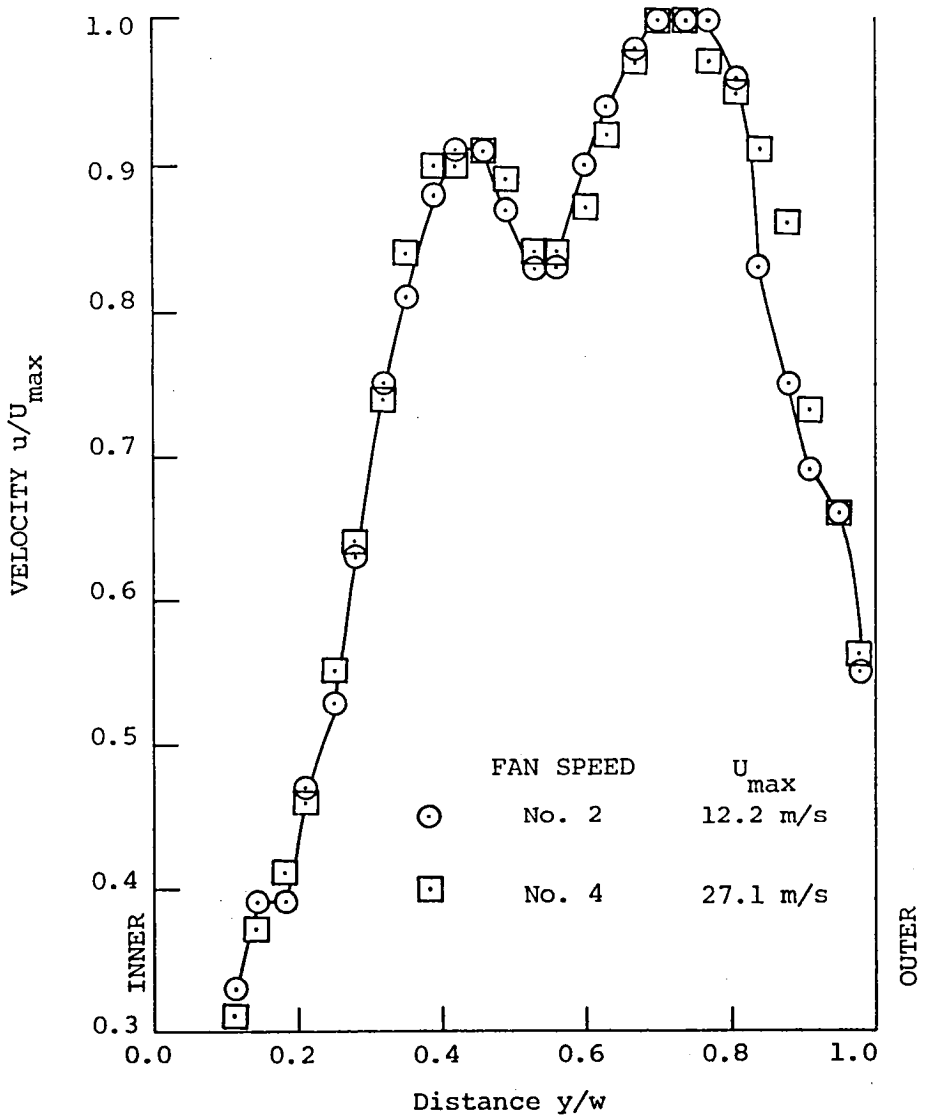

(b) Traverse station 17(H).

Figure 22. (Concluded).

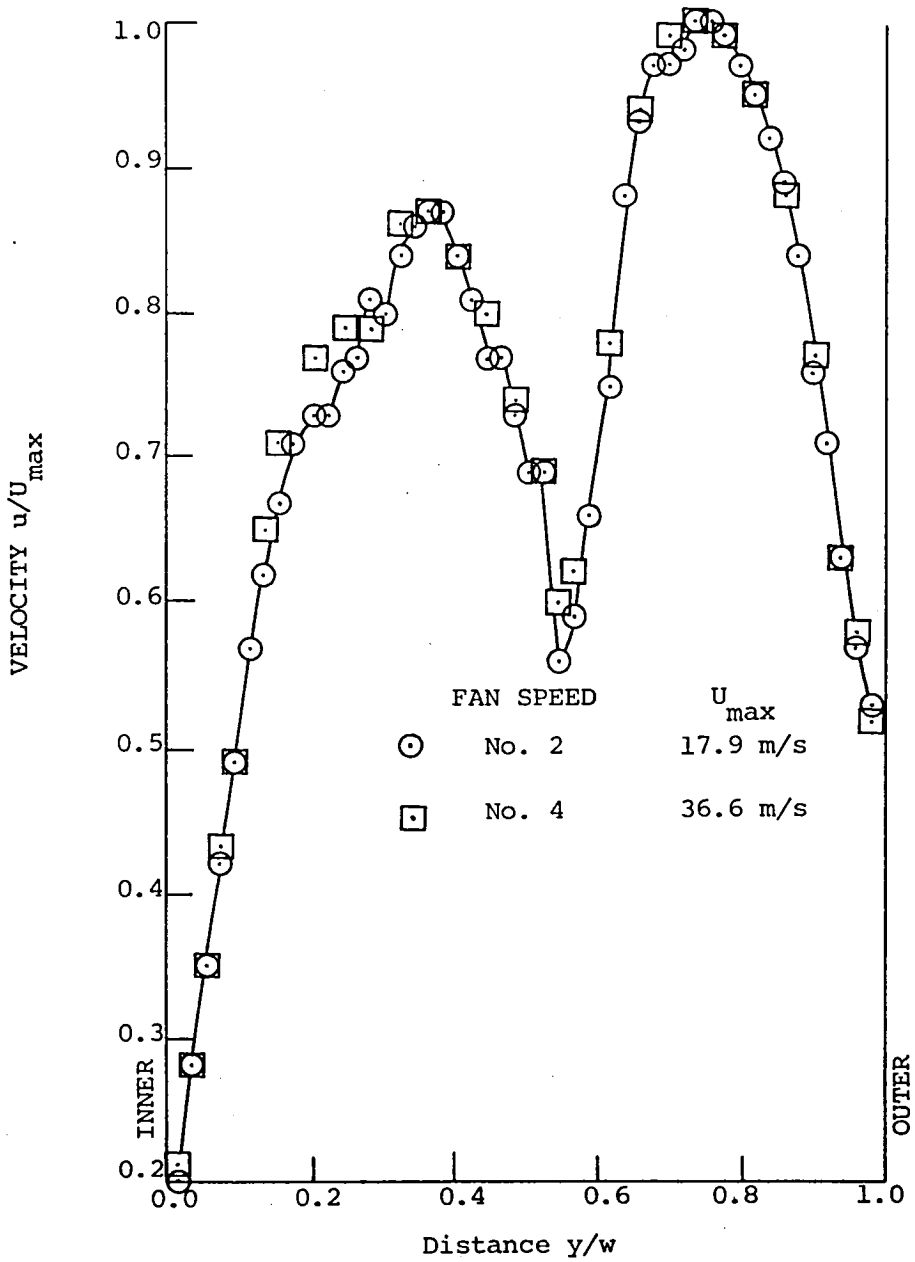

(a) Traverse station 15(H): variably spaced vanes in second corner

Figure 23. Setup H: effects on the downstream flow caused by either variably or equally spaced vanes in the second corner in presence of the third and fourth corners fitted with thick turning vanes.

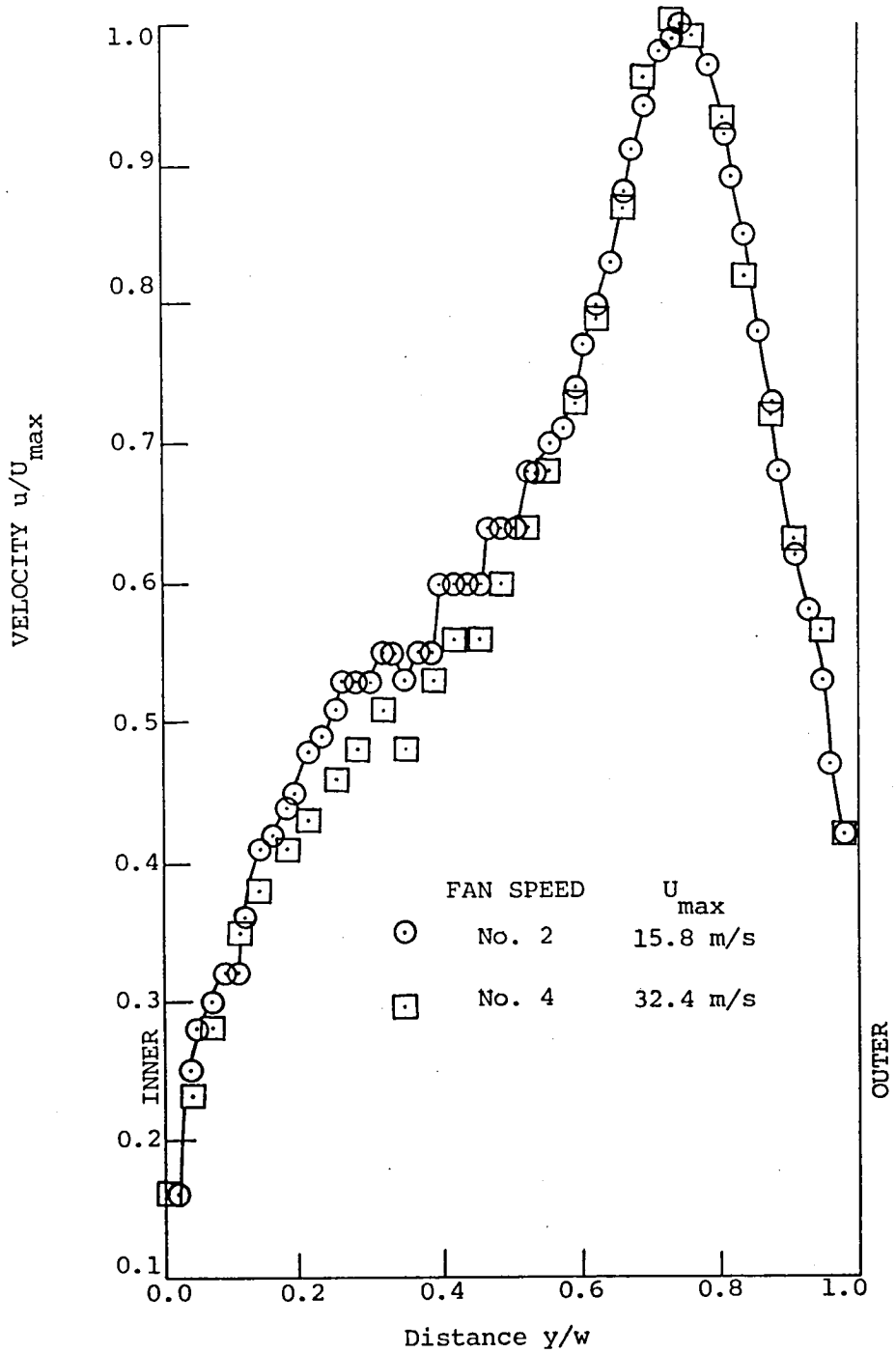

(b) Traverse station 16(H): variably spaced vanes in second corner.

Figure 23. (Continued).

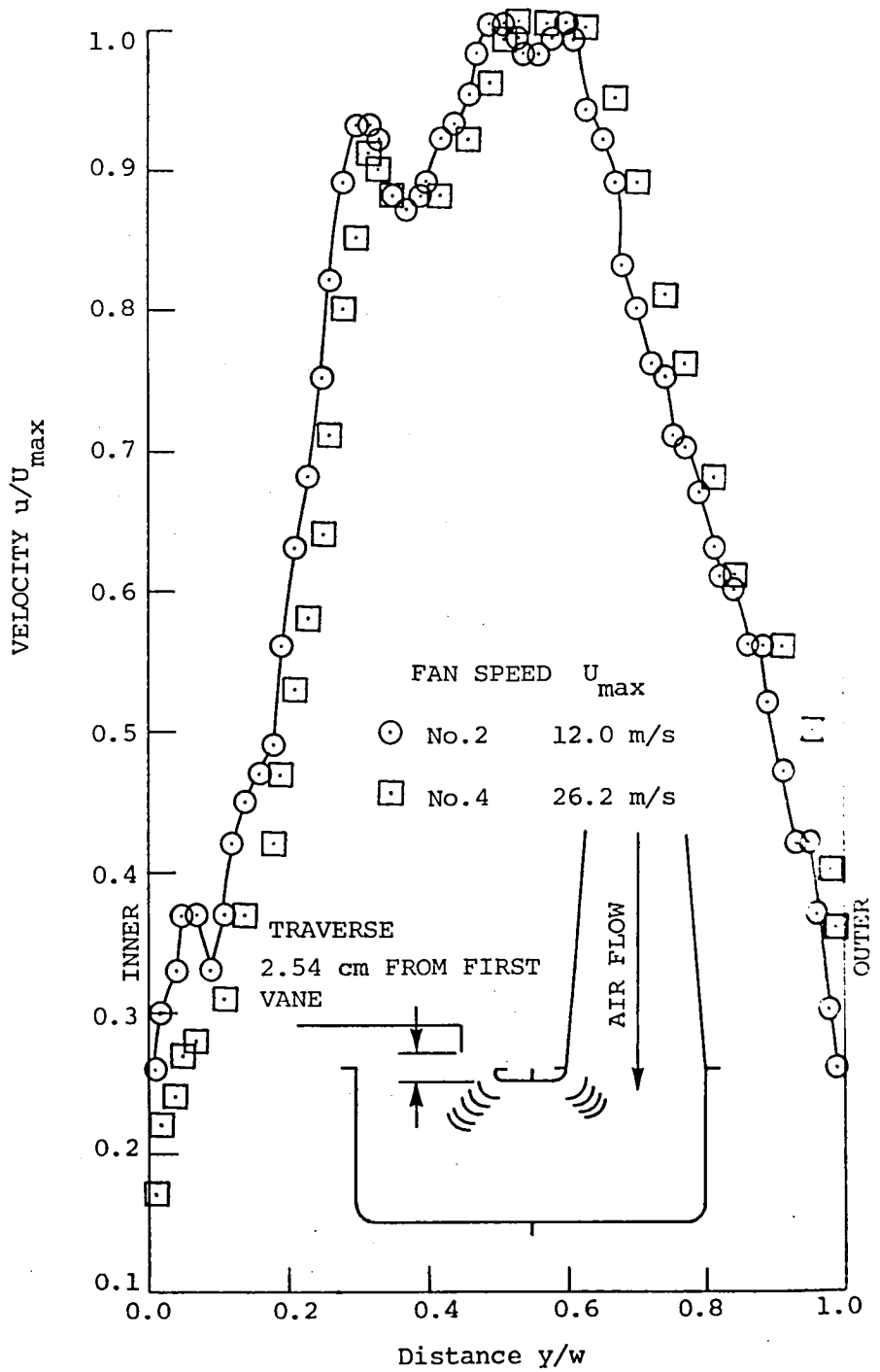

(c) Traverse station 18(H): variably spaced vanes in second corner.

Figure 23. (Continued).

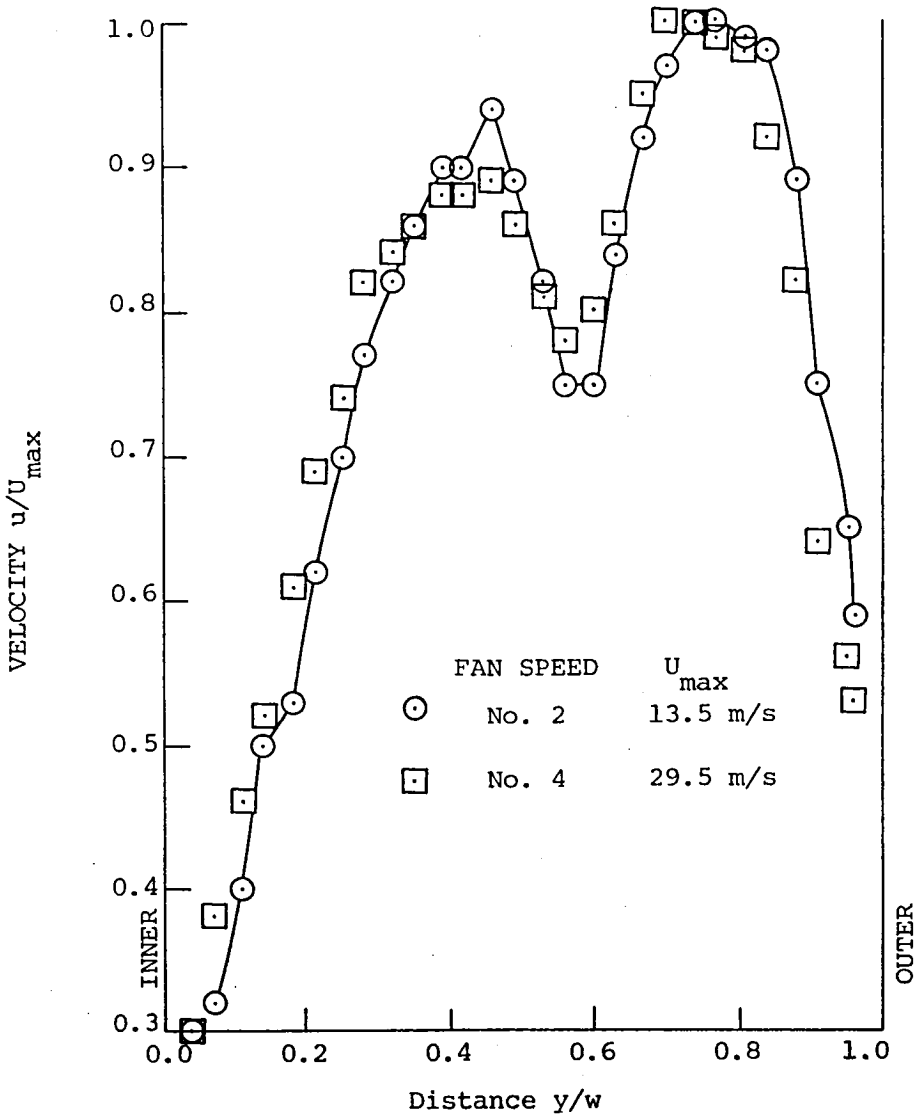

(d) Traverse station 16(H): equally spaced vanes in second corner.

Figure 23. (Concluded).

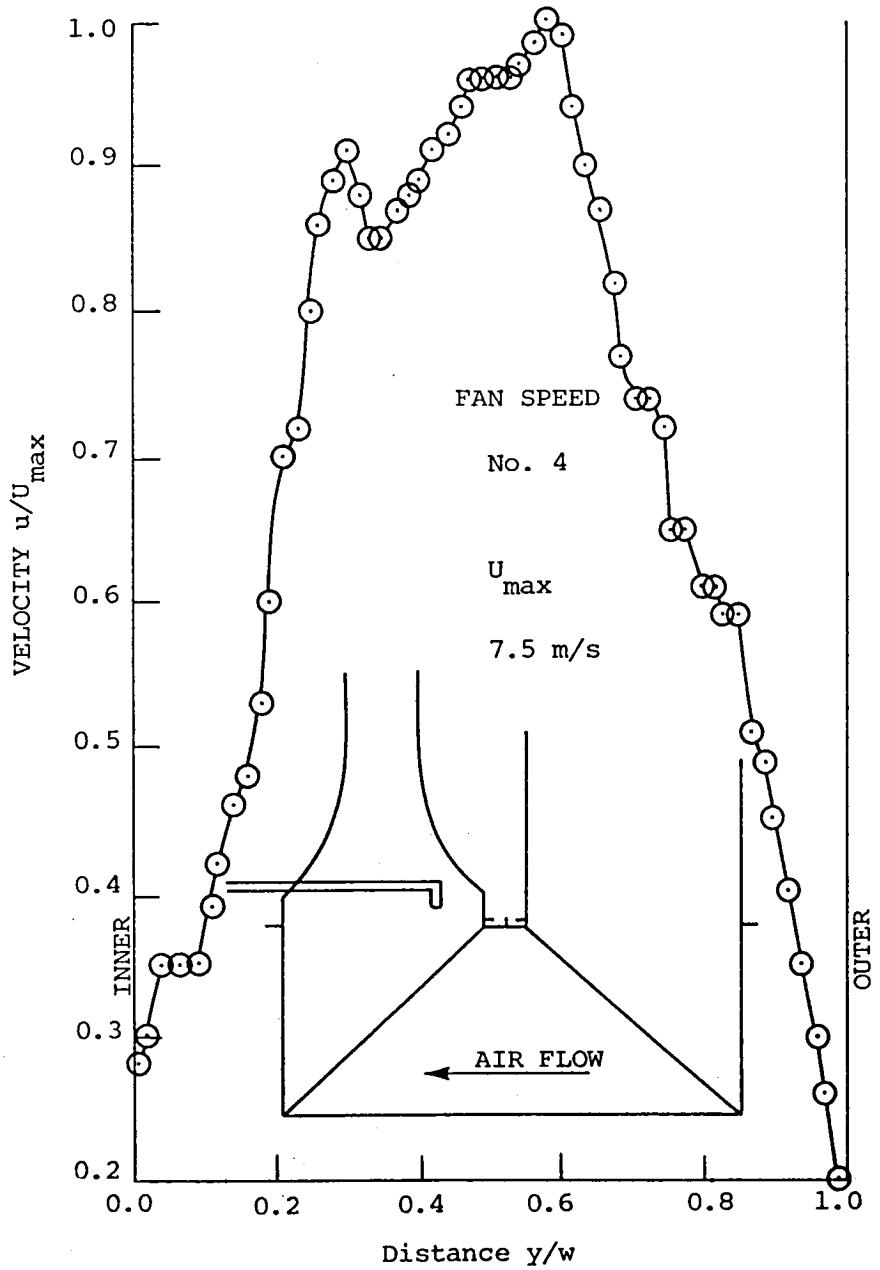

(a) Traverse station 19(H).

Figure 24. Setup I: velocity distribution at inlet and outlet of the contraction.

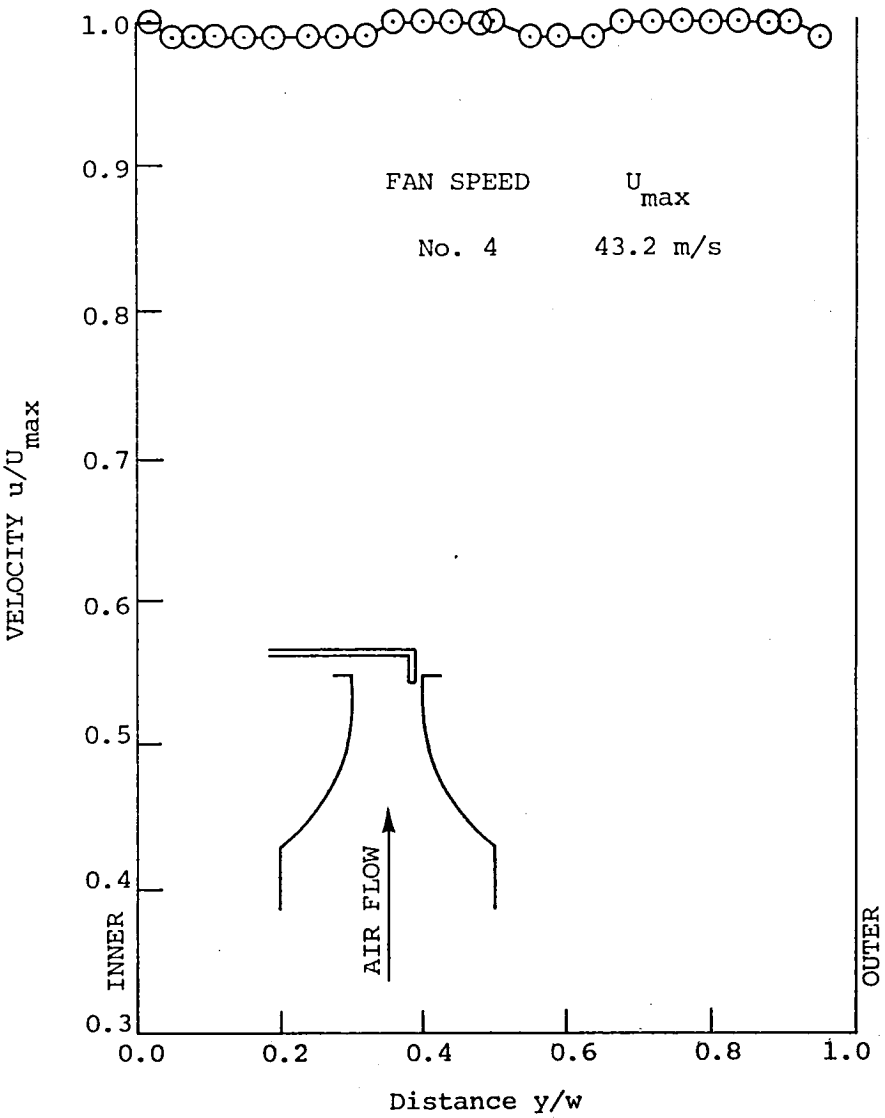

(b) Traverse station 21(H).

Figure 24. (Concluded).

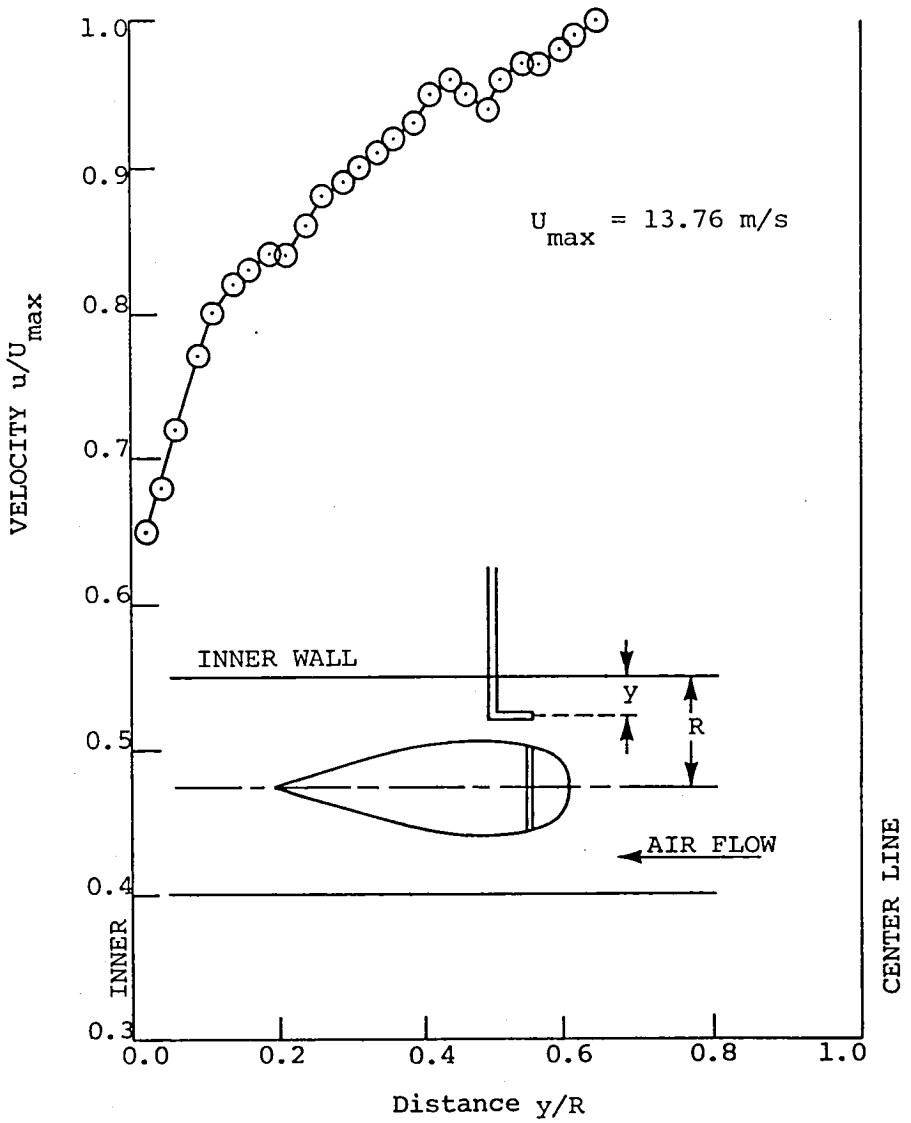

(a) Traverse station 13(H).

Figure 25. Effects on the velocity distribution at the nacelle in setup I caused by the third and fourth corners.

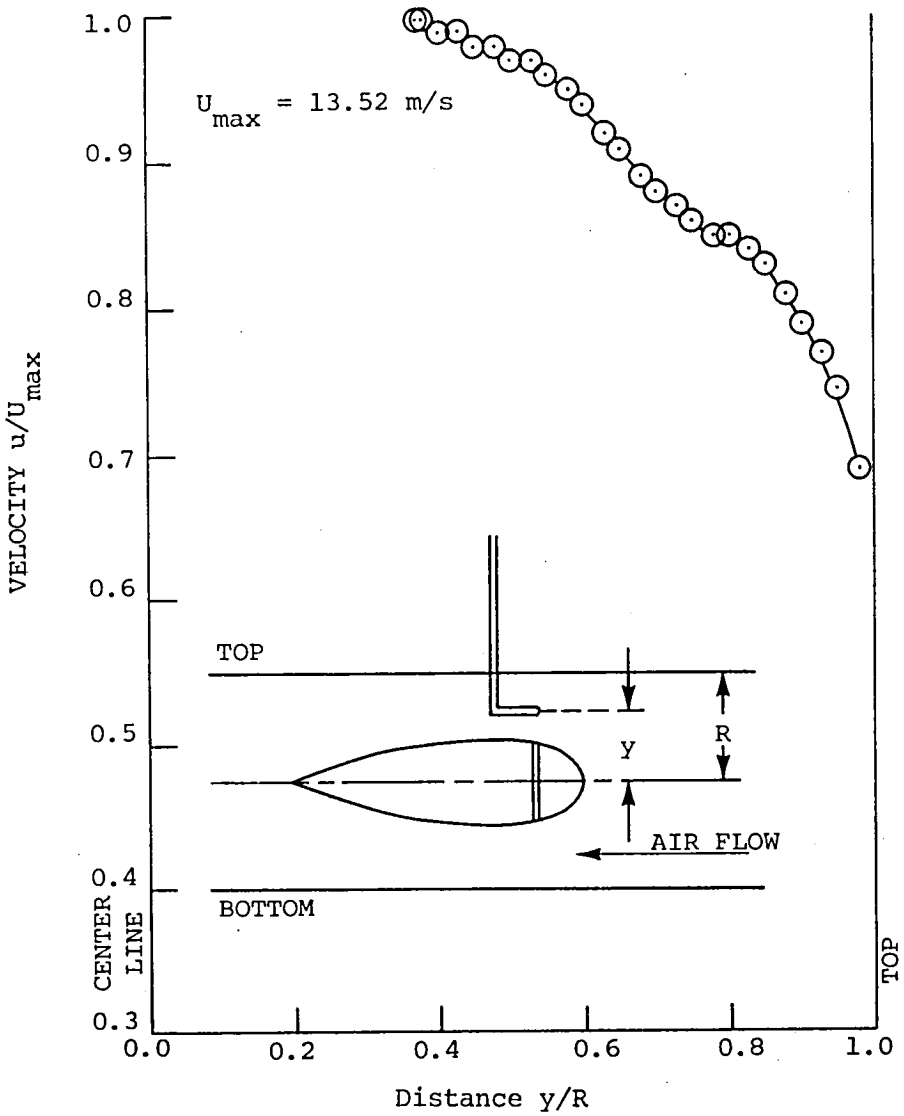

(b) Traverse station 13(V).

Figure 25. (Concluded).

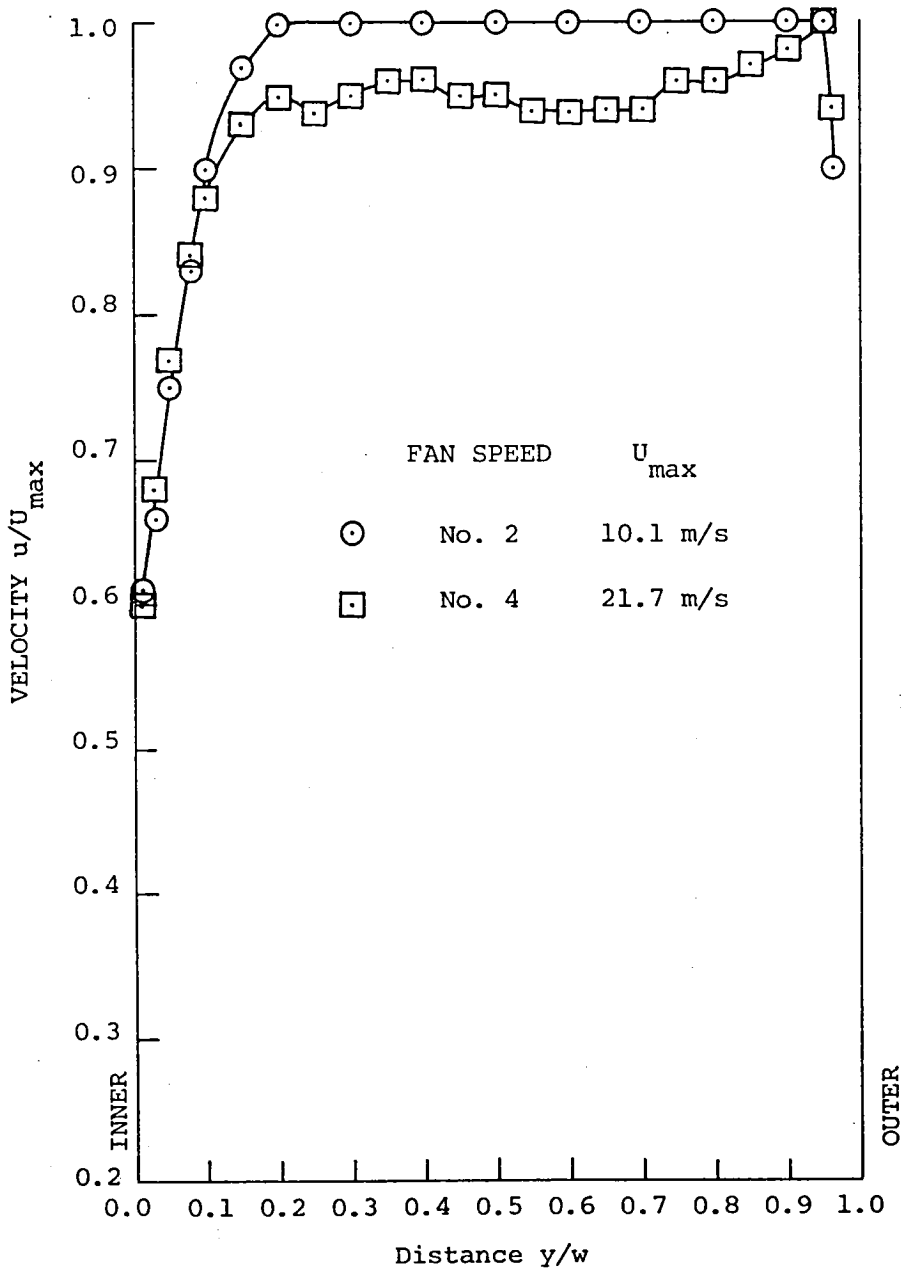

(a) Traverse station 13(H); screen at T.S. 11.

Figure 26. Effects of a screen on the velocity distribution obtained with setup A.

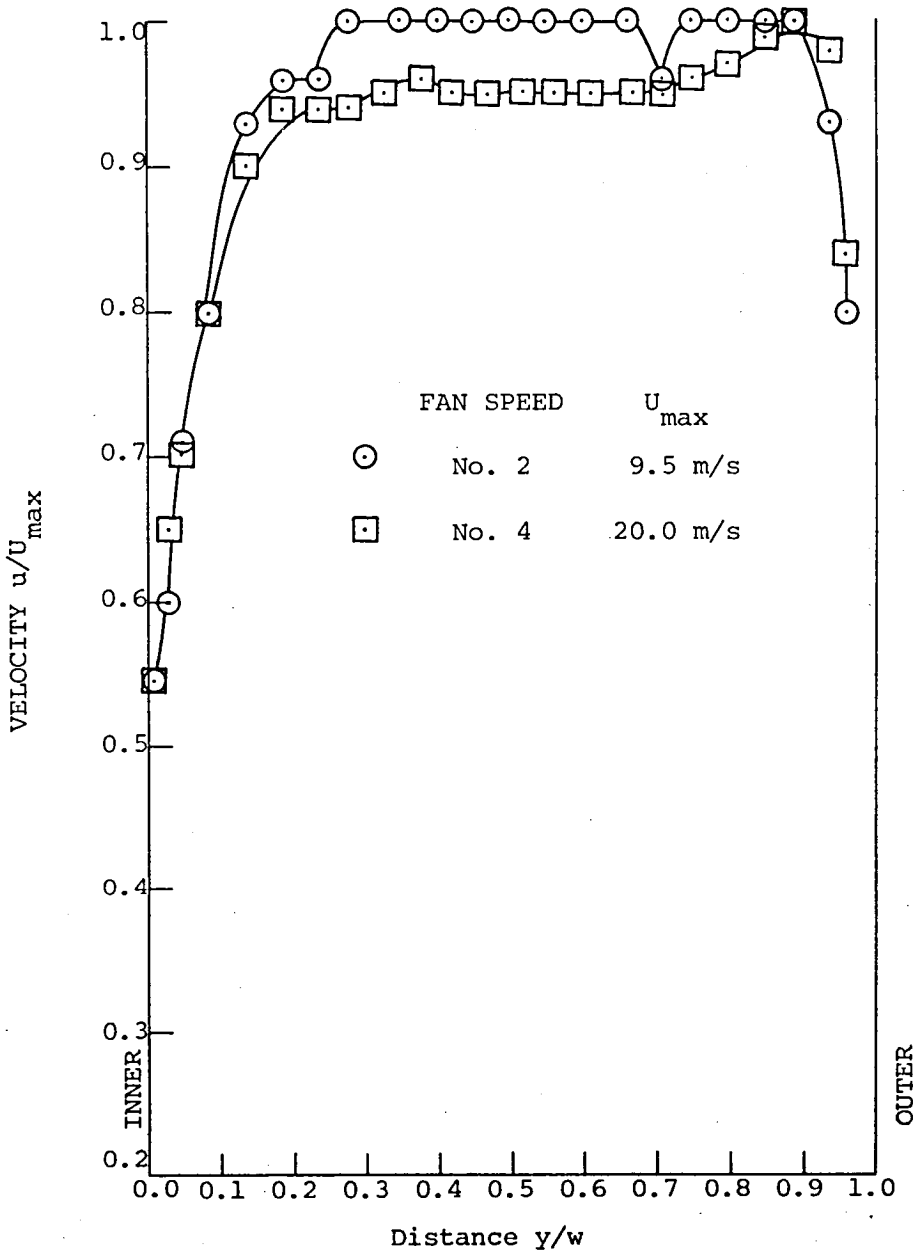

(b) Traverse station 14(H); screen at T.S. 11.

Figure 26. (Continued).

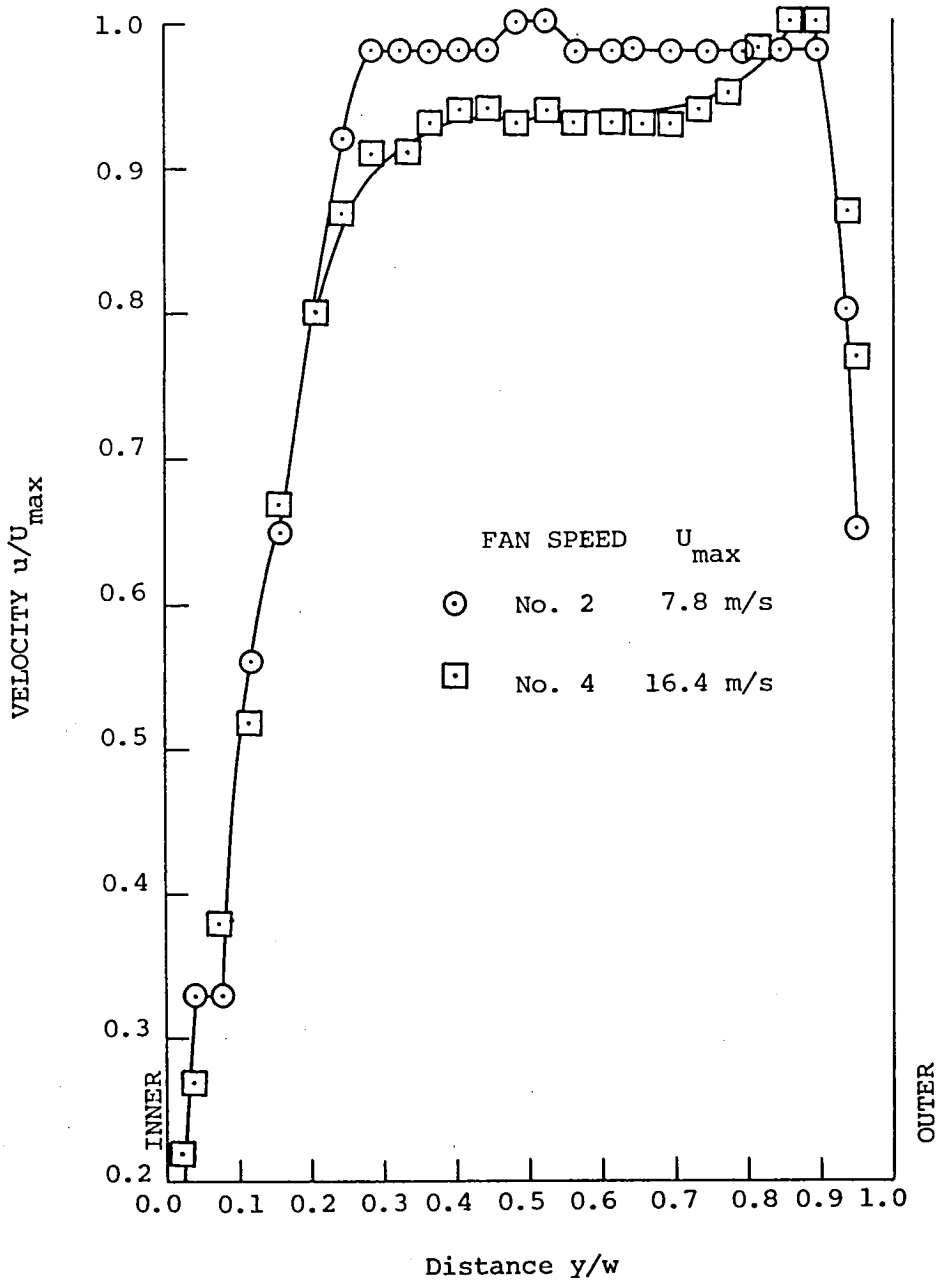

(c) Traverse station 15(H); screen at T.S. 11.

Figure 26. (Continued).

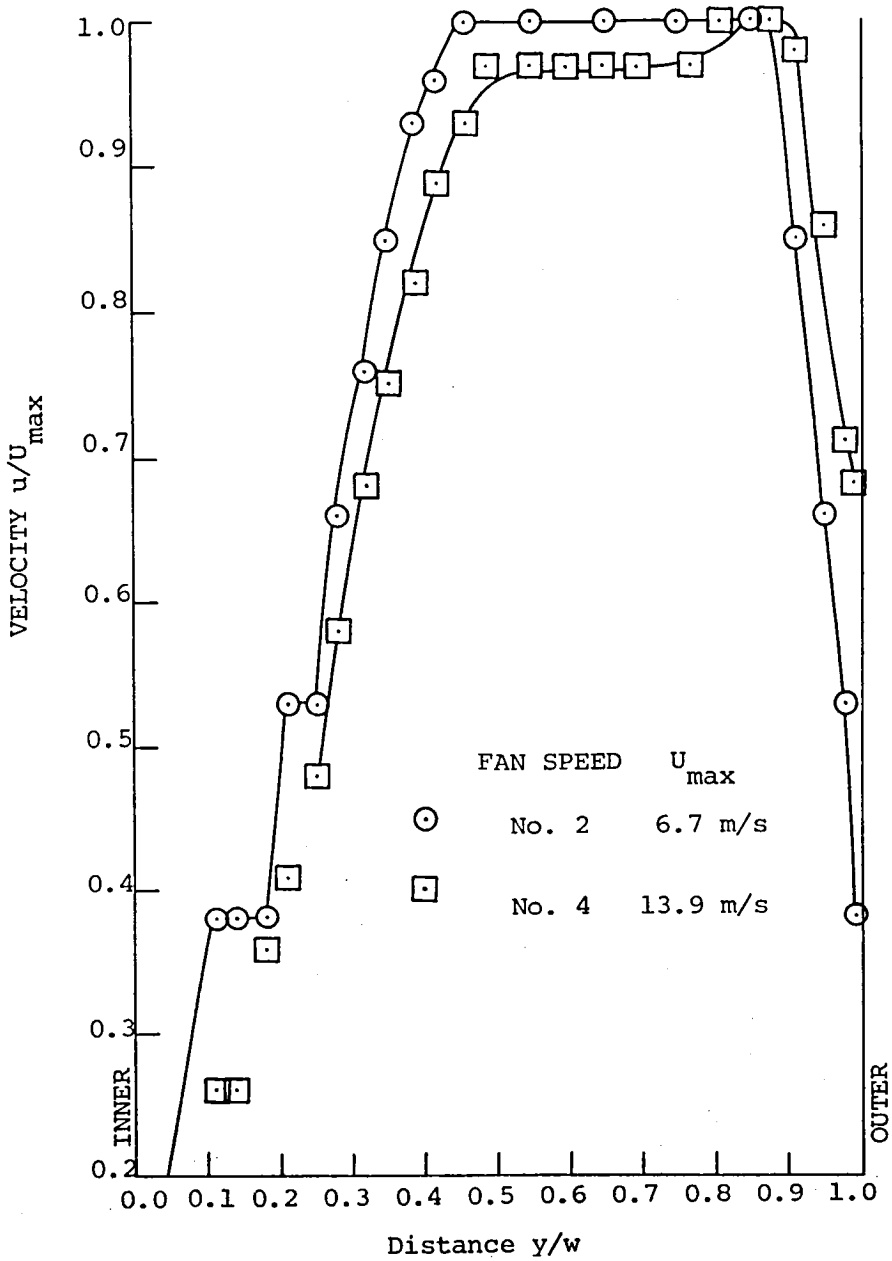

(d) Traverse station 16(H); screen at T.S. 11.

Figure 26. (Continued).

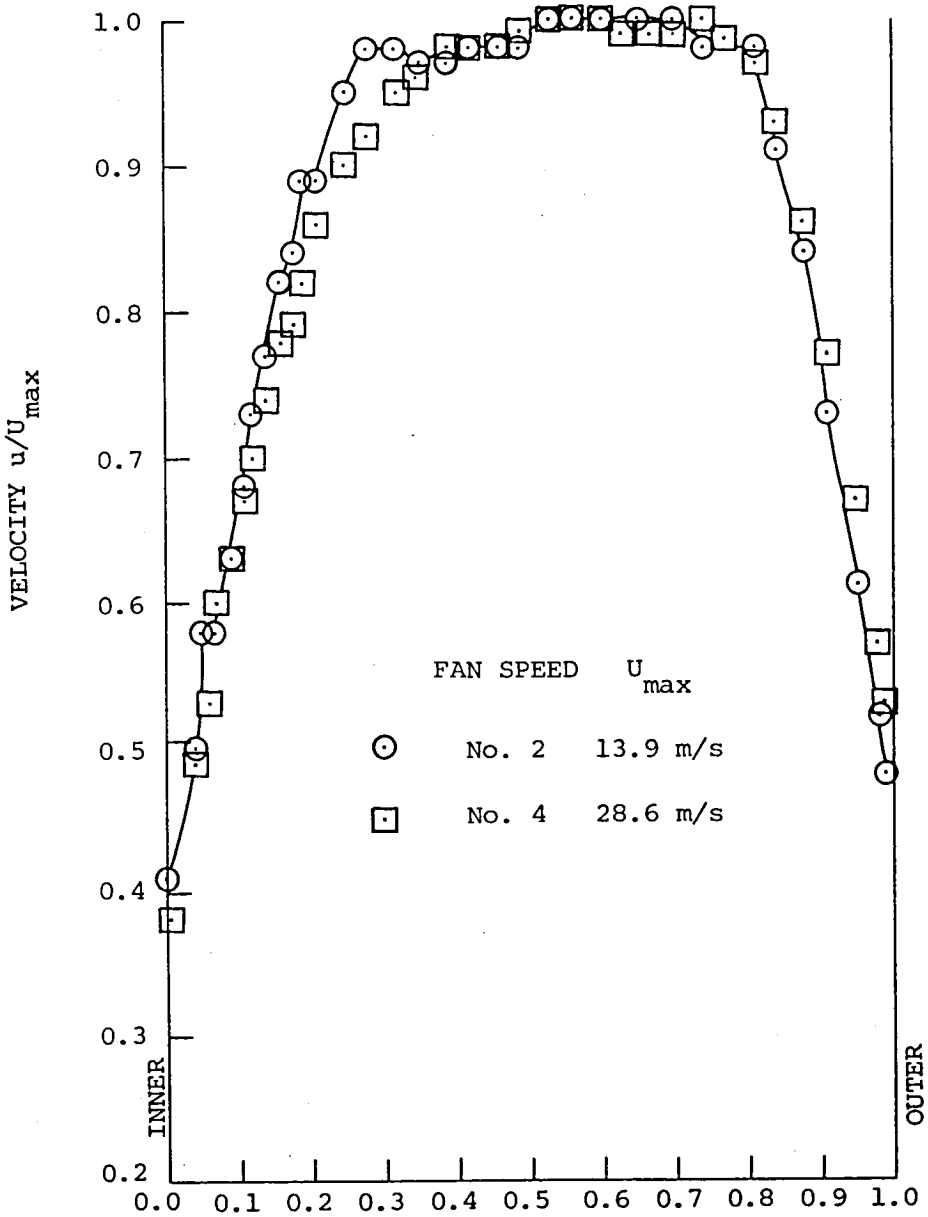

(e) Traverse station 16(H); screen at T.S. 16.

Figure 26. (Continued).

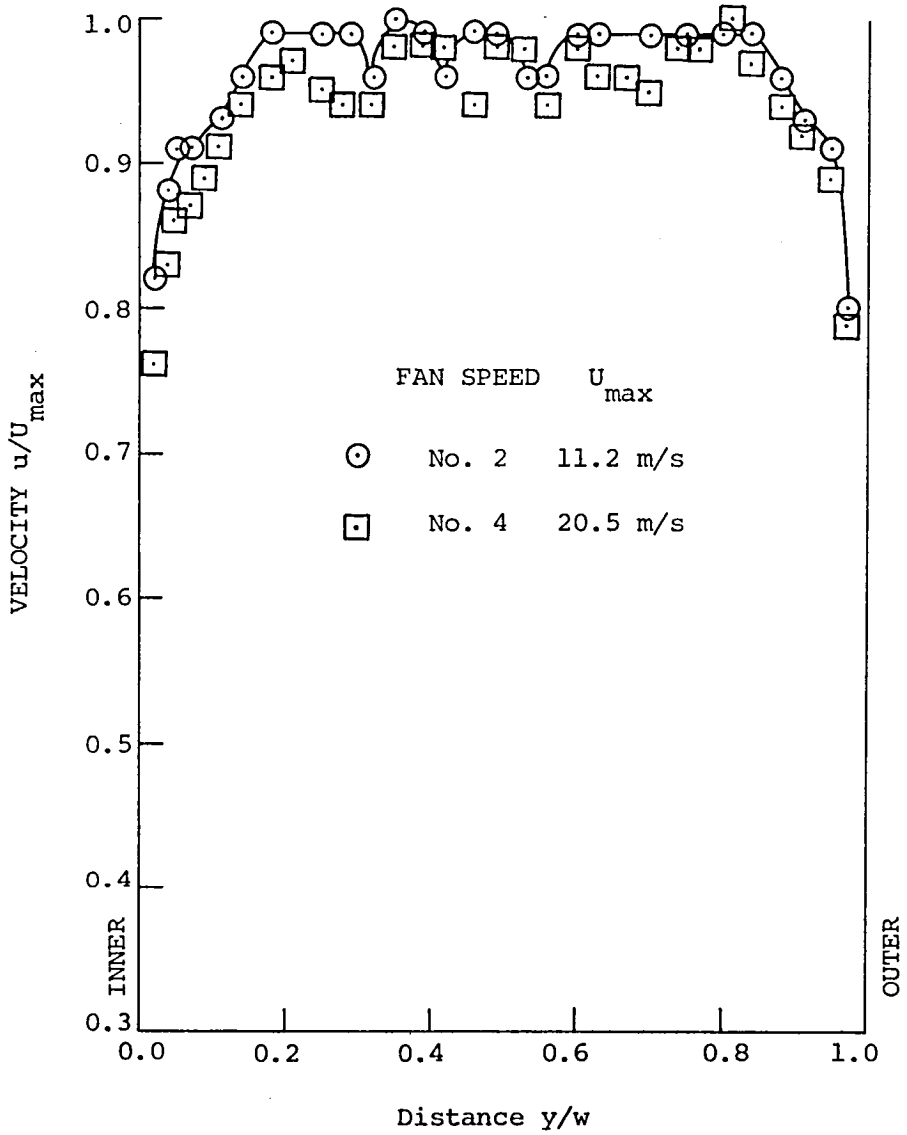

(f) Traverse station 16(H); screen at T.S. 15.

Figure 26. (Concluded).

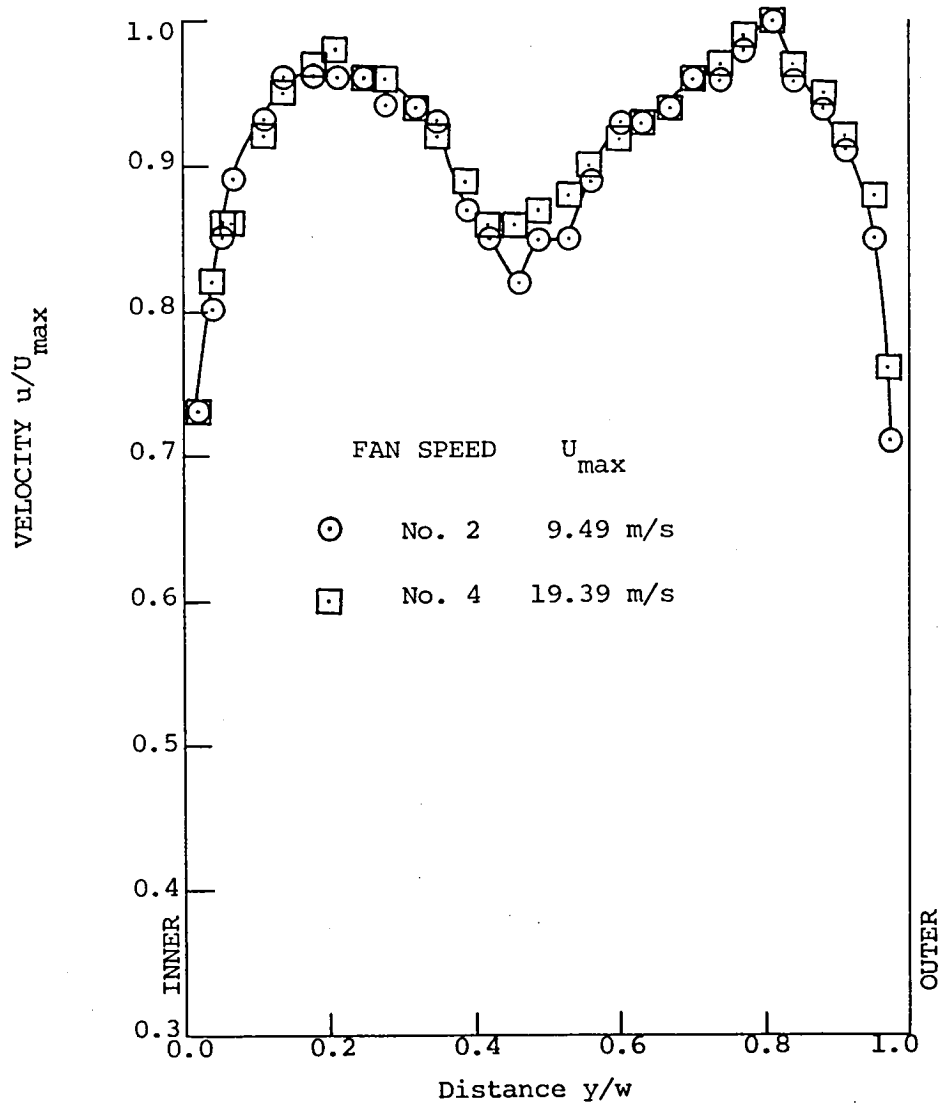

Figure 27. Traverse station 16(H): effects of screen on setup B with screen at T.S. 15.

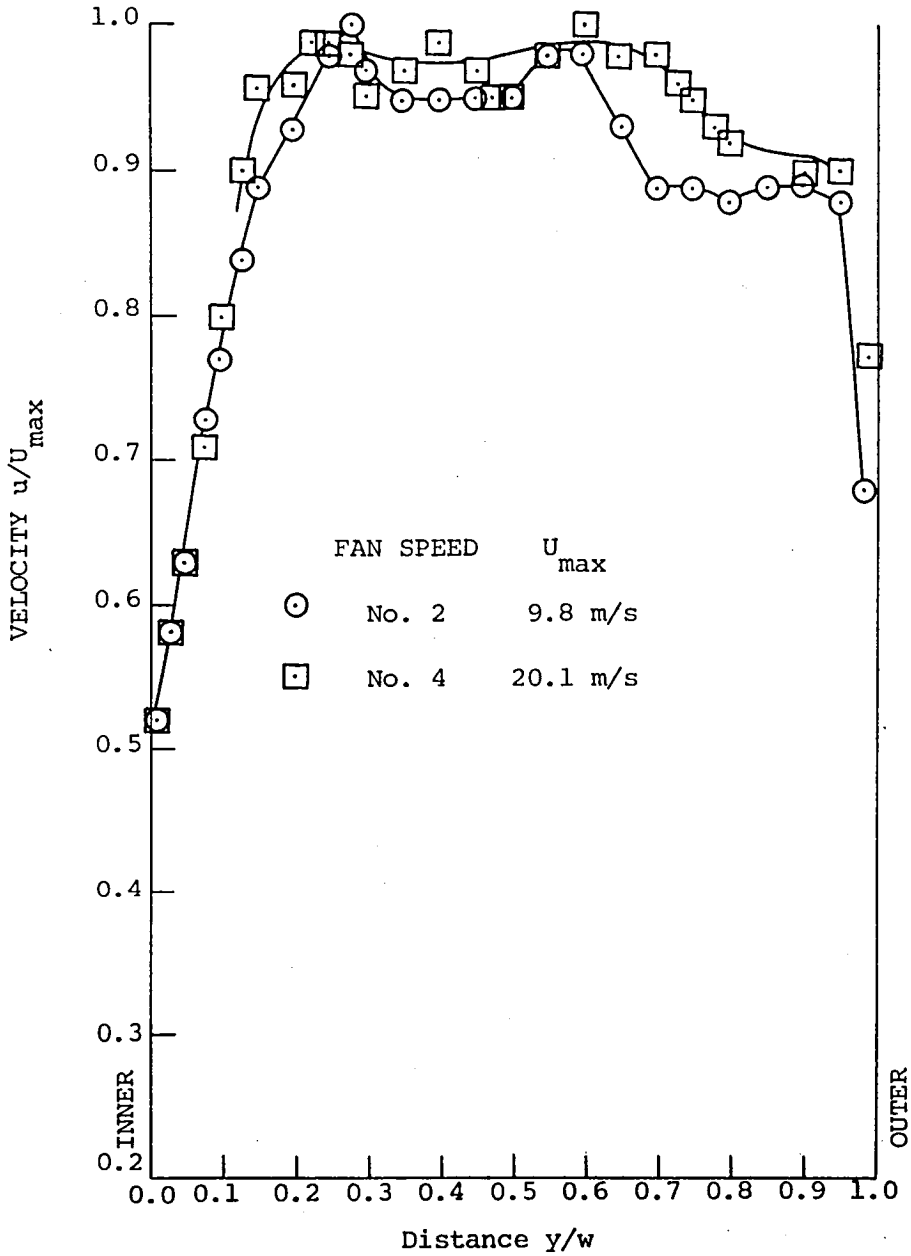

(a) Traverse station 13(H).

Figure 28. Effects of screen on setup E with screen at T.S. 11.

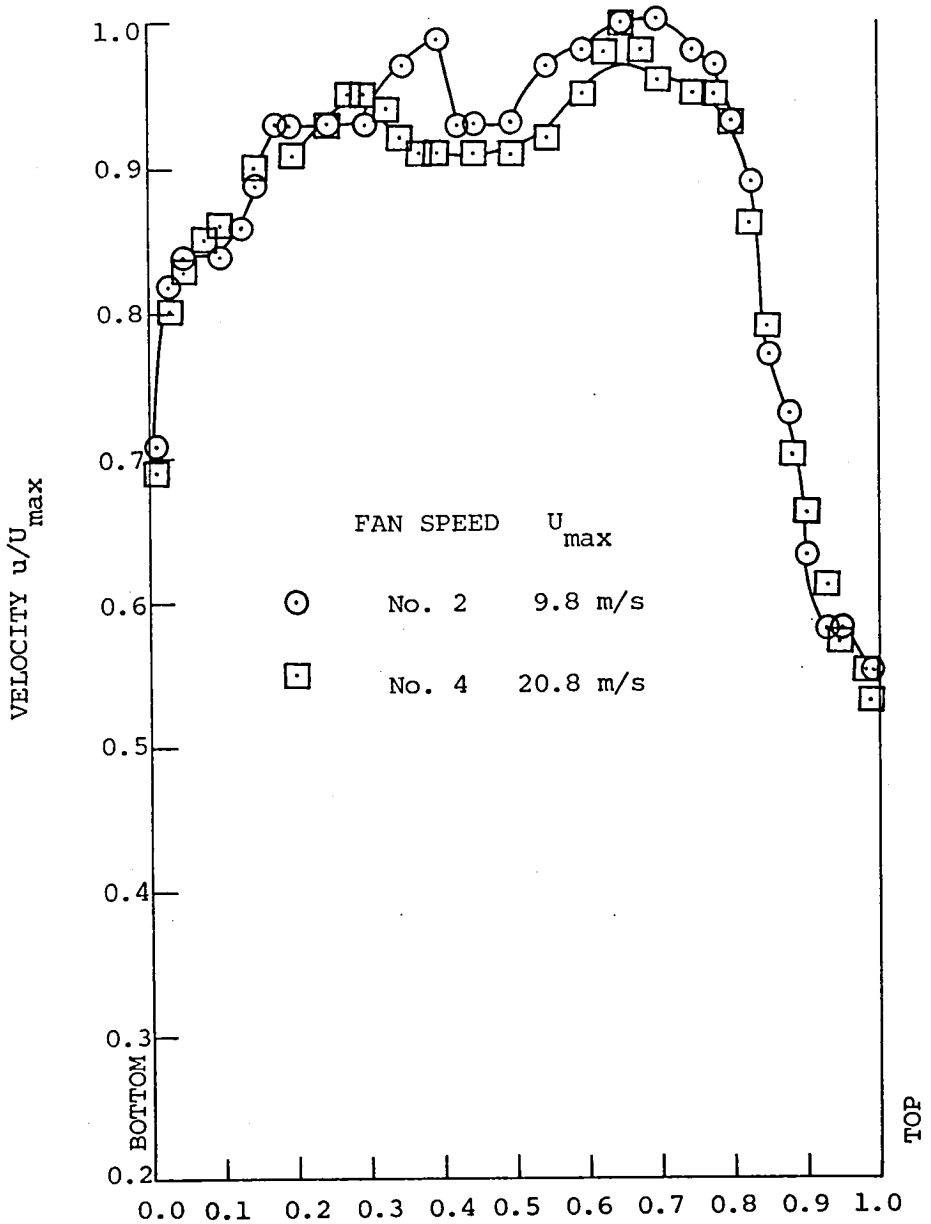

(b) Traverse station 13(V).

Figure 28. (Continued).

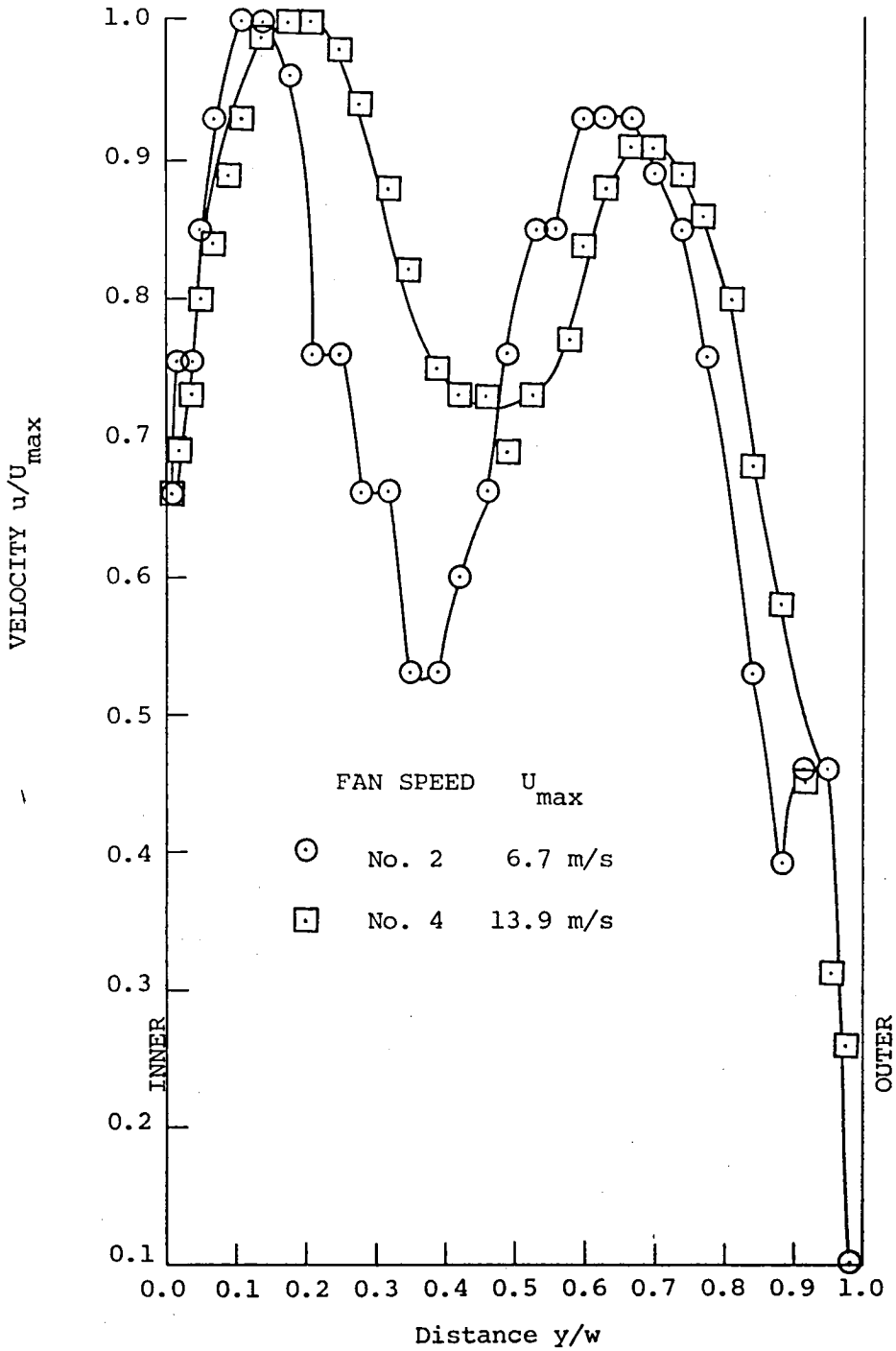

(c) Traverse station 16(H).

Figure 28. (Continued).

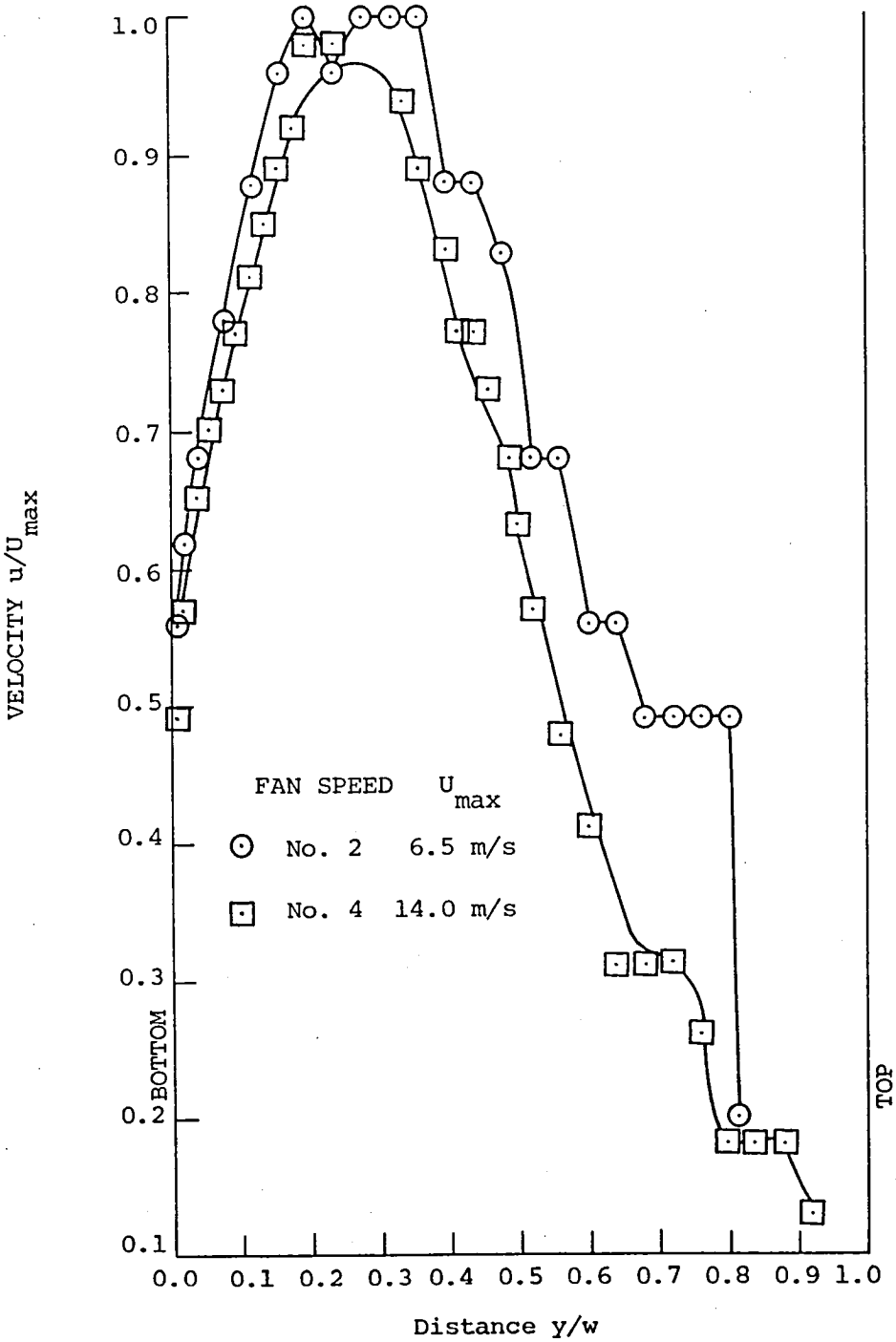

(d) Traverse station 16(V).

Figure 28. (Concluded).

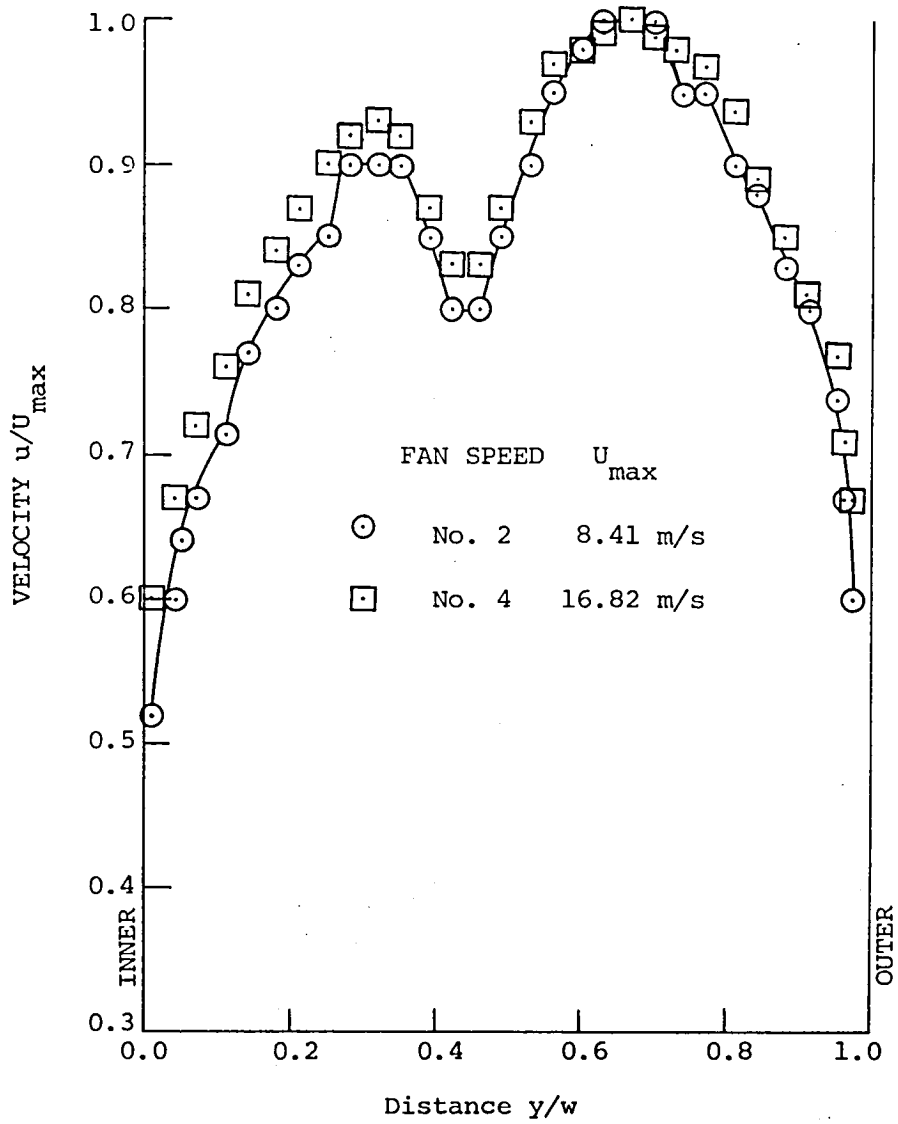

Figure 29. Traverse station 16(H): effect of screen on setup F with screen at T.S. 15.

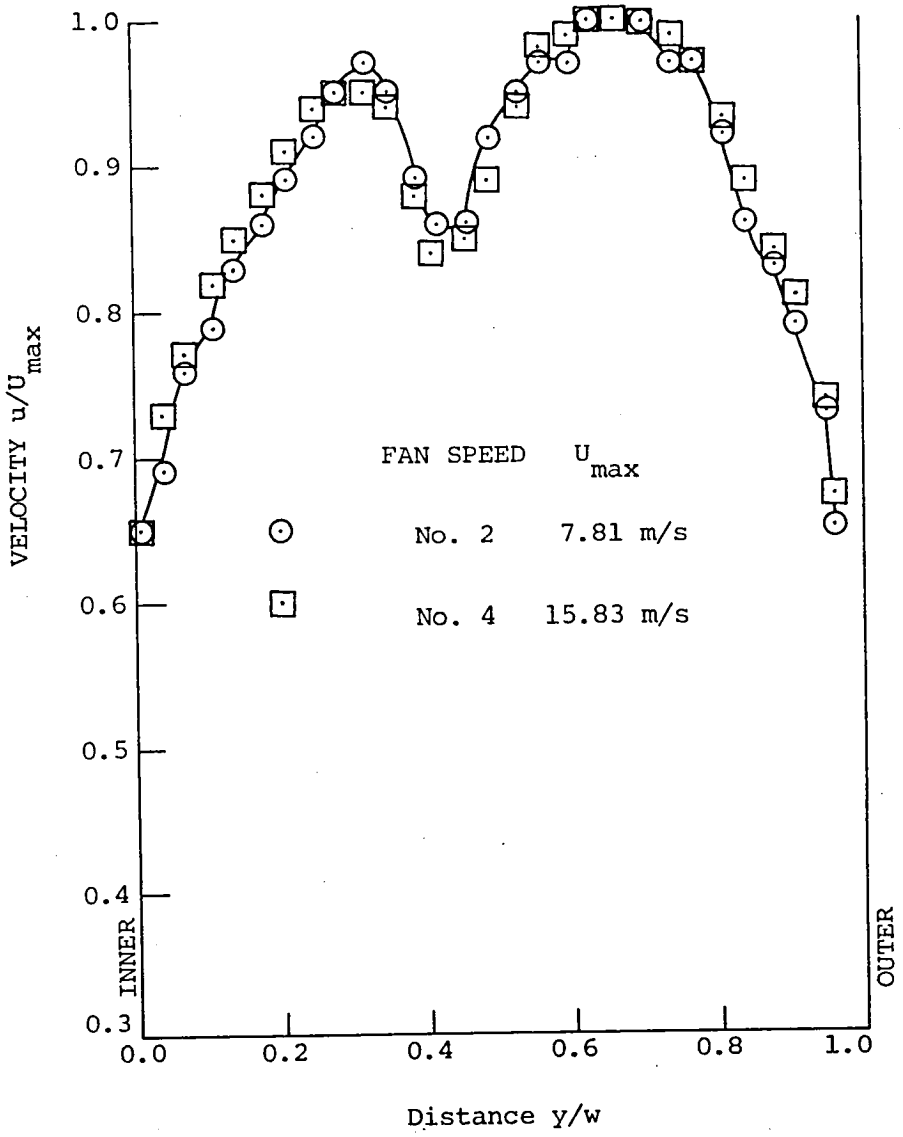

Figure 30. Traverse station 16(H): effect of screen on setup G with screen at T.S. 15.

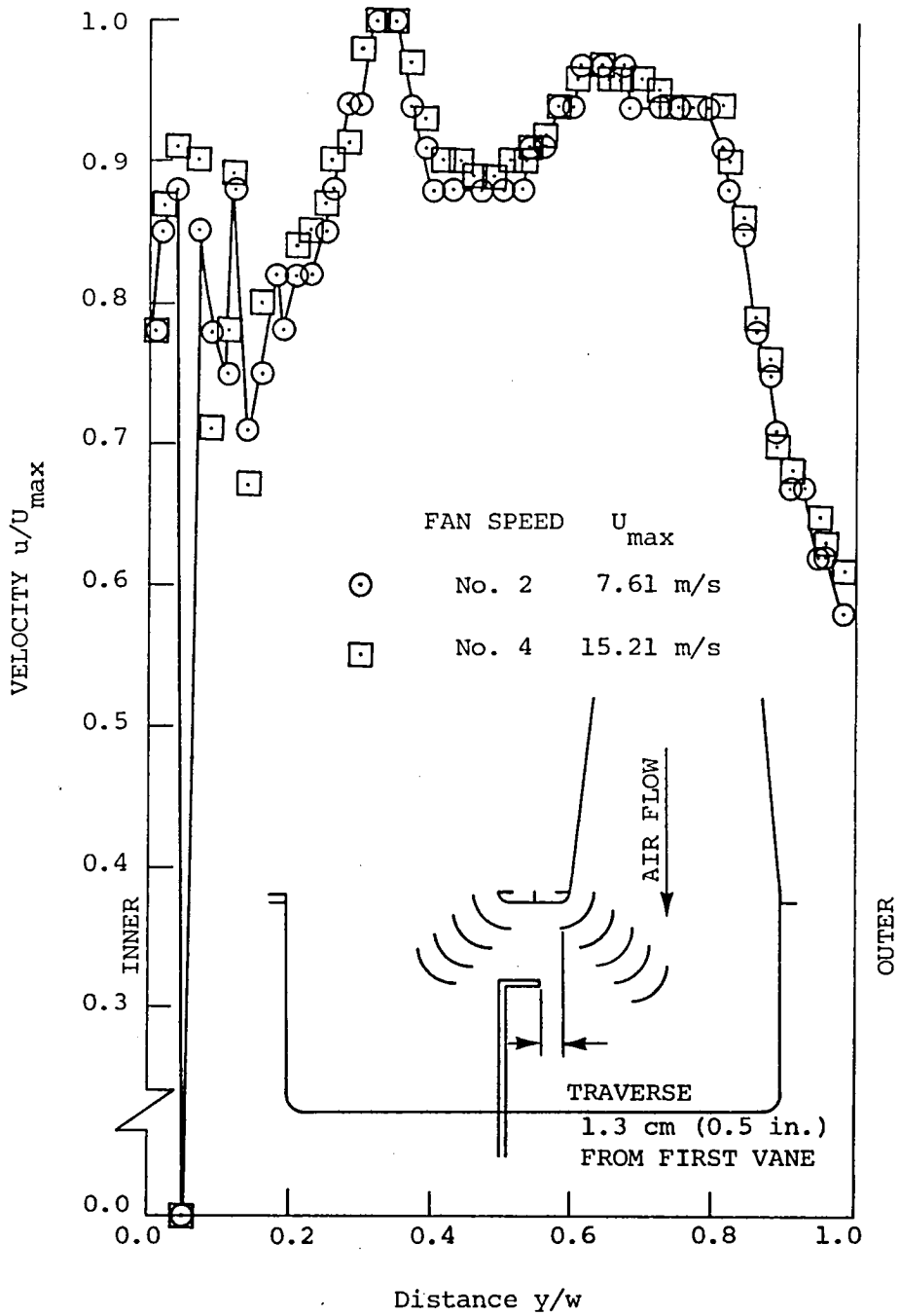

(a) Traverse station 17(H).

Figure 31. Effects of screen on setup H with screen at T.S. 15.

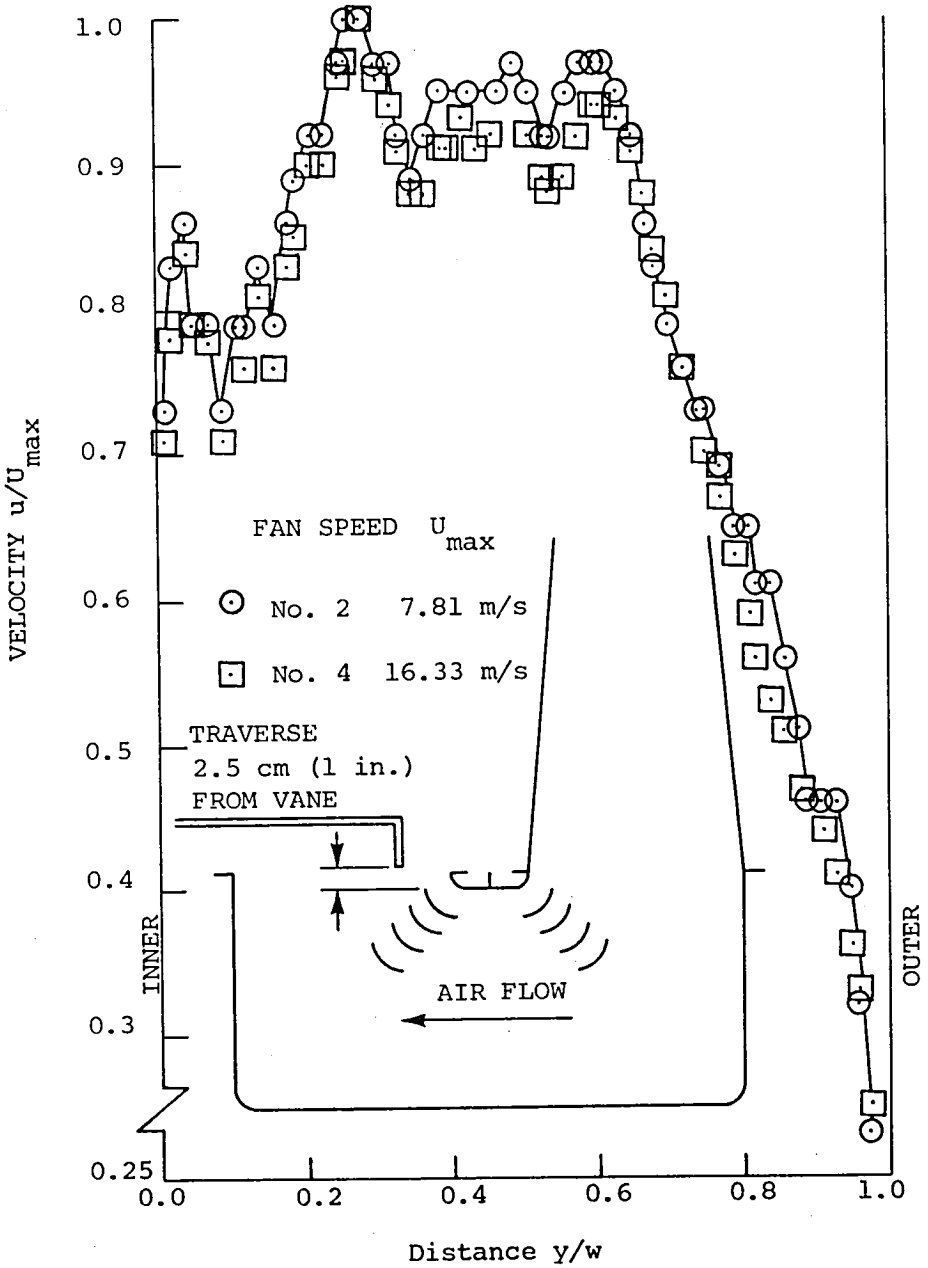

(b) Traverse station 18(H).

Figure 31. (Concluded).

1. Report No.	2. Government Accession No.	3. Recipient's Catalog No.
NASA CR-159234		

4. Title and Subtitle	5. Report Date
Scale Model Studies for Establishing the Flow Patterns of a Low-Speed Tunnel	March 1980
	6. Performing Organization Code

7. Author(s)	8. Performing Organization Report No.
P.S. Barna	10. Work Unit No.

9. Performing Organization Name and Address	11. Contract or Grant No.
Old Dominion University Research Foundation P.O. Box 6369 Norfolk, Virginia 23508	NSG 1563
	13. Type of Report and Period Covered Progress Report 3/15-9/14/79

12. Sponsoring Agency Name and Address	14. Sponsoring Agency Code
National Aeronautics and Space Administration Washington, DC 20546	

15. Supplementary Notes

Langley Technical Monitor: Richard J. Margason

16. Abstract

Experiments were conducted on a model tunnel scaled down from the full-size prototype, the V/STOL (Vertical Take-Off and Short Landing) tunnel located at NASA/Langley Research Center, in a ratio of 1:24. The purpose of the tests was to study the flow characteristics around the tunnel and to document the location and causes of flow separation and local recirculation. Cumulatively these adverse flow characteristics reduce the efficiency of tunnel performance.

Preliminary experiments performed earlier on the V/STOL tunnel indicated that adverse flow conditions existed at various locations which suggested the need for a study of the interaction between the various components from which the tunnel is built. For this purpose an experimental setup similar to the sequence of tunnel circuit components was constructed which enabled the various components to be tested either individually or in combination. These components were tested both individually and in combination by the simple technique of blowing air through them, then measuring the velocity distribution at relevant sections.

While the tests are not fully completed, results obtained so far already show effects of interaction between the components which were absent when they were tested individually and which explain to some extent why the tunnel functions at reduced efficiency.

17. Key Words (Suggested by Author(s))	18. Distribution Statement
Wind tunnels— calibration of . . . Model studies on interation of tunnel components and studies of the prevailing flow pattern around the tunnel circuit.	Unclassified-unlimited STAR category 09

19. Security Classif. (of this report)	20. Security Classif. (of this page)	21. No. of Pages	22. Price*
Unclassified	Unclassified	91	$6.00

* For sale by the National Technical Information Service, Springfield, Virginia 22161